

NUREG/CR-5720
EGG-2643

Motor-Operated Valve Research Update

Prepared by
R. Steele, Jr., J. C. Watkins, K. G. DeWall, M. J. Russell

**Idaho National Engineering Laboratory
EG&G Idaho, Inc.**

**Prepared for
U.S. Nuclear Regulatory Commission**

AVAILABILITY NOTICE

Availability of Reference Materials Cited in NRC Publications

Most documents cited in NRC publications will be available from one of the following sources:

1. The NRC Public Document Room, 2120 L Street, NW., Lower Level, Washington, DC 20555
2. The Superintendent of Documents, U.S. Government Printing Office, P.O. Box 37082, Washington, DC 20013-7082
3. The National Technical Information Service, Springfield, VA 22161

Although the listing that follows represents the majority of documents cited in NRC publications, it is not intended to be exhaustive.

Referenced documents available for inspection and copying for a fee from the NRC Public Document Room include NRC correspondence and internal NRC memoranda; NRC bulletins, circulars, information notices, inspection and investigation notices; licensee event reports; vendor reports and correspondence; Commission papers; and applicant and licensee documents and correspondence.

The following documents in the NUREG series are available for purchase from the GPO Sales Program: formal NRC staff and contractor reports, NRC-sponsored conference proceedings, international agreement reports, grant publications, and NRC booklets and brochures. Also available are regulatory guides, NRC regulations in the *Code of Federal Regulations*, and *Nuclear Regulatory Commission Issuances*.

Documents available from the National Technical Information Service include NUREG-series reports and technical reports prepared by other Federal agencies and reports prepared by the Atomic Energy Commission, forerunner agency to the Nuclear Regulatory Commission.

Documents available from public and special technical libraries include all open literature items, such as books, journal articles, and transactions. *Federal Register* notices, Federal and State legislation, and congressional reports can usually be obtained from these libraries.

Documents such as theses, dissertations, foreign reports and translations, and non-NRC conference proceedings are available for purchase from the organization sponsoring the publication cited.

Single copies of NRC draft reports are available free, to the extent of supply, upon written request to the Office of Administration, Distribution and Mail Services Section, U.S. Nuclear Regulatory Commission, Washington, DC 20555.

Copies of industry codes and standards used in a substantive manner in the NRC regulatory process are maintained at the NRC Library, 7920 Norfolk Avenue, Bethesda, Maryland, for use by the public. Codes and standards are usually copyrighted and may be purchased from the originating organization or, if they are American National Standards, from the American National Standards Institute, 1430 Broadway, New York, NY 10018.

DISCLAIMER NOTICE

This report was prepared as an account of work sponsored by an agency of the United States Government. Neither the United States Government nor any agency thereof, or any of their employees, makes any warranty, expressed or implied, or assumes any legal liability of responsibility for any third party's use, or the results of such use, of any information, apparatus, product or process disclosed in this report, or represents that its use by such third party would not infringe privately owned rights.

NUREG/CR-5720
EGG-2643
R1, RM, 1S

Motor-Operated Valve Research Update

Manuscript Completed: October 1991
Date Published: June 1992

Prepared by
R. Steele, Jr., J. C. Watkins, K. G. DeWall, M. J. Russell

G. H. Weidenhamer, O. O. Rothberg, NRC Project Managers

Idaho National Engineering Laboratory
Managed by the U.S. Department of Energy

EG&G Idaho, Inc.
Idaho Falls, ID 83415

Prepared for
Division of Engineering
Office of Nuclear Regulatory Research
U.S. Nuclear Regulatory Commission
Washington, DC 20555
NRC FINs A6857, B5529
Under DOE Contract No. DE-AC07-76ID01570

ABSTRACT

This report provides an update on the valve research sponsored by the U.S. Nuclear Regulatory Commission (NRC) that is being conducted at the Idaho National Engineering Laboratory. The update focuses on the information applicable to the following requests from the NRC staff:

- Examine the use of in situ test results to estimate the response of a valve at design-basis conditions
- Examine the methods used by industry to predict required valve stem forces or torques
- Identify guidelines for satisfactory performance of motor-operated valve diagnostics systems
- Participate in writing a performance standard or guidance document for acceptable design-basis tests.

The authors have reviewed past, current, and ongoing research programs to provide the information available to address these items.

FIN A6857, B5529—Investigation of information used to estimate valve response, methods used to predict valve stem forces/torques, guidelines for MOV diagnostics systems.

CONTENTS

ABSTRACT	iii
LIST OF FIGURES	vii
LIST OF TABLES	xi
EXECUTIVE SUMMARY	xiii
ACKNOWLEDGMENTS	xv
1. INTRODUCTION	1
2. GENERAL OBSERVATIONS	3
3. SPECIFIC OBSERVATIONS	4
3.1 Use of In Situ Test Results to Bound the Response of a Valve at Design-Basis Conditions	4
3.2 Assessment of Butterfly Valves Closing against a Compressible Fluid (Containment Purge and Vent)	4
3.2.1 Background	4
3.2.2 Flow Phenomena through a Butterfly Valve	5
3.2.3 Existing Butterfly Valve Data and Extrapolation Techniques	7
3.2.4 Butterfly Valve Dynamic Flow Testing and Results	8
3.2.5 Butterfly Valve Test Results and Torque Bounding Methods	8
3.2.6 Effect of an Upstream Elbow on the Torque Requirements of a Butterfly Valve	22
3.3 Assessment of Wedge-Gate Valves Closing against Medium to High Flow Conditions	24
3.3.1 Assessment of the Disc Factor Term in the Industry Equation	30
3.3.2 Development of a Correlation to Bound the Stem Force on a Gate Valve during Closure	37
3.3.3 A Correlation to Bound the Stem Force on a Gate Valve during Closure	42
3.3.4 Use of the Correlation to Bound the Stem Force on a Gate Valve during Closure	47
3.3.5 Identifying the Pressure Dependency Contributing to the Stem Force on a Gate Valve during Closure	51
3.3.6 Low Differential Pressure Test Verification and Bounding of the Stem Force on a Gate Valve Closing against Design-Basis Flows	51
3.3.7 Nuclear Maintenance Application Center (NMAC) Gate Valve Stem Force Equation	54

4.	UNDERSTANDING DIAGNOSTICS AND DIAGNOSTIC TESTING OF MOTOR-OPERATED VALVES	55
4.1	Overview	55
4.2	Understanding MOV Diagnostic Testing	56
4.2.1	Motor Operator Switch Position	56
4.2.2	Motor Current	56
4.2.3	Motor Voltage	59
4.2.4	Motor Operator Torque	62
4.2.5	Valve Stem Force	62
4.3	Load-Sensitive Motor-Operated Valve Behavior	67
4.4	Direct Current Powered Motor Operators	79
5.	WRITING A PERFORMANCE STANDARD	83
5.1	Overview	83
5.2	Detailed Observations	84
6.	REFERENCES	85

LIST OF FIGURES

1.	Effect of low pressure zones on butterfly valve torque—disc oriented with the flat face of the disc facing upstream	6
2.	Effect of low pressure zones on butterfly valve torque—disc oriented with the curved face of the disc facing upstream	6
3.	Cross section of Valve 1, the first 8-in. butterfly valve	9
4.	Cross section of Valve 2, the second 8-in. butterfly valve, and Valve 3, the 24-in. butterfly valve	10
5.	Containment butterfly valve disc overlay	11
6.	Typical installation—butterfly valve uniform inlet flow test section	11
7.	Uniform inlet flow butterfly valve positions	11
8.	Typical installation—butterfly valve nonuniform inlet flow test section	12
9.	Nonuniform inlet flow butterfly valve positions	12
10.	Butterfly valve differential pressure to upstream pressure ratio versus valve position	13
11.	Static pressure 15 diameters downstream of a butterfly valve versus valve position	13
12.	Torque versus upstream pressure and angle for Valve 1, the first 8-in. butterfly valve, FFF orientation	14
13.	Torque versus upstream pressure and angle for Valve 2, the second 8-in. butterfly valve, FFF orientation	15
14.	Torque versus upstream pressure and angle for Valve 3, the 24-in. butterfly valve, FFF orientation	15
15.	Torque versus upstream pressure and angle for Valve 1, the first 8-in. butterfly valve, CFF orientation	16
16.	Torque versus upstream pressure and angle for Valve 2, the second 8-in. butterfly valve, CFF orientation	16
17.	Torque versus upstream pressure and angle for Valve 3, the 24-in. butterfly valve, CFF orientation	17
18.	Peak torque versus static upstream pressure for Valve 1, the first 8-in. butterfly valve	17
19.	Peak torque versus static upstream pressure for Valve 2, the second 8-in. butterfly valve	18
20.	Peak torque versus static upstream pressure for Valve 3, the 24-in. butterfly valve	18
21.	Extrapolation exponent, butterfly valve oriented with the curved face of the disc facing upstream	20

22.	Extrapolation exponent, butterfly valve oriented with the flat face of the disc facing upstream	20
23.	Actual to predicted butterfly valve torque (percent) as a function of extrapolation exponent versus valve diameter ratio	21
24.	Predictions for a 48-in. butterfly valve based on extrapolating the torques of an 8-in. and a 24-in. butterfly valve at upstream pressures of 15 and 60 psig	23
25.	Torque versus upstream pressure and angle for Valve 3, the 24-in. butterfly valve in the CFF orientation	25
26.	Peak torque versus static upstream pressure for Valve 3, the 24-in. butterfly valve, comparing the response of the peak torque with elbow and peak torque without elbow orientations	25
27.	Comparison of the standard industry gate valve stem force equation with selected test results	29
28.	Comparison of the NMAC gate valve stem force equation with selected test results	30
29.	Disc factor for Gate Valve 2 closing on line break flow, effect of subcooling at 1000 psig	32
30.	Disc factor for Gate Valve 2 closing on line break flow, effect of pressure at 100°F subcooling	33
31.	Disc factor for Gate Valve 2 opening on line break flow, effect of pressure at 100°F subcooling	34
32.	Gate valve disc cross section showing pressure forces and measurement locations	36
33.	Gate valve internal pressure distribution	36
34.	Gate valve disc cross section showing unbalanced forces just before wedging	37
35.	Resolution of horizontal and vertical gate valve disc forces into surface normal and sliding forces	39
36.	Gate-valve stem-force history, indicating severe damage to the guides	40
37.	Gate-valve stem-force history, indicating damage to the guides but not to the seats	41
38.	Normalized surface sliding force versus normalized surface normal force for gate valves closing against less than 70°F subcooled fluid	45
39.	Normalized surface sliding force versus normalized surface normal force for gate valves closing against 70°F, or greater, subcooled fluid	46
40.	Stem-force history of a small gate valve during an opening test	48
41.	Stem-force history of a large gate valve during an opening test	49

42. Gate valve load-dependent friction factor using the INEL correlation	53
43. Limit switch history showing stroke time for a position-controlled valve. Limit switch actuation points are important when analyzing other data	57
44. Torque switch history showing torque switch trip and the termination of current flow to the motor controller holding coil	57
45. Current history from a design-basis test showing current increasing as the valve closes; the rapid increase in current indicates torque switch trip. The test began with the valve 75% open	58
46. Motor torque-speed curve showing the speed-torque-current relationship for the ac motor test results shown in Figure 45. Beyond the knee of the curve, the torque increase is small in proportion to the speed loss and the current increase. For some motor configurations there is no increase; for some there is actually a decrease in torque beyond the knee of the speed curve.	58
47. Current history from a design-basis test showing the motor going into a stall, saturating the current transducer. The test began with the valve 30% open	59
48. Motor torque-speed curve showing the speed-torque-current relationship for a dc motor. The torque (load) continues to increase as the speed drops and the current increases.	60
49. Disc position histories from three dc-powered closing tests showing that the stroke time is longer with higher loads	60
50. Motor heating under load caused the current demand of this dc motor to decrease at a rate of 1 amp per second during the 20-second test, resulting in a decrease in the output torque of approximately 1 ft-lb every 2 seconds	61
51. Disc position histories from four dc-powered MOV closing tests, showing that the stroke time is longer with higher loads. Three of the tests did not fully seat the valve, and the test at the highest load stalled the motor	61
52. Ratio of torque spring force to stem torque from MOVLS Test 1, with a small stem force	63
53. Ratio of torque spring force to stem torque from MOVLS Test 4 at a higher stem force	63
54. Ratio of torque spring force to stem torque from MOVLS Test 5, at a high stem force, in which final seating was not achieved, showing that the average torque spring force to stem torque ratio was not influenced by the load on the operator	64
55. Stem force history from MOVLS Test 4, showing a 3000 lb _f margin between the peak stem force and the stem force at final seating	64
56. Stem force history from MOVLS Test 5, showing that a 1000 lb _f increase in the initial stem force eliminated the 3000 lb _f final seating stem force margin observed in MOVLS Test 4	65

57.	Typical torque spring calibration plot shows the initial force offset at zero deflection. This figure also confirms that for this spring, the spring force to deflection relationship is linear. The actual values are omitted from this figure because the data are proprietary until the MOV diagnostic equipment validation effort is complete	65
58.	MOVLS layout drawing	68
59.	Traces of thrust versus time for Tests 8 through 10 of the MOVLS test sequence. These are identical low-thrust tests	69
60.	Traces of thrust versus time for Tests 10 through 14 of the MOVLS test sequence	69
61.	Traces of thrust versus time for the final three tests of the MOVLS test sequence. Tests 12–14, which exhibit load-sensitive MOV behavior, were followed by a series of low-thrust tests (Tests 15–17), with resistance to closing much like the first three of the series	70
62.	The design of the operator allows two potential output motion paths	71
63.	The application of spring pack force to the operator mechanism at an offset distance from the stem centerline generates the torque input to the mechanism	73
64.	Potential causes of torque loss in the operator are identified	73
65.	Traces of spring pack force versus time for Tests 8 through 10 of the MOVLS test sequence. These traces correspond to the thrusts of Figure 59	75
66.	Traces of spring pack force versus time for Tests 10 through 14 of the MOVLS test sequence. These traces correspond to the thrusts of Figure 60. Spring pack force does not change significantly from test to test	75
67.	Traces of spring pack force versus time for Tests 14 through 17 of the MOVLS test sequence. These traces correspond to the thrusts of Figure 61. Spring pack force does not change significantly from test to test	76
68.	The ratio of spring pack force to stem torque for Tests 8 through 10 of the MOVLS test sequence. These traces correspond to the thrusts of Figure 59	76
69.	The ratio of spring pack force to stem torque for Tests 10 through 14 of the MOVLS test sequence. These traces correspond to the thrusts of Figure 60	77
70.	The ratio of spring pack force to stem torque for Tests 14 through 17 of the MOVLS test sequence. These traces correspond to the thrusts of Figure 61. Spring pack force does not change significantly from test to test	77
71.	Traces of coefficient of friction in the stem nut versus time for the first three tests of the MOVLS test sequence. Very little change in coefficient of friction is observed at the low thrust levels of these tests	78
72.	Traces of coefficient of friction in the stem nut versus time for Tests 10 through 14 of the MOVLS test sequence. A steady increase in coefficient of friction is evident in these tests. Coefficient of friction is highest during Test 14, the test exhibiting load sensitive MOV behavior	78

73. Traces of coefficient of friction in the stem nut versus time for the last four tests of the MOVLS test sequence. A full opening/closing low-thrust cycle (Test 15) is needed following the test exhibiting load-sensitive MOV behavior (Test 14) before the coefficient of friction returns to the levels recorded for the initial low-thrust level tests	80
74. Typical stem thrust histories from the dc-powered MOVLS tests	80
75. Typical stem nut coefficient of friction histories from the dc-powered MOVLS test. Note the increase in friction between low-load Test 1 and high-load Test 12. The load was doubled between Tests 12 and 15 without a significant increase in stem nut coefficient of friction	82

LIST OF TABLES

1. Comparison of torque prediction methods butterfly versus valve orientation	22
2. Ratio of peak torque to uniform flow peak torque for a butterfly valve in the CFF orientation	23
3. Phase I gate valve flow interruption test temperatures and pressures	26
4. Phase II gate valve flow interruption test temperatures and pressures	26
5. Phase II gate valve test data supporting extrapolation	43
6. Phase I gate valve test data supporting extrapolation	44
7. Comparison of gate valve stem forces, estimates versus actual	52

EXECUTIVE SUMMARY

The U.S. Nuclear Regulatory Commission (NRC) is supporting motor-operated valve (MOV) research at the Idaho National Engineering Laboratory (INEL). The MOV test programs performed as part of the research provide the basis for assessing the effects various factors have on the valves and for evaluating current industry standards. This report discusses several research items, including

- Use of in situ test results to estimate the response of a valve at design basis conditions
- Methods used by industry to predict required valve stem forces or torques
- Guidelines for satisfactory performance of MOV diagnostics systems
- Composition of a performance standard or guidance document for acceptable design-basis tests.

We have reviewed all of our past, current, and ongoing valve research that included full-scale

valve test programs to address these items. This review revealed that (a) use of in situ test results to estimate the response of gate and butterfly valves at design-basis conditions is possible, but a long list of caveats exists; (b) the methods used by industry to predict the required stem force for a gate valve and the required stem torque for a butterfly valve are incomplete; (c) satisfactory performance of MOV diagnostic systems is possible, but very few of the currently available systems measure enough parameters to be completely effective; and (d) our participation in writing a performance standard or guidance document for acceptable design-basis tests requires us to continue to exchange information with the American Society of Mechanical Engineers standards writing committees.

The research documented in this report forms the basis for the technical presentations given at the NRC inspector training courses, and has also enabled the INEL to create a PC-based computer program to assist NRC personnel during their MOV inspections.

ACKNOWLEDGMENTS

Researchers at the Idaho National Engineering Laboratory (INEL) developed the basis for the INEL gate valve stem force correlation presented in Section 3.3 and have presented the results to a wide range of industry and utility experts for review. We wish to thank the following reviewers, who responded with comments and insights to this effort:

Siemens/Kraftwerk Union	Dr. Nabil Schauki, Dr. Norbert Rauffmann, Dr. U. Simon, Helmut Knoedler
Duke Power	Neal Estep, W. Scheffler
Consumers Power	George Smith
Portland General Electric	M. Lee Kelly
Nuclear Management and Resources Council	Review Team
Electric Power Research Institute	John Hosler
Idaho National Engineering Laboratory	Dr. Romney Duffy, Tim Boucher, Vic Berta.

We would also like to thank the following individuals from Limitorque who have reviewed our research on load-sensitive, motor-operated valve behavior: Bob Bailey, Pat McQuillan, Mike Bailey, Greg Pence, Charles Cox, and Walt Sykes. Their comments and insights are appreciated.

Motor-Operated Valve Research Update

1. INTRODUCTION

The Idaho National Engineering Laboratory (INEL) is performing motor-operated valve (MOV) research in support of the U.S. Nuclear Regulatory Commission's (NRC's) efforts regarding Generic Issue 87, "Failure of HPCI [High-Pressure Coolant Injection] Steam Line Without Isolation," and Generic Letter 89-10, "Safety-Related Motor-Operated Valve Testing and Surveillance."

This report updates the research reported in NUREG/CR-5558, *Generic Issue 87 Flexible Wedge Gate Valve Test Program, Phase II Results and Analysis* (Steele et al., 1990). This update also provides research results on program objectives not covered completely in that report. These objectives include

- Examine the use of in situ test results to estimate the required forces of a valve at design-basis conditions
- Examine the methods used by industry to predict required valve stem forces or torques
- Identify guidelines for satisfactory performance of MOV diagnostics systems
- Participate in writing a performance standard or guidance document for acceptable design-basis tests.

In preparing this report, we reanalyzed selected results from all four of the full-scale valve test programs performed for the NRC Equipment Operability Program, as well as results from the ongoing separate effects testing currently being conducted at the INEL. The full-scale valve test programs include

- The Test Program for Containment Purge-and-Vent Valves is reported in NUREG/CR-4648, *A Study of Typical Nuclear Containment Purge Valves in an Accident*

Environment (Watkins et al., 1986). In this test program, three butterfly valves, two 8-in. and one 24-in., were tested at line break flows at closing differential pressures of 5 to 60 psig.

- The testing reported in NUREG/CR-4977, *SHAG Test Series: Seismic Research on an Aged United States Gate Valve and on a Piping System in the Decommissioned Heissdampfreaktor (HDR)* (Steele and Arendts, 1989). A 25-year old, 8-in., dc powered, motor-operated Crane gate valve was refurbished and installed in an experimental reactor flow loop. Test loadings included flow, pressure, temperature, and seismic excitations.
- The Phase I Generic Issue 87 Test Program reported in NUREG/CR-5406, *BWR [Boiling Water Reactor] Reactor Water Cleanup System Flexible Wedge Gate Isolation Valve Qualification and High Energy Flow Interruption Test Program* (DeWall and Steele, 1989). This test program subjected two 6-in., motor-operated, flexwedge, containment isolation gate valves to (a) the applicable hydraulic qualification test outlined in American National Standards Institute (ANSI)/American Society of Mechanical Engineers (ASME) B16.41, (b) a test at normal reactor water cleanup (RWCU) system flow and pressure, and (c) tests at full line break flows at design-basis and other parametric fluid conditions.
- The Phase II Generic Issue 87 Test Program, reported in NUREG/CR-5558 (Steele et al., 1990). This test program subjected three 6-in. and three 10-in. flexwedge, motor-operated gate valves to (a) applicable hydraulic qualification tests outlined in ANSI/ASME B16.41, (b) tests at normal system pressure and flow, and (c) full line break flow tests at design-basis and other

Introduction

parametric fluid conditions for the BWR containment isolation valves. The valves were representative of those installed in the BWR HPCI turbine steam supply line, the RWCU system, and the reactor core isolation cooling turbine steam supply line.

The ongoing separate effects testing in our laboratory uses the INEL motor-operated valve load simulator (MOVLS). This device uses actual motor operators and valve stems, which are loaded using a hydraulic cylinder to produce rising stem valve loadings typical of those we have observed in field testing. The MOVLS is currently instrumented to directly measure the following:

- Force and torque on the stem
- Position of the stem
- Force on the torque spring

- Displacement of the torque spring
- Torque and limit switch actuation
- Root mean squared (rms) current and voltage
- Peak to peak current
- Power, power factor, and speed of the electric motor.

Through the Data Acquisition System, the MOVLS can also display real time calculations such as stem factor.

The design and calibration of the MOVLS has been upgraded from strictly a research device to a standard that can be used by the industry to evaluate their diagnostic equipment. Current research includes load-sensitive motor-operator behavior and comparison testing of ac- and dc-powered motor operators.

2. GENERAL OBSERVATIONS

Manufacturing tolerances, piping geometry effects, and specific installation effects all influence whether a valve can be grouped with other like valves and categorically qualified by similarity. The following examples provide some insights into why we believe such influences need to be considered:

- When the same 6-in. gate valve was tested with flow in one direction, then refurbished and tested with flow in the other direction, the failure mechanism changed from guiding surface failure to seating surface failures. We believe this to be the result of the internal valve tolerances stacking up differently.
- A 6-in. and a 10-in. gate valve from the same manufacturer were design-basis flow tested. The 6-in. valve passed the tests with good results. However, with the 10-in. valve the flow forces plastically deformed the valve body guide rails, which increased the required stem force to close. Upon disassembly and inspection of the valve, it was observed that the guide rails were not welded far enough down into the body. The current nuclear valve qualification standard ANSI/ASME B16.41 would have allowed similar 3- to 12-in. valves to be qualified, based on the 6-in. qualification test.
- Two like 4-in. gate valves were recently disassembled, inspected, and tested by a utility. The internal tolerances of both valves were within the manufacturer's tolerances, but the utility lapped and polished the second valve until it was as similar to the first valve as possible. The first valve was subjected to both no-flow static tests and design-basis flow tests. The second valve was also subjected to no-flow static tests and

required a higher torque switch setting to produce the same stem force as the first valve. Both motor operators had been dynamometer tested by Limitorque,^a showing equal output for the same torque switch settings. The need for the higher torque switch setting may have been caused by a difference in the stem factor.

- Testing of containment purge-and-vent valves revealed that butterfly valves installed in certain orientations downstream of an elbow could require up to 133% of the torque required to close the same valve in a straight piece of pipe.
- Two like valves at the same utility, but at two different units, performed quite differently. One valve burned up two dc motors. The fault was traced to cable sizing. The cables supplying power to the valve were undersized, resulting in excessive voltage drop and motor stall. The cable size at the other unit was larger, thus avoiding the voltage drop, motor stall, and subsequent motor burnout.

The list could go on, but the point is that we do not know that like valves will behave alike until sufficient testing can show that they will perform in the generic group. Since all valves cannot be design-basis tested in situ, we believe it will be necessary to conduct both testing and analysis to prove that a given valve can be related to a prototype test or a generic qualification group.

a. Mention of specific products and/or manufacturers in this document implies neither endorsement or preference nor disapproval by the U.S. Government, any of its agencies, or EG&G Idaho, Inc., of the use of a specific product for any purpose.

3. SPECIFIC OBSERVATIONS

The first two research update objectives, (a) to examine the use of in situ test results to estimate the response of a valve at design-basis conditions, and (b) to examine the methods used by industry to predict required stem force or torques, will be covered in this section. At this time, the INEL can provide information only on butterfly valves used in purge-and-vent-valve applications and on wedge-gate valves used in a number of medium- and high-flow applications. Testing currently being performed in Europe and at selected utilities in the United States may provide information on other valve designs and flow applications later this year.

We have found it useful to distinguish between predictable valves (those whose performance is repeatable) and nonpredictable valves (those whose performance is not repeatable, usually because they experience internal damage when subjected to high loads during operation). In the previous section, we discussed the pitfalls associated with predicting the performance of various kinds of valves, both predictable and non-predictable. The remainder of this report will be limited to discussing predictable valves only. Valves that do not exhibit predictable behavior under load are discussed extensively in NUREG/CR-5558 (Steele et al., 1990).

3.1 Use of In Situ Test Results to Bound the Response of a Valve at Design-Basis Conditions

The results of INEL testing indicate that the response of a valve can be bounded for specific valve types and fluid conditions from in situ test results obtained from either small-scale test valves or low differential pressure tests. The results of recent European testing support this conclusion. The fact that valves of a given type respond linearly with pressure for a specific fluid condition leads one to believe that, with a sufficient amount of testing, bounding the response of a valve is possible. On the other hand, the

equations the industry has used in the past to predict the performance of gate and butterfly valves are incomplete. The INEL has confidence in bounding the stem force of predictable wedge-gate valves closing against medium to high flows and in bounding the torque of high aspect ratio offset disc butterfly valves used in purge-and-vent applications closing against compressible flows.

3.2 Assessment of Butterfly Valves Closing against a Compressible Fluid (Containment Purge and Vent)

3.2.1 Background. The expression "butterfly valve" is a generic term for a rotating-disc, in-line valve. Of interest to this discussion is the application of butterfly valves in nuclear containment purge-and-vent systems. These systems penetrate the containment boundary and allow air to circulate through the containment; however, in the event of an accident, these systems must close to isolate the environment inside the containment. Consequently, the butterfly valve installed in these systems must be functional both during and following an accident. Industry operability assumptions have been based to a large degree on empirical information obtained from work with incompressible fluids or from small valves tested with compressible fluids. Previous experimental work with incompressible fluids has, for the most part, been done at very low pressures, with very low pressure drops with large valves, or with small valves. The operability issue concerning containment purge-and-vent valves was raised after the Three Mile Island Unit 2 incident. The first question dealt with valve actuator sizing: Would an actuator stall and fail to close a valve because of the dynamic loads that might be produced by a high differential pressure across the containment boundary resulting from a design-basis loss-of-coolant accident? The second question dealt with stress margins to withstand the loads imposed during the closure. The

stress margins are totally dependent on the analysis of the predicted loads and are not part of this discussion.

3.2.2 Flow Phenomena through a Butterfly Valve

As a part of the program for testing butterfly valves, reported in NUREG/CR-4648 (Watkins et al., 1986), we conducted a study into the physics of a butterfly valve closing against a compressible flow to better understand the torque response of a butterfly disc. We observed that a butterfly disc responds as an airfoil from the full-open position to the position where maximum lift occurs (peak torque). With the exception of a disc that is perfectly symmetric and oriented so that flow is evenly split over both faces, the flow that passes around the disc, and the resulting flow perturbation and pressure distribution, will depend not only on the degree of closure of the valve, but also on which surface of the disc is closing into the flow. The torque characteristics of a valve are the result of the pressure that acts over the surface of the disc, which must be counter-balanced to move or control the motion of the disc. With the valve partially closed and the disc oriented so that the flat face of the disc is facing upstream when the valve is fully closed (Figure 1), the flow will separate around the disc, with vortices and a low-pressure region developing at location "L." The result of this low-pressure region is a torque acting on the disc in the opening direction. However, if the valve is partly closed, with the disc oriented so that the curved face of the disc is facing upstream when the valve is fully closed (Figure 2), the flow separation and resultant low-pressure region (location "L") will result in a torque acting on the disc in the closing direction. However, the fact that this torque acts in the closing direction is not necessarily helpful or even benign, because most butterfly valve designs do not have positive stops. Without actuator control, the disc would go beyond the fully closed position to some partially open position in the other direction.

Immediately after peak torque occurs, the airfoil will stall. The disc then becomes an increasingly larger flow obstruction, with a more uniform pressure distribution and decreasing

torque requirements as the valve completes its closing cycle. Based on this hypothesis, one might believe that the pressure acting on a disc can be directly related to the torque for any degree of valve closure, any type of fluid, or any flow velocity through the valve. Unfortunately, test results indicate that, unlike many other valve designs, there are no proven equations for predicting the torque required for a butterfly valve to close against a compressible fluid flow. Torque predictions must come from valid testing and extrapolation. The validity of test results is influenced by the following:

- A compressible flow medium must be used during the tests because of the phenomena of flow separation around a disc and the creation of a low-pressure region. An incompressible fluid will usually cavitate, resulting in a less pronounced low-pressure region. If the fluid is cavitating, the low-pressure region acting on the disc will be limited to the vapor pressure of the fluid.
- The inlet pressure, rather than the differential pressure, should be used for extrapolation, because flow rates through the valve that cause the flow to become choked can result in supersonic flow downstream of the valve. The sonic plane in the valve will depend heavily on the degree of valve closure, the shape of the disc surface, the relative location of the valve seals to the disc, and the properties of the fluid. These effects should be minimal, resulting in a torque extrapolating ability for a given valve, provided the smaller valve is geometrically representative of the larger valve.
- The flow rates and pressure drops achieved during testing must be typical of conditions expected in the actual plant installation. If the flow rate through a valve is too low, it will produce a minimal pressure drop, which in turn eliminates the effect of compressibility. Consequently, the flow field through the valve and around each side of the disc will be much more uniform, as will the resultant pressure profile acting on

Specific Observations

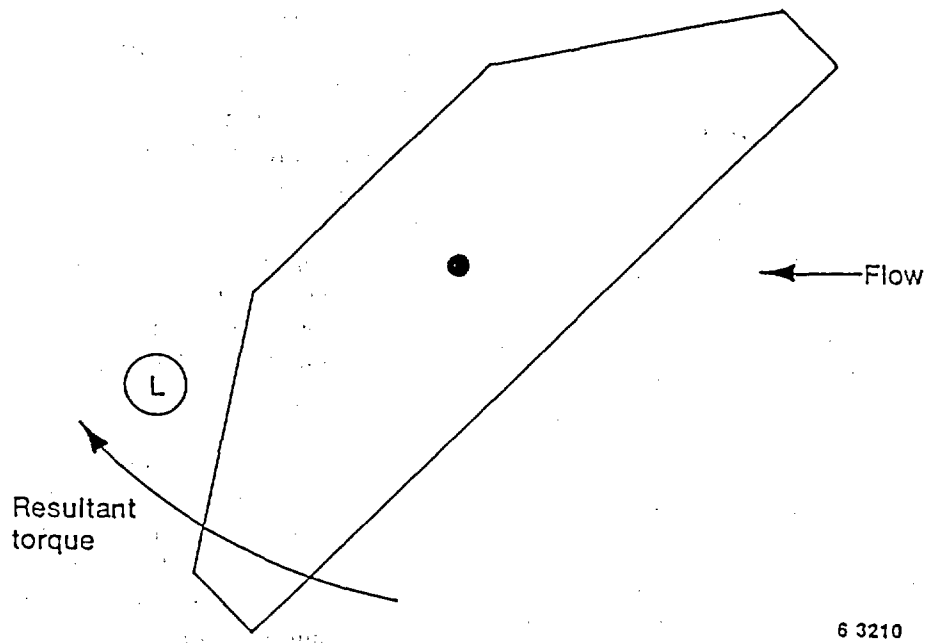


Figure 1. Effect of low pressure zones on butterfly valve torque—disc oriented with the flat face of the disc facing upstream.

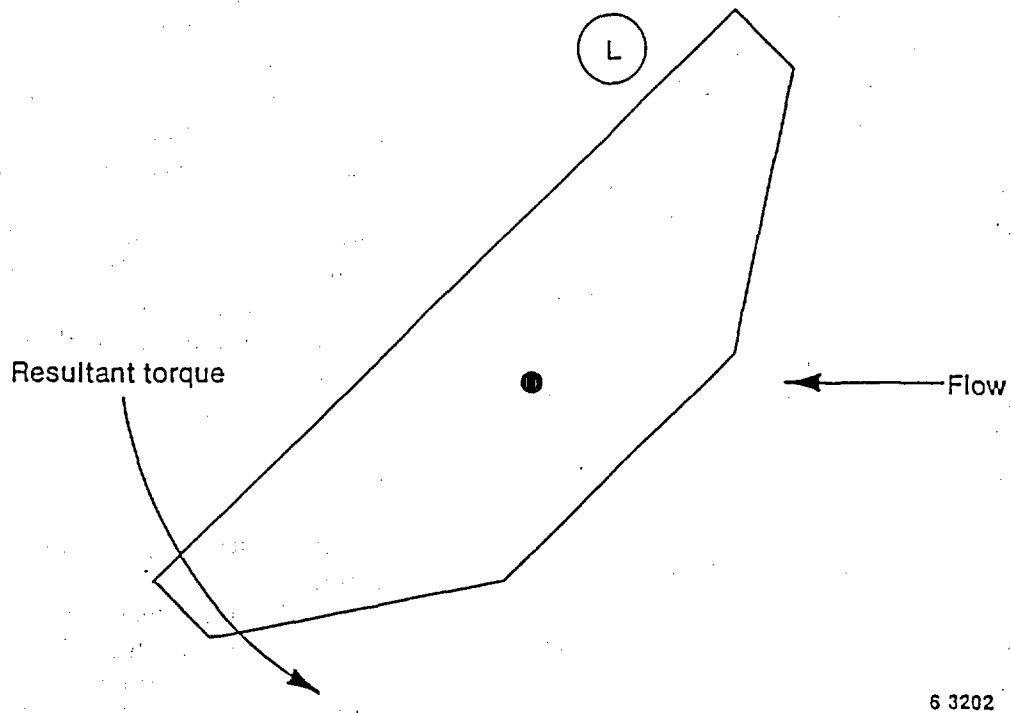


Figure 2. Effect of low pressure zones on butterfly valve torque—disc oriented with the curved face of the disc facing upstream.

the disc. Thus, the resultant torque will be less than expected at high flow.

- For test purposes, the valve should always be oriented so that the curve face of the disc would be facing upstream when the valve is fully closed. This orientation results in a bounding extrapolation of the closing torque using the methods proposed in this report, whereas the other valve orientation does not.
- For very low flow applications, the last 20 degrees of disc closure should be included in the test, because the torque reaction from the seals and bearings in the valve may be much larger than the corresponding dynamic torque and will always work against valve closure.

3.2.3 Existing Butterfly Valve Data and Extrapolation Techniques. An analytical assessment of the loads on a butterfly valve resulting from the increasing pressure environment of a design-basis accident is difficult because of the complex geometries and flows through such a valve and the lack of empirical information on the dynamic response of a butterfly valve in a compressible fluid flow. Also, nonuniform inlet flow configurations will impact the dynamic response of a butterfly valve. Consequently, we performed a number of tests to determine the response characteristics of nuclear containment isolation (butterfly) valves during accident conditions, in an attempt to ensure that the flow dynamics of such a valve were understood. Prior to this work, the only public domain information was that produced for the Allis Chalmers Company by the National Aeronautics and Space Administration Langley Research Center (Allis-Chalmers Corporation, 1979). The Langley Research Center conducted this testing using a 6-in. valve body and three interchangeable butterfly valve discs. The program did not include testing a larger-sized valve to verify the extrapolation theory. Also, Langley performed the testing for a specific vendor, and did not compare the results to other vendor designs.

Because of the very high volumetric flow rates of concern, testing a large butterfly valve under a simulated accident environment is not always economical or even feasible. Consequently, the valve manufacturers have developed a method for testing scale-model test valves and then extrapolating their performance to predict the torque requirements of a larger valve. All of the extrapolation techniques used to predict the torque requirements of a larger butterfly valve have a common underlying assumption as to the nature of the flow. Specifically, the flow is assumed to be quasi-one-dimensional, and the response is assumed to be linear. Again, unfortunately, the flow through a butterfly valve has very real and complicated three-dimensional flow perturbations; therefore, an inherent compromise must be accepted when extrapolating the performance of a scale-model test valve to a larger valve. To further complicate the flow field, the effects of compressibility must be acknowledged. Compressibility effects can cause the flow through a valve to become choked and allow the downstream pressure to vary independent of the upstream pressure.

Each of the extrapolation techniques used by the manufacturers contains a common extrapolation term that relates the size of a large valve to the size of the scale-model test valve. This term is the cube of the nominal diameter of the valve being predicted, divided by the cube of the nominal diameter of the scale-model test valve. Later sections of this report will show that this term will yield a bounding prediction, if data are used with the scale-model test valve oriented so that the curved face of the disc is facing upstream when the valve is fully closed. A nonbounding prediction could result if the flat face of the disc is facing upstream when the valve is fully closed.

Most of the extrapolation techniques have a differential pressure term. The manufacturers assume that the differential pressure across a scale-model test valve will be the same as in a larger valve. Consequently, if the differential pressure term is eliminated from the equation, the torque extrapolation technique reduces to the torque being a direct function of the diameter ratio cubed.

Specific Observations

For our testing, we selected three nuclear-designed butterfly valves typical of those used in commercial nuclear power plant containment purge-and-vent applications. For a comparison of response, we tested two 8-in. nominal-pipe-size butterfly valves with differing internal designs. For extrapolation insights, we also tested a 24-in. nominal-pipe-size butterfly valve (made by the same manufacturer who made one of the 8-in. valves). Figures 3 and 4 show cross-sectional views of the valves, which were ASME Code Class III, ANSI 150 pound class, in-line, off-set disc, elastomer-sealed, high aspect ratio butterfly valves (thickness of the disc is relative to the diameter). These valves are typical of designs up to, and including, 24-in. nominal diameter. In Figure 3, the elastomer seal is part of the body; in Figure 4, the elastomer seal is part of the disc assembly. Figure 5 is a composite cross-sectional view of all three discs, with the 24-in. disc reduced by a factor of 3.

3.2.4 Butterfly Valve Dynamic Flow Testing and Results. The results of the testing of butterfly valve dynamic flow were analyzed to assess the butterfly valve closing torque extrapolation methodology used by the industry and to quantify the influence of piping geometry on the torque response of a butterfly valve.

We performed the experiments with various piping configurations and disc orientations to simulate various installation options that could be encountered in the field. As a standard for comparing the effects of the various installation options, we initially performed our testing in a standard ANSI test section. The nominal or uniform inlet flow ANSI test section is shown in Figure 6, and the valve test positions for this configuration are shown in Figure 7. During the flat face forward (FFF) tests, the disc was oriented so that the flat face of the disc would be facing upstream when the valve was fully closed. Likewise, during the curved face forward (CFF) tests, the disc was oriented so that the curved face of the disc would be facing upstream when the valve was fully closed.

The test section for nonuniform inlet flow is shown in Figure 8; the valve test positions for

this configuration are shown in Figure 9. As the flow bends around the elbow immediately upstream of the test valve, the resultant flow profile results in higher velocities near the outside radius of the elbow. Unlike the uniform inlet flow test section, this nonuniform flow profile will interact with the disc differently, depending on the direction in which the disc is rotating toward the closed position. As such, the clockwise (CW) and counterclockwise (CCW) notations associated with the nonuniform inlet flow tests identify orientations with the disc rotating clockwise or counterclockwise relative to the figure.

Each test was performed while the valve upstream pressure was controlled at a relatively constant pressure throughout the valve closure cycle. Each test cycle consisted of stabilizing the valve upstream pressure with the valve in the fully open (90-degree) position. We then closed the valve at 18 degrees/second to the fully closed (0-degree) position and reopened it after a 250-ms delay. Testing cycles were performed with the upstream pressure varied up to the design-basis pressure of 60 psig while monitoring the position and torque of the valve shaft, the mass flow rate, and the temperature and pressure at various locations throughout the system (shown in Figures 6 and 8).

3.2.5 Butterfly Valve Test Results and Torque Bounding Methods. The test results were first reduced and entered into a computer data base. This data base was then used as a common base for presentation, comparison, analysis, and plotting. The ratio of valve differential pressure to upstream pressure versus valve position was plotted at pressures of 15, 30, 45, and 60 psig for one of the 8-in. CFF valve tests. The results (Figure 10) indicate that the response for the 15-psig test is very different from the response for the higher-pressure tests. However, the response for the higher-pressure tests is very similar beyond the 40-degree position. This difference is indicative of choked flow at the higher test pressures and results in a supersonic flow region downstream of the valve that fluctuates as the valve closes. This, in turn, results in a downstream pressure profile (Figure 11) that is

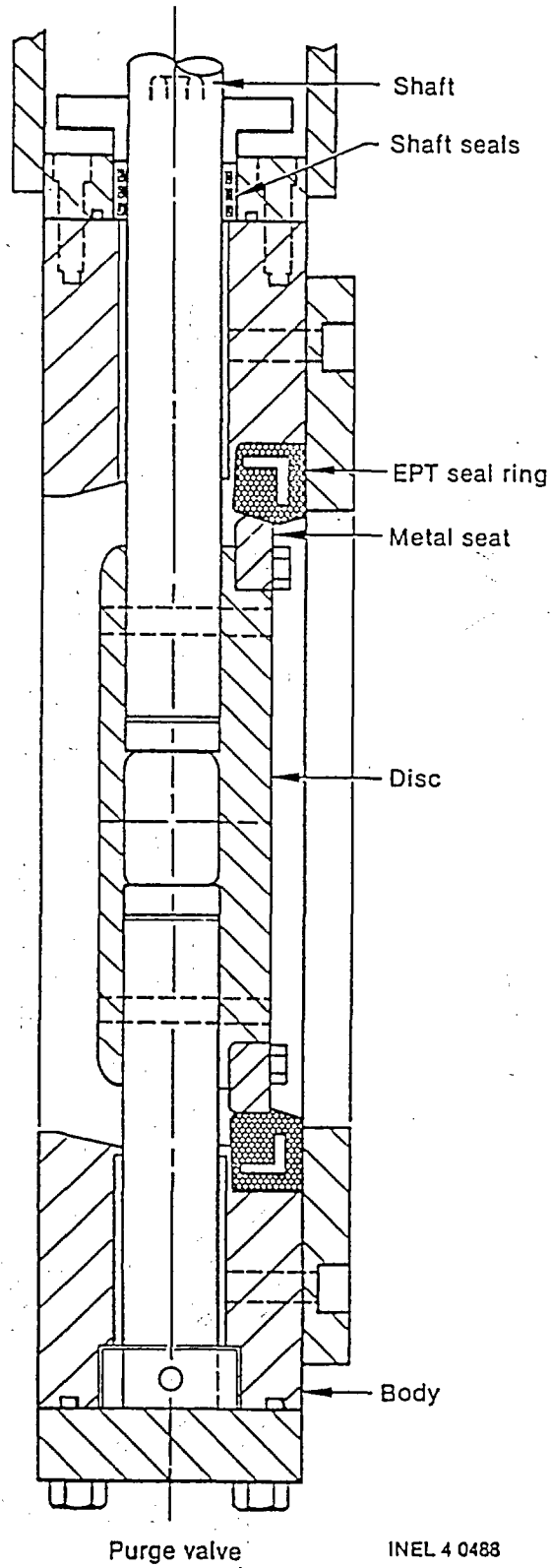


Figure 3. Cross section of Valve 1, the first 8-in. butterfly valve.

Specific Observations

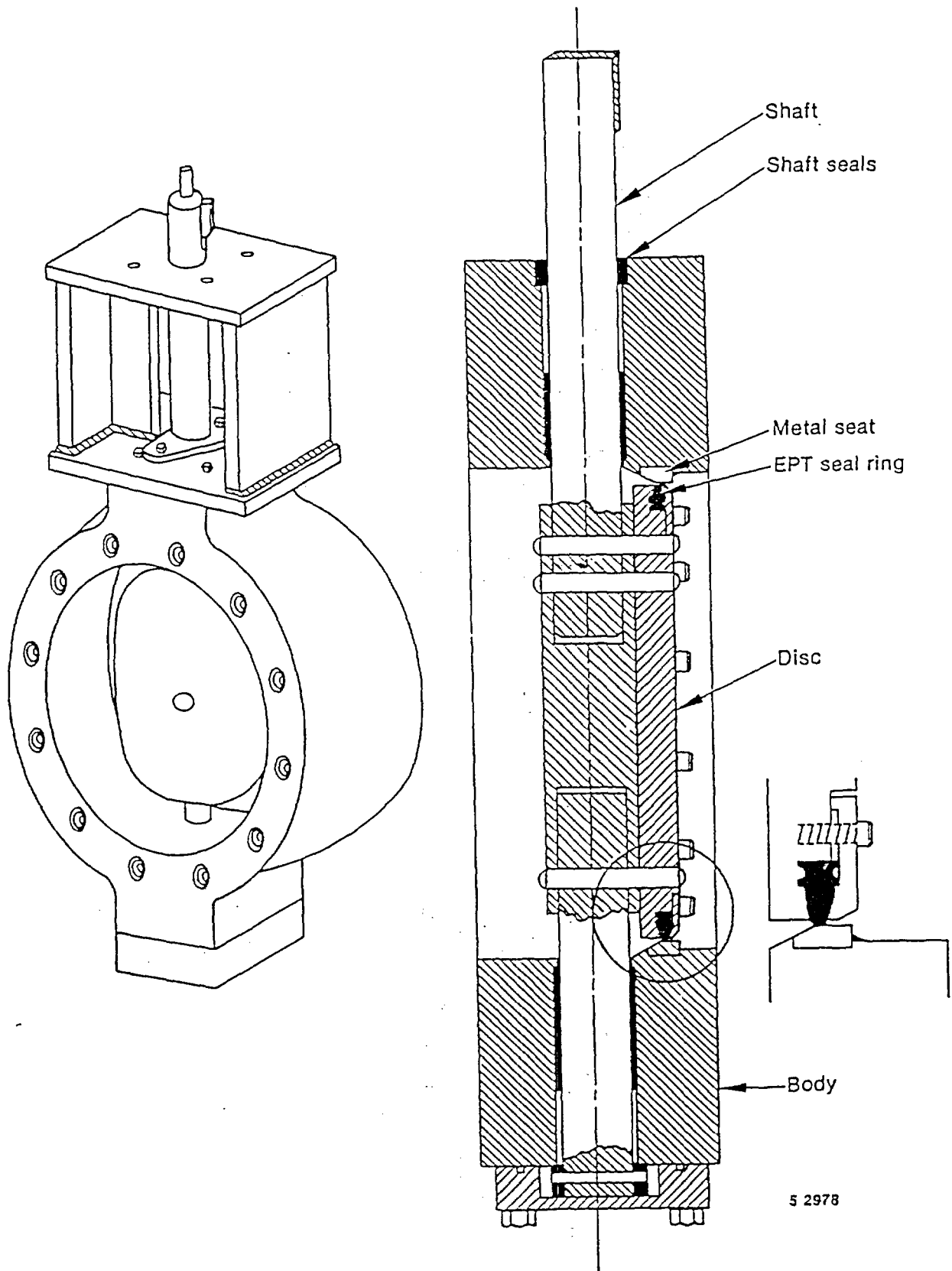


Figure 4. Cross section of Valve 2, the second 8-in. butterfly valve, and Valve 3, the 24-in. butterfly valve.

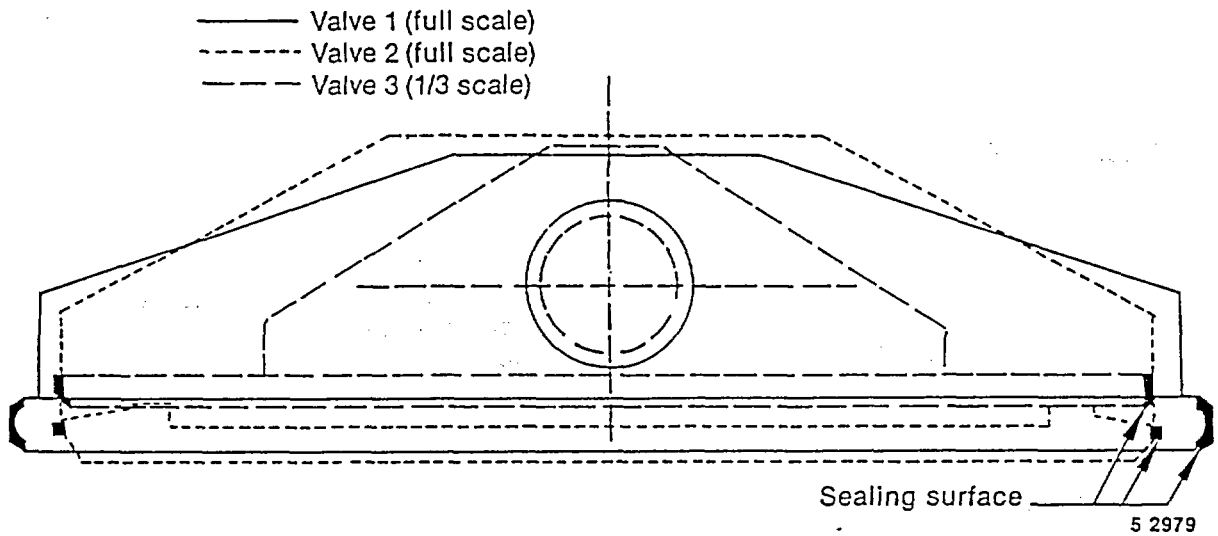


Figure 5. Containment butterfly valve disc overlay.

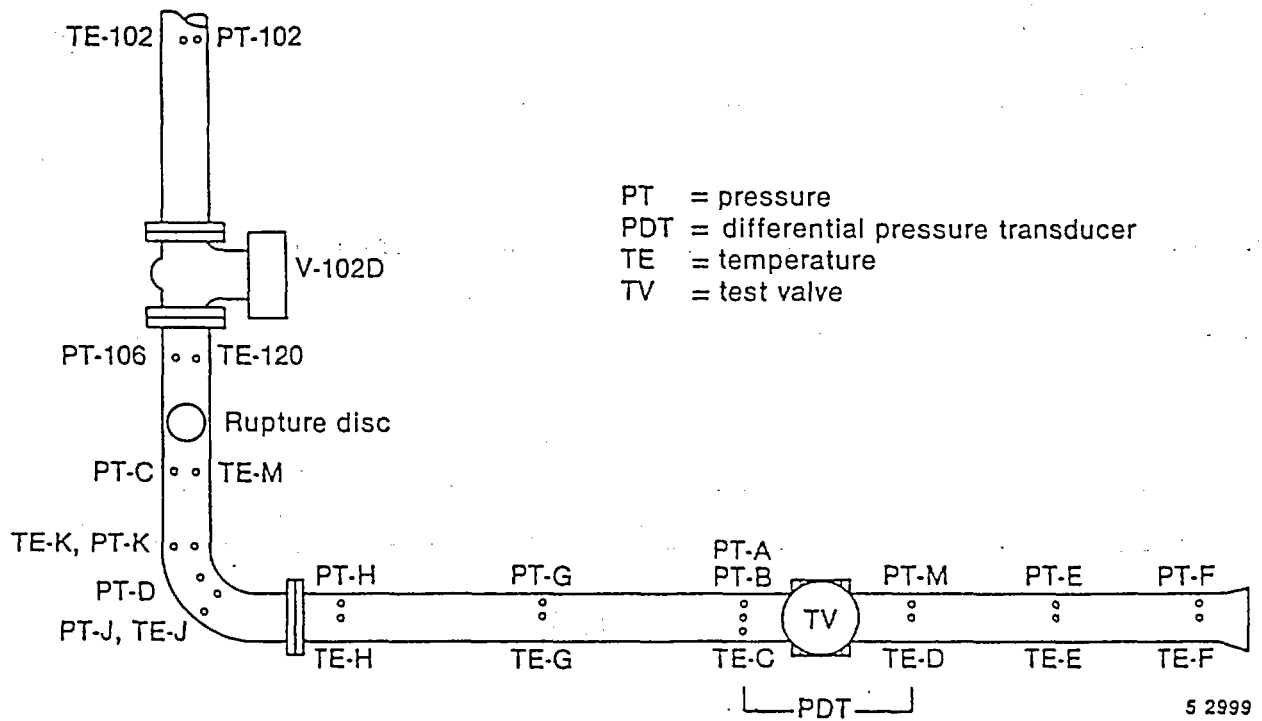


Figure 6. Typical installation—butterfly valve uniform inlet flow test section.

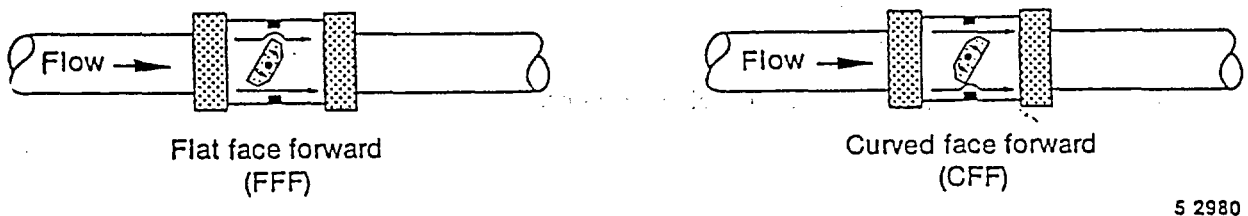


Figure 7. Uniform inlet flow butterfly valve positions.

Specific Observations

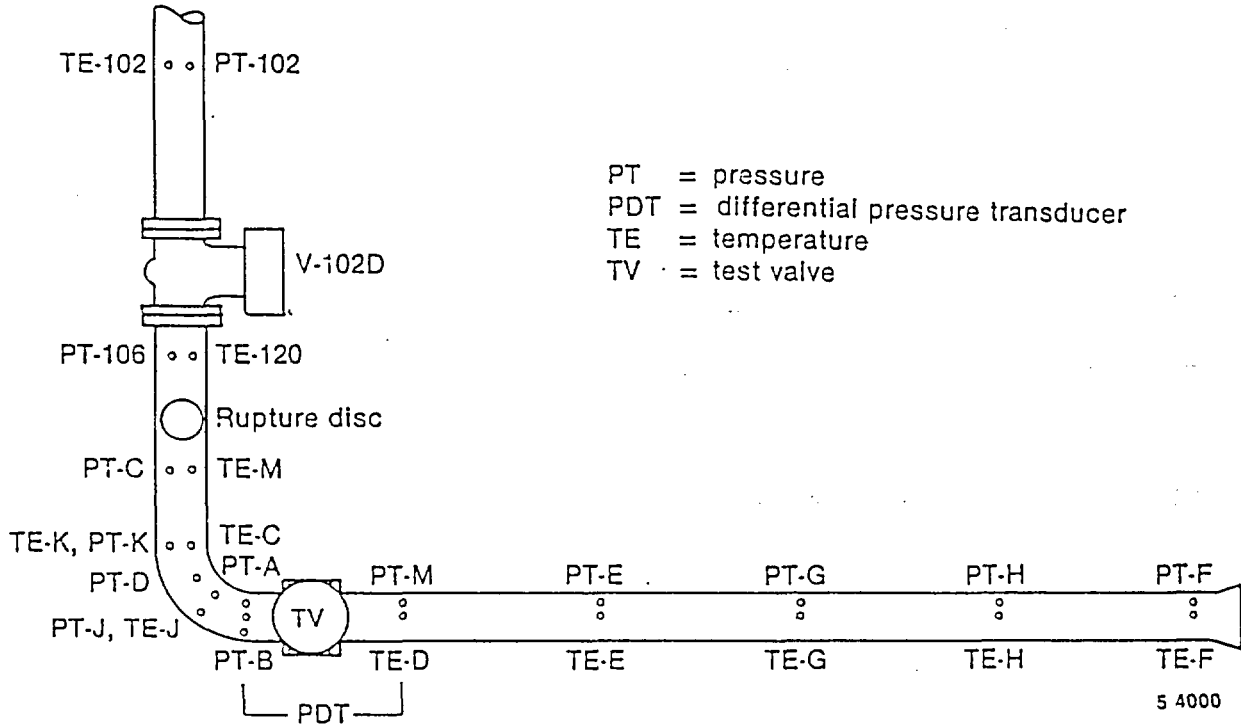


Figure 8. Typical installation—butterfly valve nonuniform inlet flow test section.

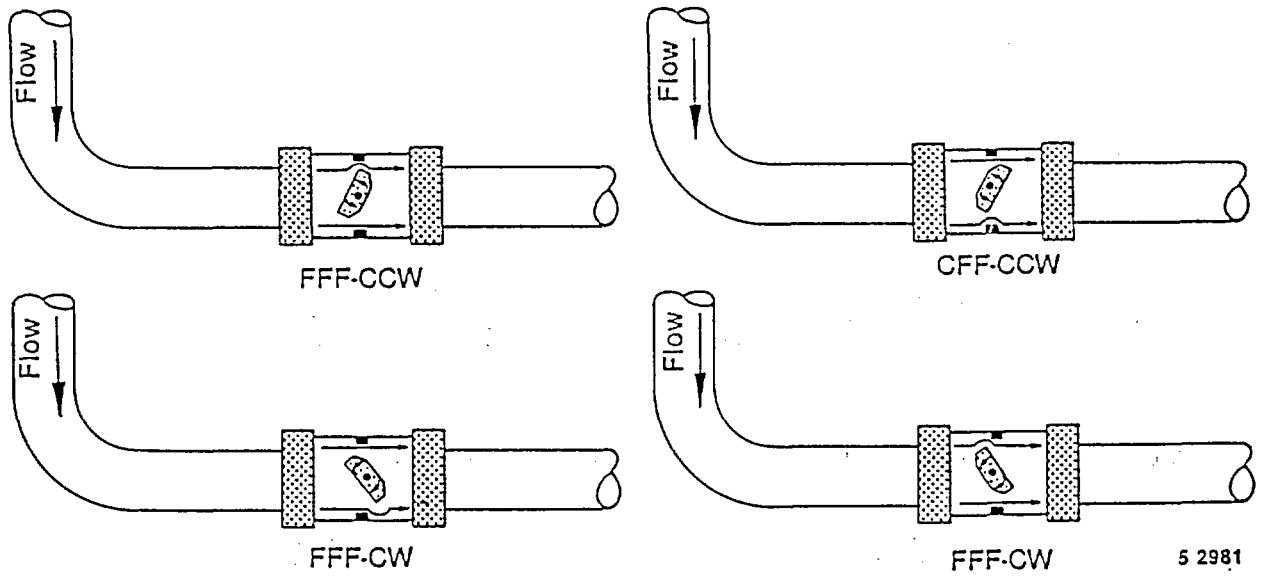


Figure 9. Nonuniform inlet flow butterfly valve positions.

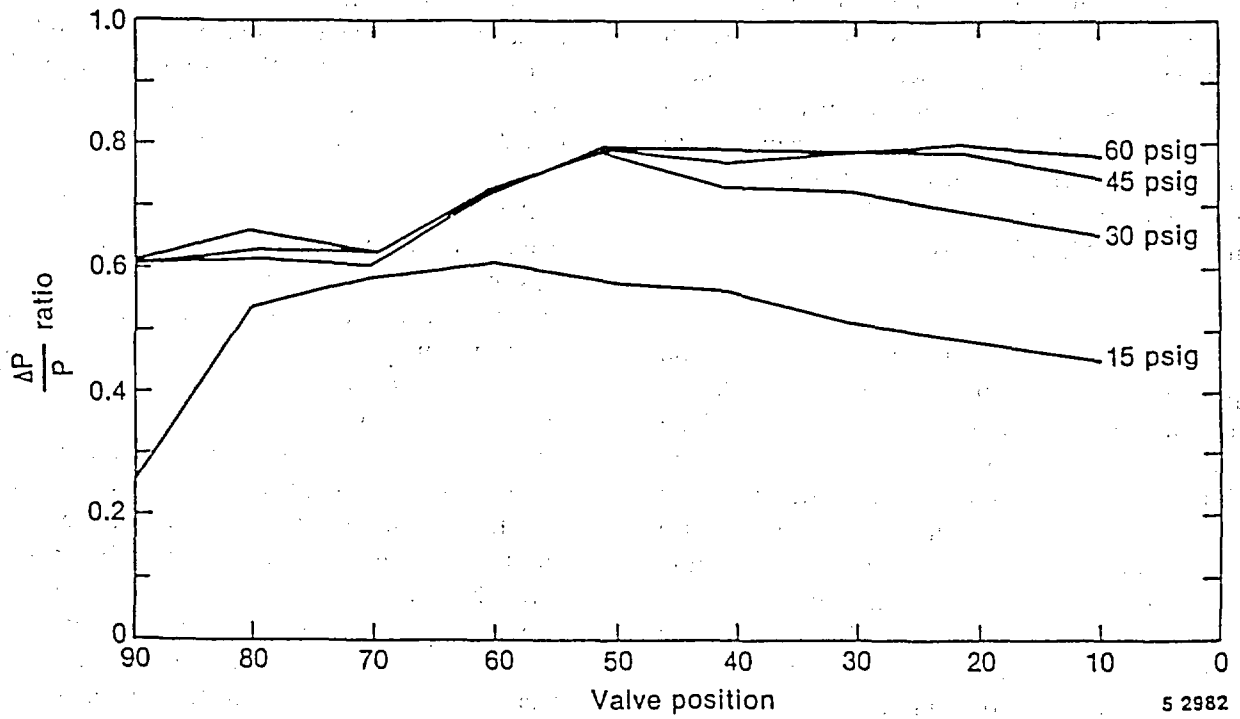


Figure 10. Butterfly valve differential pressure to upstream pressure ratio versus valve position.

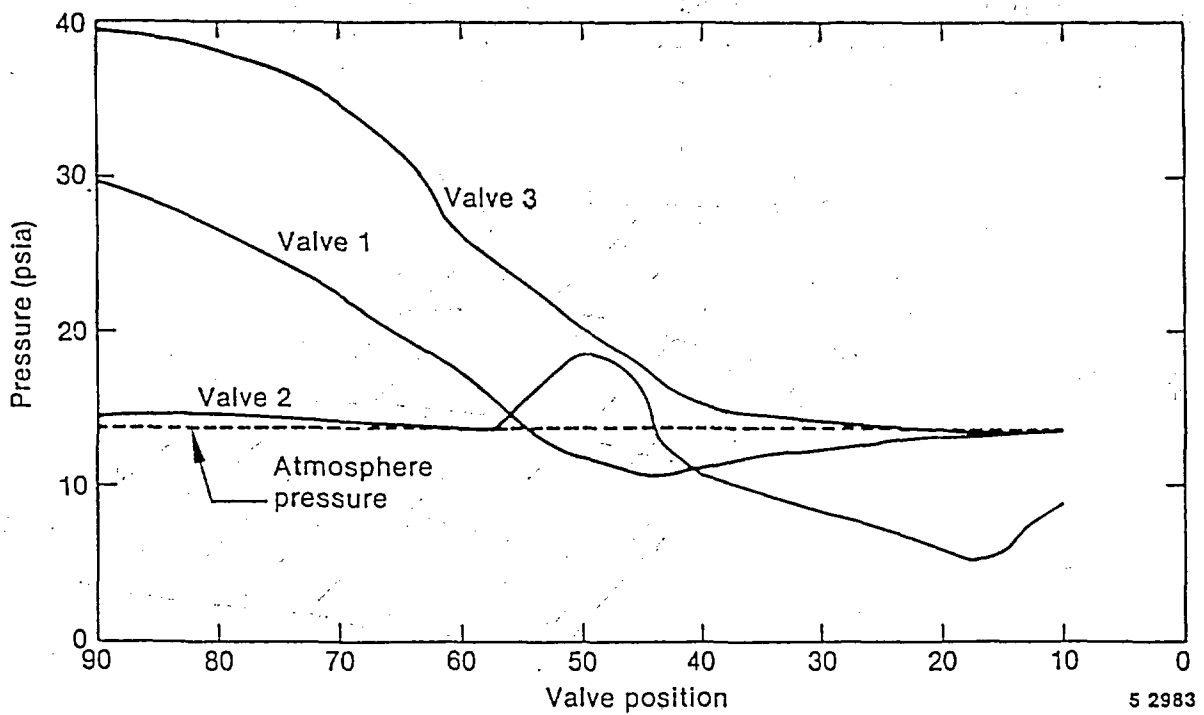


Figure 11. Static pressure 15 diameters downstream of a butterfly valve versus valve position.

Specific Observations

very different from that experienced during incompressible flow and very different for each of the valves tested. Specifically, the downstream pressure, as measured 15 diameters downstream of each test valve, did not always recover from the flow perturbation during certain portions of the valve closure cycle. This indicates that the measurement location was in a supersonic region.

These results suggest that torque extrapolation practices using the differential pressure do not account for supersonic flow downstream of the valve and its resulting effect on valve torque during a design-basis accident. Therefore, we introduced a new parameter (upstream pressure) and developed plots of valve response, relating valve upstream pressure, dynamic torque, and the position of the disc. Figures 12 through 17 are the response plots for the three valves tested in the uniform inlet flow configuration. The figures for the CFF orientation indicate a butterfly valve responding with a positive or self-closing torque. In this orientation, the operator must supply torque to keep the valve from shutting too rapidly. The figures for the FFF orientation indicate a butterfly valve responding with a negative or self-

opening torque. In this orientation, the operator must supply torque to close the valve. Therefore, butterfly valves in the FFF orientation will be harder to close, and butterfly valves in the CFF orientation will be harder to open.

Analysis of the response plots shows that the magnitude of the dynamic torque when the valve was in the CFF orientation (a positive response) was greater than the magnitude of the dynamic torque when the valve was in the FFF orientation (a negative response). Also, the positive dynamic torque curves of the three valves in the CFF orientation, as shown in Figures 12 through 14, are very similar in appearance. Conversely, the negative dynamic torque curves of the three valves in the FFF orientation, as shown in Figures 15 through 17, are very different in appearance. This provides some assurance that limited extrapolation is possible using the upstream pressure (rather than the pressure drop) across the butterfly valve if the valve is in the CFF orientation.

The peak torque for each of the three butterfly valves tested with a uniform inlet flow configuration was plotted against upstream pressure in Figures 18 through 20. The results indicate

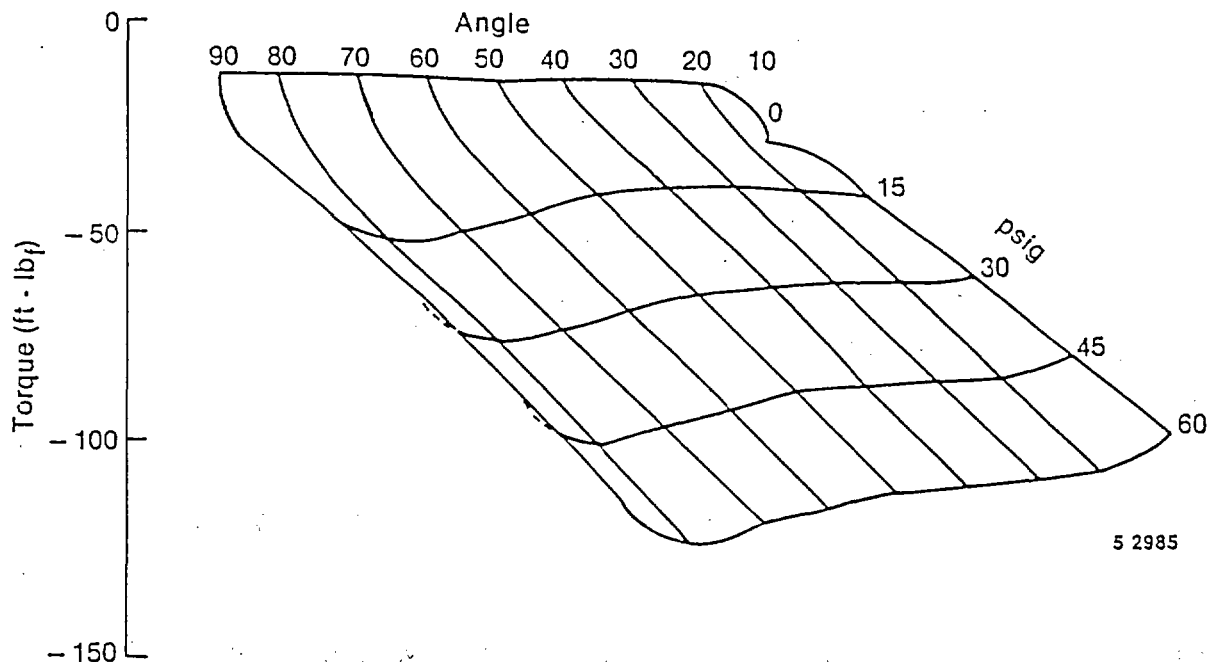


Figure 12. Torque versus upstream pressure and angle for Valve 1, the first 8-in. butterfly valve, FFF orientation.

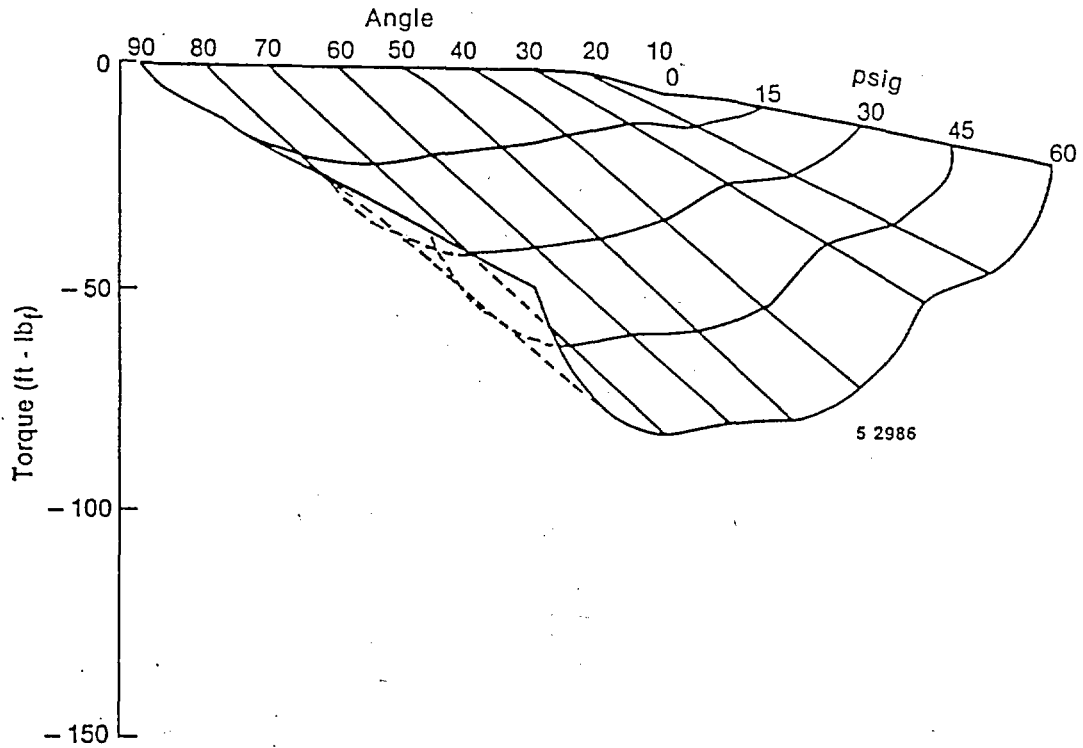


Figure 13. Torque versus upstream pressure and angle for Valve 2, the second 8-in. butterfly valve, FFF orientation.

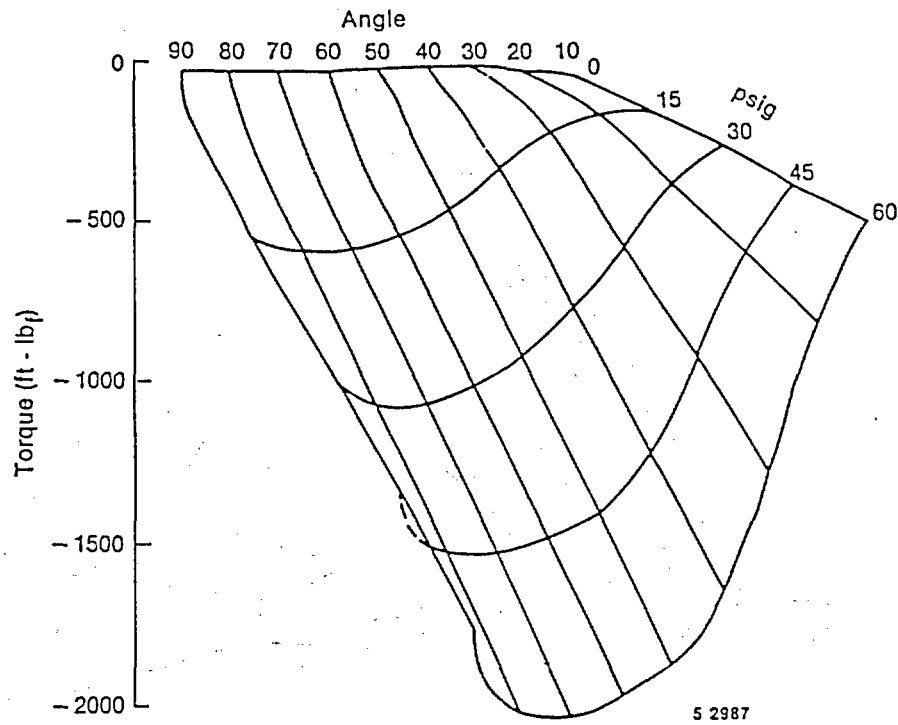


Figure 14. Torque versus upstream pressure and angle for Valve 3, the 24-in. butterfly valve, FFF orientation.

Specific Observations

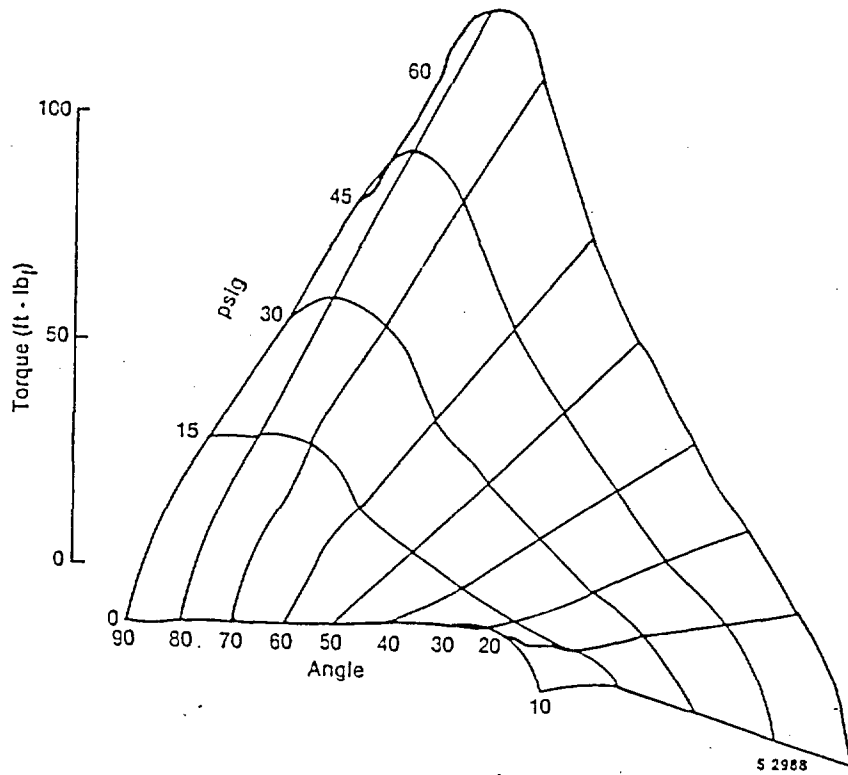


Figure 15. Torque versus upstream pressure and angle for Valve 1, the first 8-in. butterfly valve, CFF orientation.

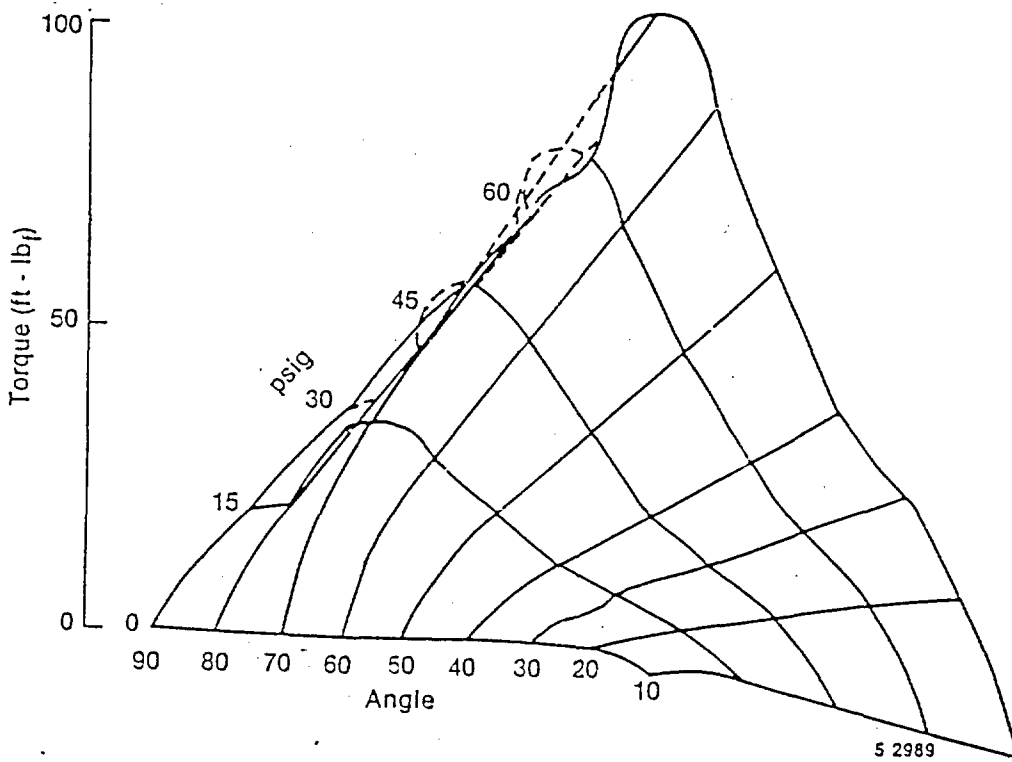


Figure 16. Torque versus upstream pressure and angle for Valve 2, the second 8-in. butterfly valve, CFF orientation.

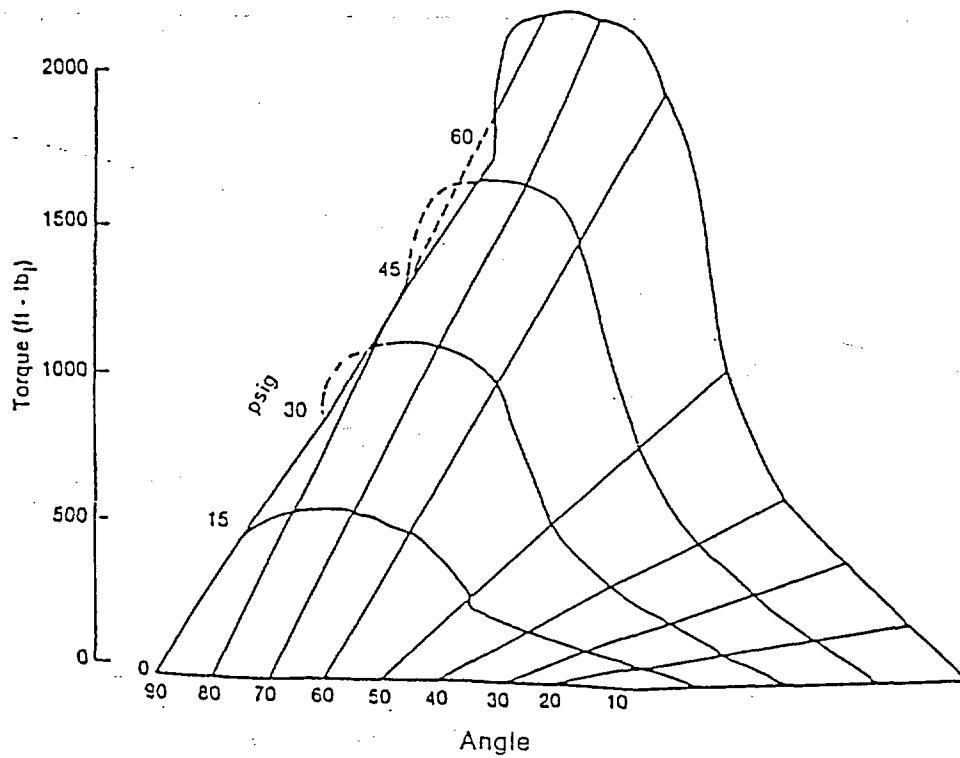


Figure 17. Torque versus upstream pressure and angle for Valve 3, the 24-in. butterfly valve, CFF orientation.

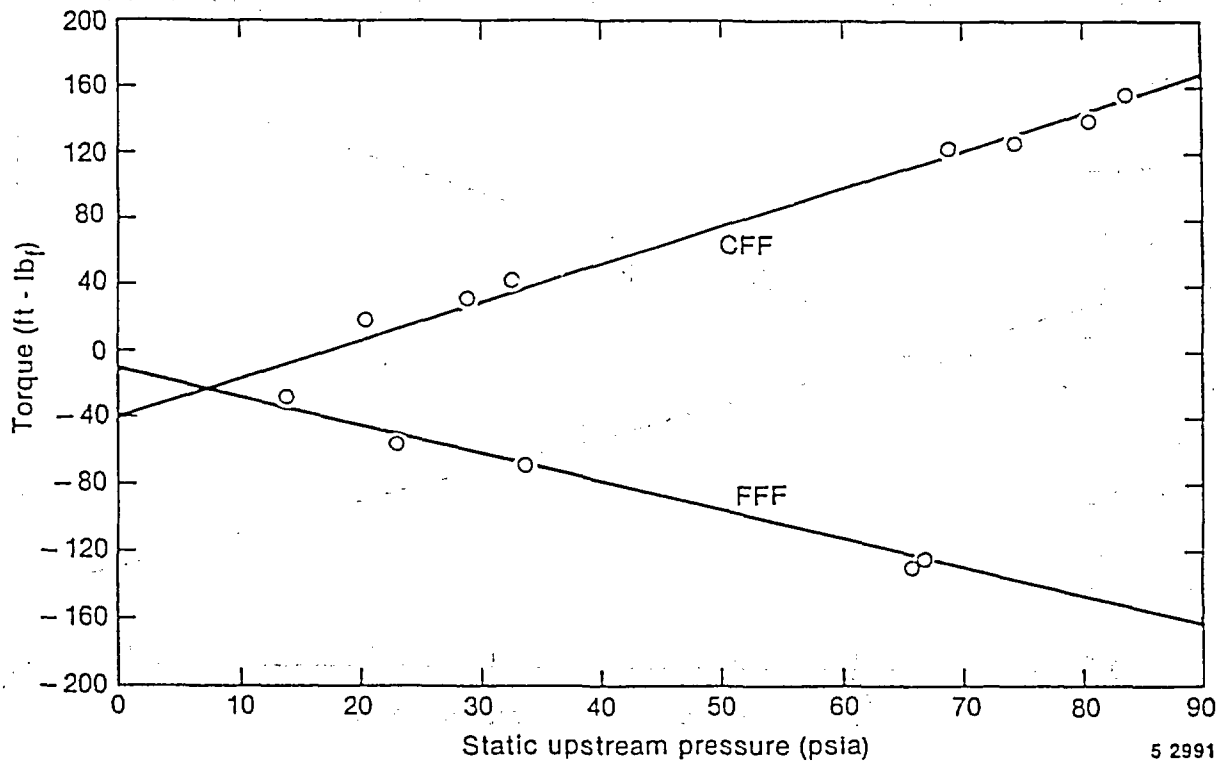


Figure 18. Peak torque versus static upstream pressure for Valve 1, the first 8-in. butterfly valve.

Specific Observations

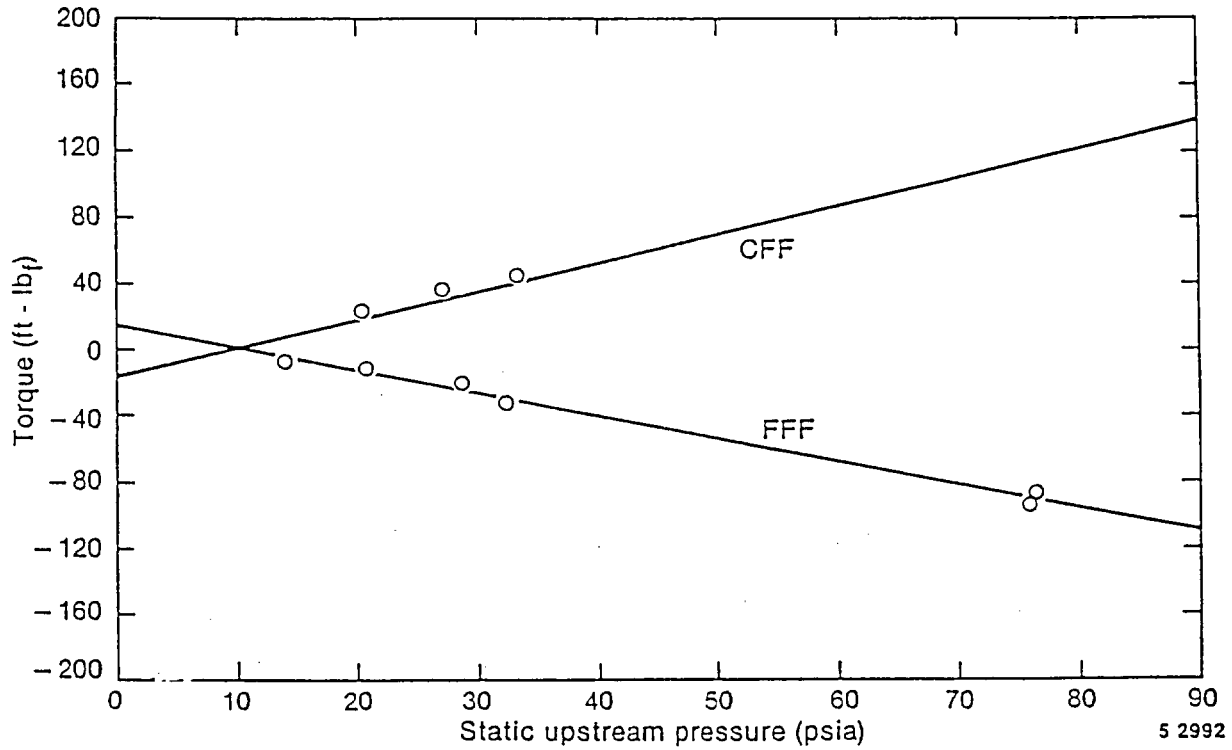


Figure 19. Peak torque versus static upstream pressure for Valve 2, the second 8-in. butterfly valve.

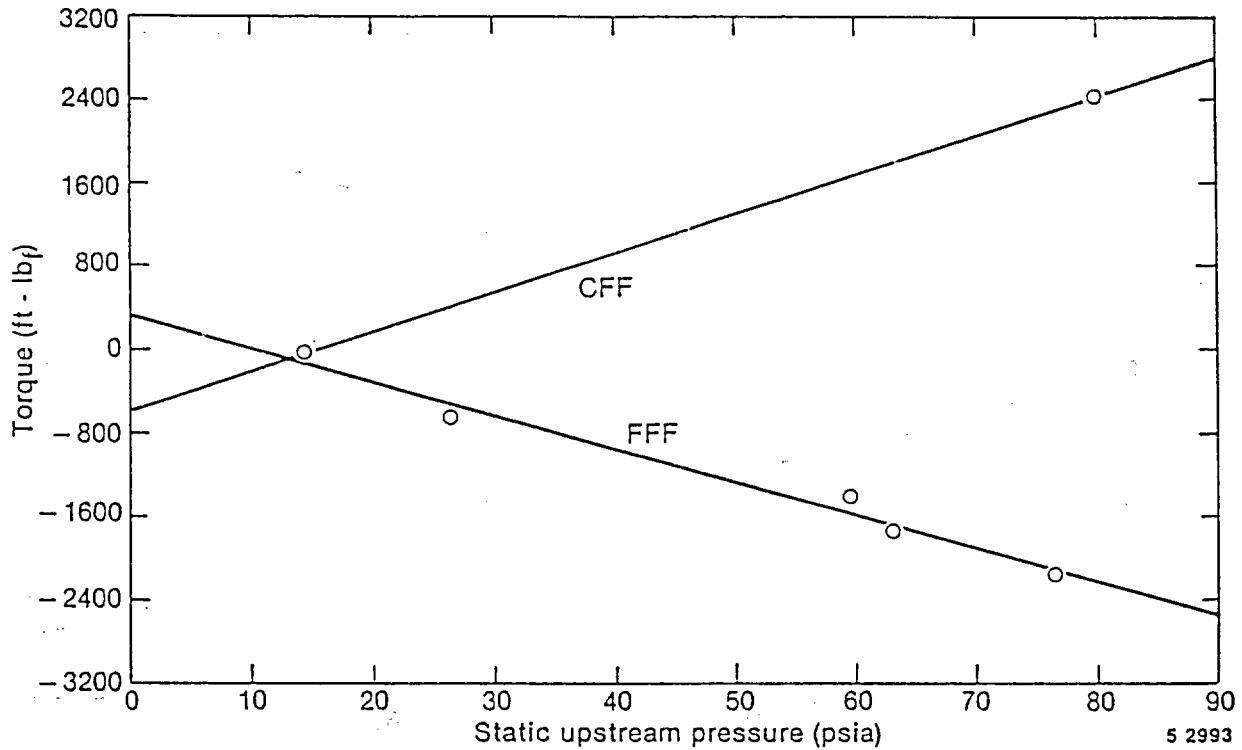


Figure 20. Peak torque versus static upstream pressure for Valve 3, the 24-in. butterfly valve.

that a linear relationship exists between the two parameters, although the angle where peak torque occurs varies with pressure. The fact that the response is linear reinforces the confidence that the response of a butterfly valve can be extrapolated using the upstream pressure.

The validity of a diameter ratio cubed term, as used in typical extrapolation relationships, was also evaluated. The dynamic torque of the 8- and 24-in. valves from the same manufacturer, with both valves in the CFF orientation, was compared from the fully open position (90 degrees) to near the fully closed position (20 degrees) at upstream pressures of 15, 30, 45, and 60 psig. The results of this evaluation are shown in Figure 21. The extrapolation exponent was always below 3 except for one position at an inlet pressure of 60 psig. These results indicate that use of an extrapolation exponent of 3 will result in the predicted torque of a larger valve being slightly greater than the actual torque, provided the inlet pressure does not exceed 60 psig. The trend of the data indicates that an extrapolation exponent of 3 could underpredict the actual torque of the larger valve at higher inlet pressures.

This evaluation was then repeated for tests with each valve in the FFF orientation. The results are shown in Figure 22. This evaluation indicates that the extrapolation exponent, when the flat face of the disc is facing upstream, with the valve fully closed, will frequently be above 3, ranging as high as 3.47 in these tests. Thus, using an extrapolation exponent of 3 could result in the predicted torque of a larger valve being less than the actual torque. To examine the effect the extrapolation exponent has on the estimated torque, we calculated torques for large valves, using an extrapolation of small-valve data and extrapolation exponents ranging from 2.8 to 3.5. The results are shown in Figure 23. This figure indicates that the torque requirements of a larger valve could be seriously underestimated if an extrapolation exponent of 3 is used when a larger exponent should be used. For example, if the torque requirements of a 42- to 48-in. valve were being predicted from the results of a 3- to 4-in. scale-model test valve, an extrapolation range on the order of 10 to 12, the torque of the larger valve could be underestimated by 50% or

more, if an extrapolation exponent of 3 is used instead of, for example, 3.2.

Consequently, a diameter-ratio-cubed formulation appears justified if (a) torques are obtained with the scale-model test valve oriented with the curved face of the disc facing upstream when the butterfly valve is fully closed, and (b) the upstream pressure does not exceed 60 psig. We developed the following equations to more consistently envelop the response of a larger valve based on the response of a smaller scale-model test valve. Note that, in the CFF orientation, the bearing torque (the torque that must be supplied to move the valve disc against the resistance of the bearings and seal only) and the dynamic torque (the torque that must be supplied to move the valve disc against the resistance of the flowing fluid only) are acting in opposite directions, the dynamic torque assisting valve closure and the bearing torque resisting it. Either equation can be used, depending on the information available (i.e., whether the total and bearing torques or just the dynamic torque of the smaller scale-model test valve is known). In either case, an estimate of the bearing torque of the larger valve must be known.

$$T_{t, \ell} = \frac{D_{\ell}^3}{D_s^3} T_{d, s} - T_{b, \ell} \quad (1)$$

$$T_{t, \ell} = \frac{D_{\ell}^3}{D_s^3} (T_{t, s} - T_{b, s}) - T_{b, \ell} \quad (2)$$

where

T_t	=	valve total torque (dynamic + bearing torque)
ℓ	=	a parameter of the large valve
D	=	valve diameter
s	=	a parameter of the small, scale-model test valve
T_d	=	valve dynamic torque only
T_b	=	valve bearing torque only

Specific Observations

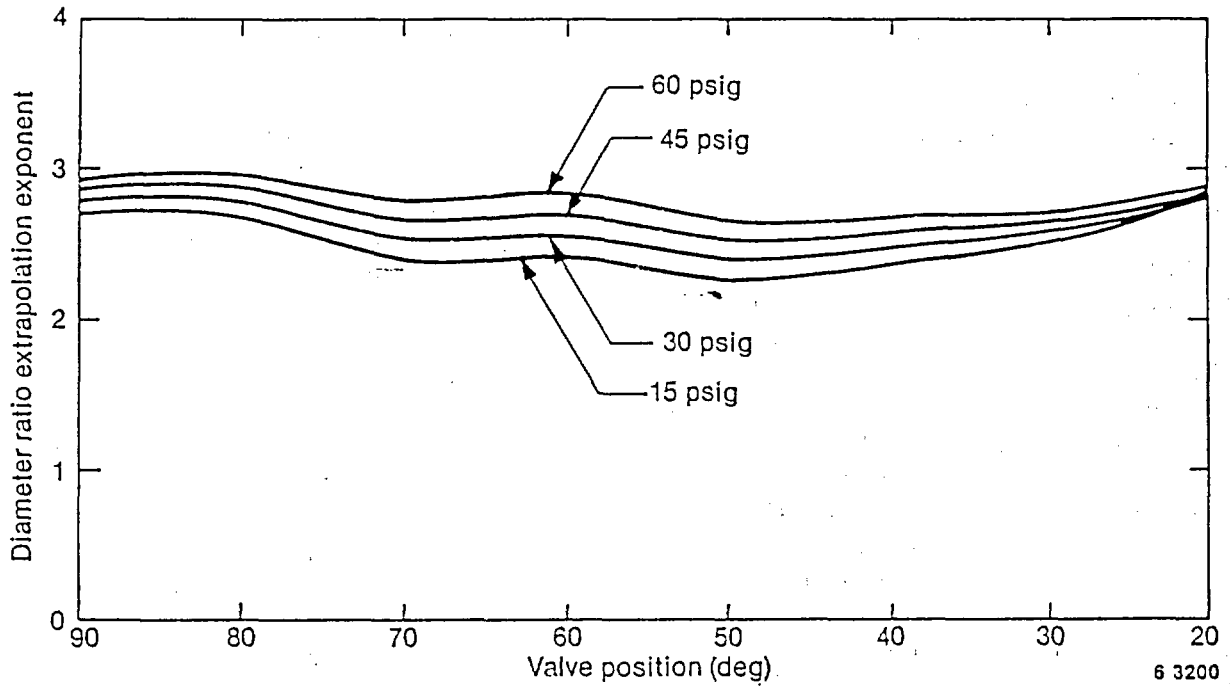


Figure 21. Extrapolation exponent, butterfly valve oriented with the curved face of the disc facing upstream.

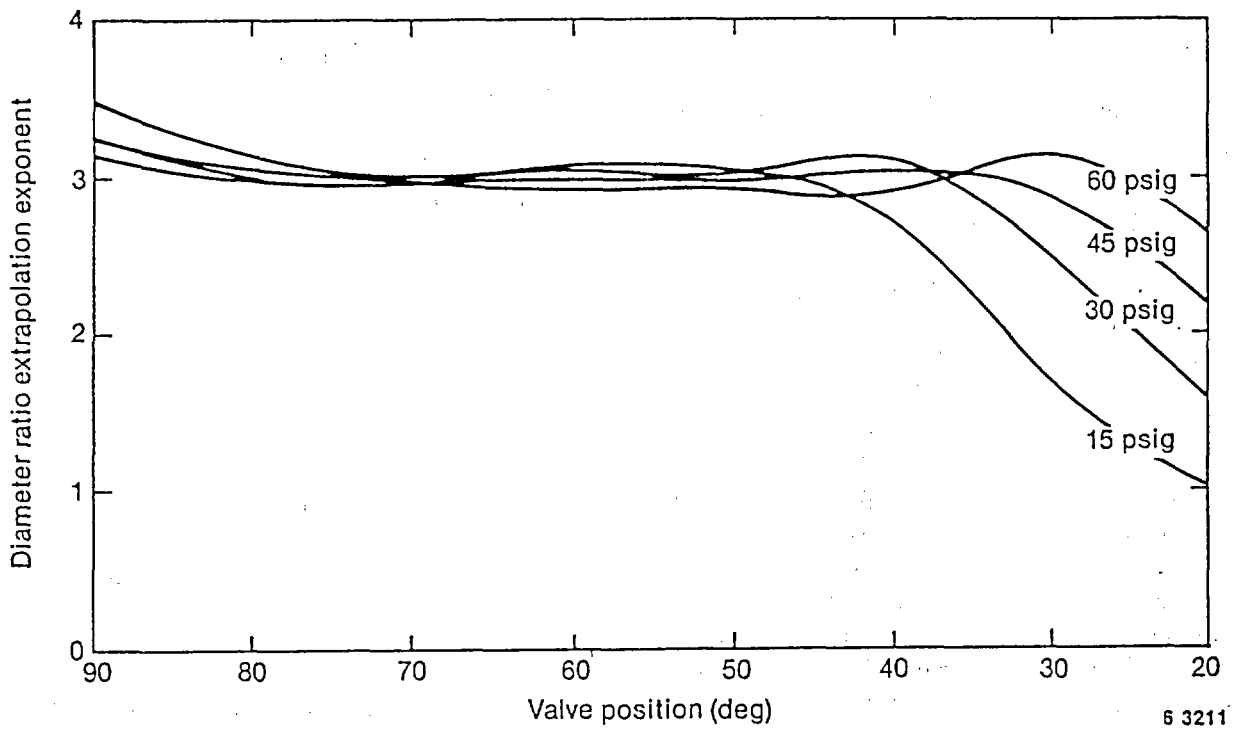
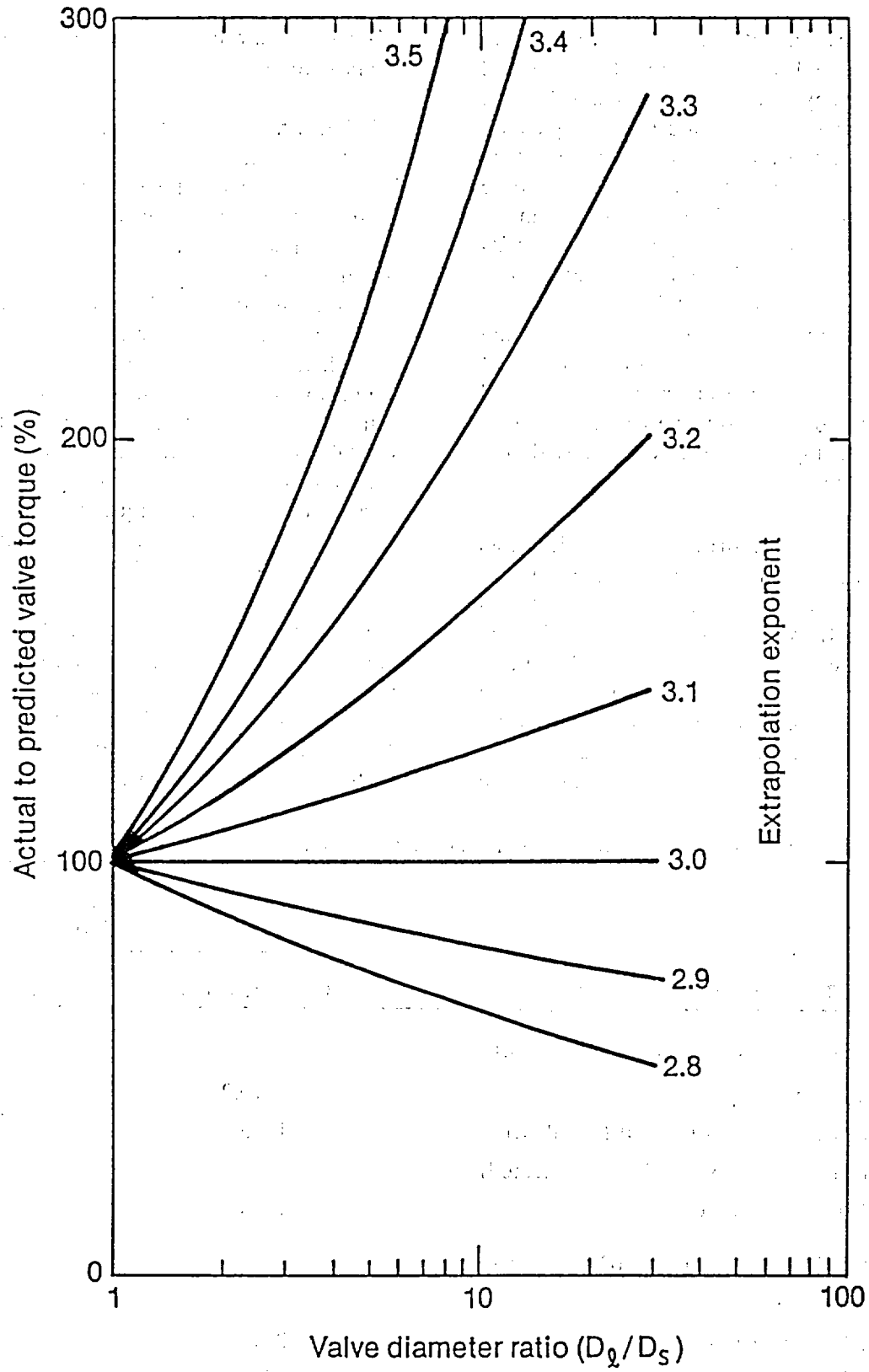


Figure 22. Extrapolation exponent, butterfly valve oriented with the flat face of the disc facing upstream.



6 3201

Figure 23. Actual to predicted butterfly valve torque (percent) as a function of extrapolation exponent versus valve diameter ratio.

Specific Observations

A comparison between the results of the method presented here and the results of a method typically used by industry is presented in Table 1. This table also provides a direct comparison between the test results from this program and the methods used by industry to predict the torque requirements of a 24-in. butterfly valve from the test results of an 8-in. butterfly valve. The results indicate that, as expected, torque extrapolations performed with test data obtained from a valve oriented with the curved face of the disc facing into the flow will bound the torque demands of either orientation. However, extrapolations based on the results from a test valve with the flat face of the disc facing into the flow typically do not bound the data.

We then used the proposed technique, as reflected in Equation (1), to predict the response of a 48-in. butterfly valve using both the 8- and 24-in. butterfly valves as the scale-model test valves. The results, shown in Figure 24, indicate some differences between the two 48-in. valve predictions. However, the extrapolations for 8-in. to 48-in. valves generally result in higher (more conservative) values than the extrapolations from

24-in. to 48-in. valves. This is particularly true for the peak torque.

3.2.6 Effect of an Upstream Elbow on the Torque Requirements of a Butterfly Valve. We also investigated the effects of system upstream geometry on the closing torque requirements of a butterfly valve. We compared the test results for valves located immediately downstream of an elbow to the results with uniform inlet flow. (The valves were installed as close as possible to the elbows in order to expose them to the maximum nonuniform flow anticipated in an actual installation.) The peak torque at 60 psig was tabulated for all three valves in each of the six orientations tested. These torques were then normalized to the peak torque at 60 psig for each valve in the uniform flow CFF orientation and tabulated for easy comparison (Table 2).

Using this table, we can assess the effect non-uniform inlet flow relative to uniform inlet flow has on valve torque. The worst-case elbow effect was noted for one of the 24-in. valve orientations, 1.33 times the uniform inlet torque. This was followed closely by one of the 8-in. valve

Table 1. Comparison of torque prediction methods butterfly versus valve orientation.

Torque prediction method	Torque (ft-lb _f)	
	CFF orientation	FFF orientation
Predicted 24-in. valve torque at 90° and 60 psig		
Actual 8-in. valve torque	70.2	-52.1
Predicted 24-in. valve torque (INEL method)	1895	-1895
Predicted 24-in. valve torque (Industry method)	1895	-1407
Actual 24-in. valve torque	1754	-1828
Predicted 24-in. valve torque at 80° and 60 psig		
Actual 8-in. valve torque	99.2	-58.0
Predicted 24-in. valve torque (INEL method)	2373	-2373
Predicted 24-in. valve torque (Industry method)	2984	-1875
Actual 24-in. valve torque	2257	-1986

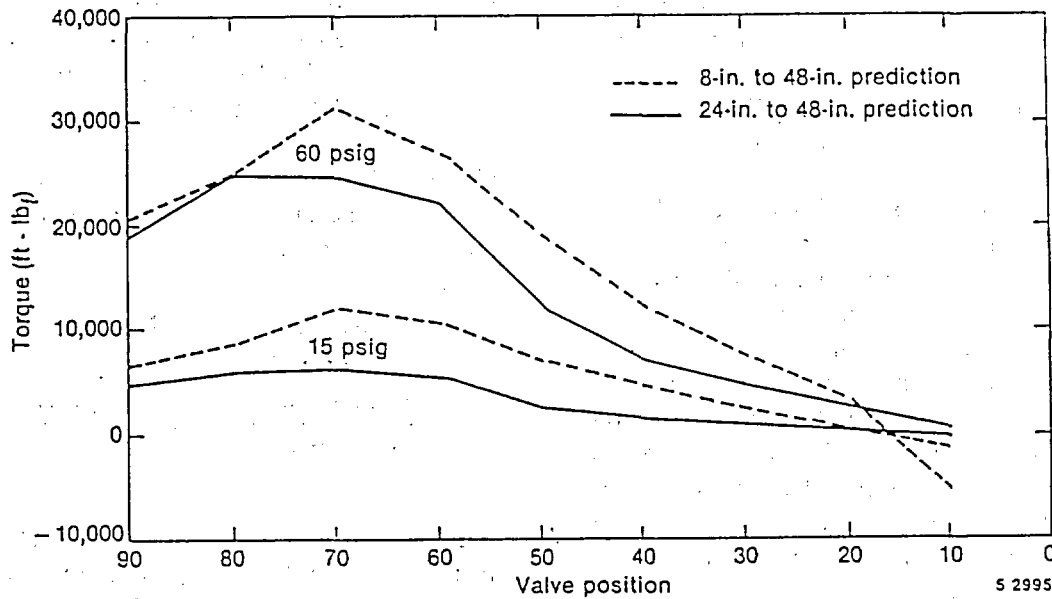


Figure 24. Predictions for a 48-in. butterfly valve based on extrapolating the torques of an 8-in. and a 24-in. butterfly valve at upstream pressures of 15 and 60 psig.

Table 2. Ratio of peak torque to uniform flow peak torque for a butterfly valve in the CFF orientation.^a

Valve position	Valve 1	Valve 2	Valve 3
FFF	1.06	0.81	0.94
CFF	1.00	1.00	1.00
FFF-CCW	0.90	0.83	1.33
CFF-CCW	1.29	1.00	1.04
FFF-CW	1.02	0.84	0.87
CFF-CW	1.14	0.95	0.92

a. Valve position identification is given in Figures 7 and 9.

orientations, which was 1.29 times the uniform inlet torque. Based on these results, the maximum torque expected from a nonuniform inlet flow configuration can be bounded by using 1.5 times the torque from the uniform inlet flow configuration, if the curved face of the disc is facing upstream when the valve is fully closed.

Next, a valve response plot was developed (Figure 25) for the 24-in. butterfly valve in the CFF orientation, with the shaft of the valve perpendicular to the plane of an upstream elbow. The similarity of the shape of this response plot to the response plot of the same valve without an upstream elbow (Figure 17) is clear. This comparison suggests that, although the torques resulting from a nonuniform inlet flow configuration may be higher, the response can still be bounded with a factor of 1.5 times the torque from the uniform inlet flow configuration, if the curved face of the disc is facing upstream when the valve is fully closed.

Finally, Figure 26 compares the linearity of the peak torque versus inlet pressure for the 24-in. butterfly valve with and without an upstream elbow. Generally, the torque in the presence of an upstream elbow is higher, but the response remains linear. This comparison provides added confidence that the results of the nonuniform inlet flow configuration can be bounded.

This study has shown a weakness in the industry's extrapolation procedures for butterfly valves closing against a compressive fluid. The industry (a) has not identified a dominant orientation for the small valve to be tested in, (b) has used differential pressure (which is influenced non-conservatively by downstream pressure) instead of upstream pressure, and (c) has not identified the effect that the upstream piping geometry has on the torque requirements of these valves, all of which were shown to be important. Most butterfly valve vendors are aware of the NRC test program, but it is not known to what extent they have incorporated the test results into their proprietary calculations. It is known that most large purge-and-vent valves are either closed or blocked at small angles of opening and that all purge-and-vent valves required plant submittals and NRC

Safety Evaluation Reports (SERs) in response to Three-Mile Island Action Plans NUREG-0660 and NUREG-0737 (NRC, 1980a; NRC, 1980b). A large percentage of the purge-and-vent valves were reviewed before these test results were available, and the status of purge-and-vent valves replaced in the last five years is not known. Generic Letter 89-10 will not cause many re-reviews, because many purge-and-vent valves are not motor operated.

3.3 Assessment of Wedge-Gate Valves Closing against Medium to High Flow Conditions

Flexwedge gate valves were tested in two NRC test programs referenced earlier in this report; those tests were reported in NUREG/CR-5406 (DeWall and Steele, 1989) and NUREG/CR-5558 (Steele et al., 1990). The latter was published in support of Generic Issue 87. After that report was published, we developed a technique to (a) bound the stem force of a 5-degree flexwedge gate valve closing against medium to high flow conditions, and (b) validate a low differential pressure closure test and then bound the stem force of a flexwedge gate valve closing against design-basis conditions.

In the two test programs mentioned above, the authors tested six valves with a total of seven different internal designs. One valve was tested with two different discs, one with hardfaced disc guides (Valve B Phase I), and one without hardfaced guides (Valve 2 Phase II). Under the high loadings encountered during the testing of this particular valve, there was no difference in the performance of the two discs.

The valves were tested under a broad range of fluid conditions and flow rates, from normal system flows to design-basis line break flows. Initial conditions for each valve tested are shown in Tables 3 and 4. These conditions were established before the normal system flow isolation and the design-basis flow isolation portions of each test. Two of the valves, including the valve

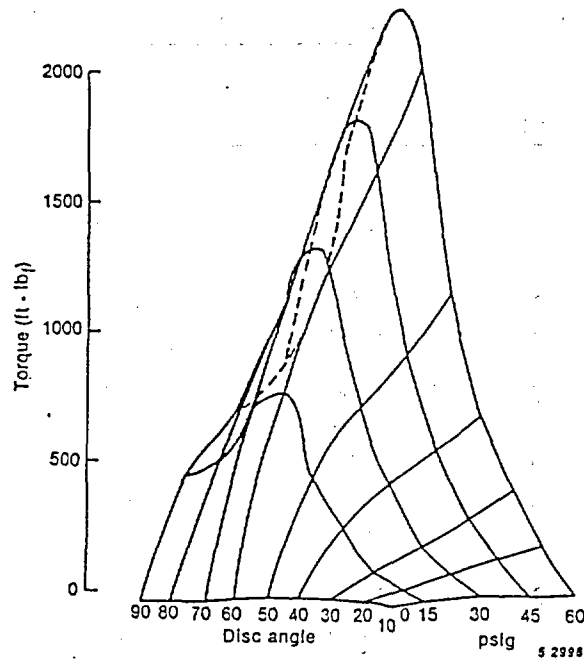


Figure 25. Torque versus upstream pressure and angle for Valve 3, the 24-in. butterfly valve in the CFF orientation.

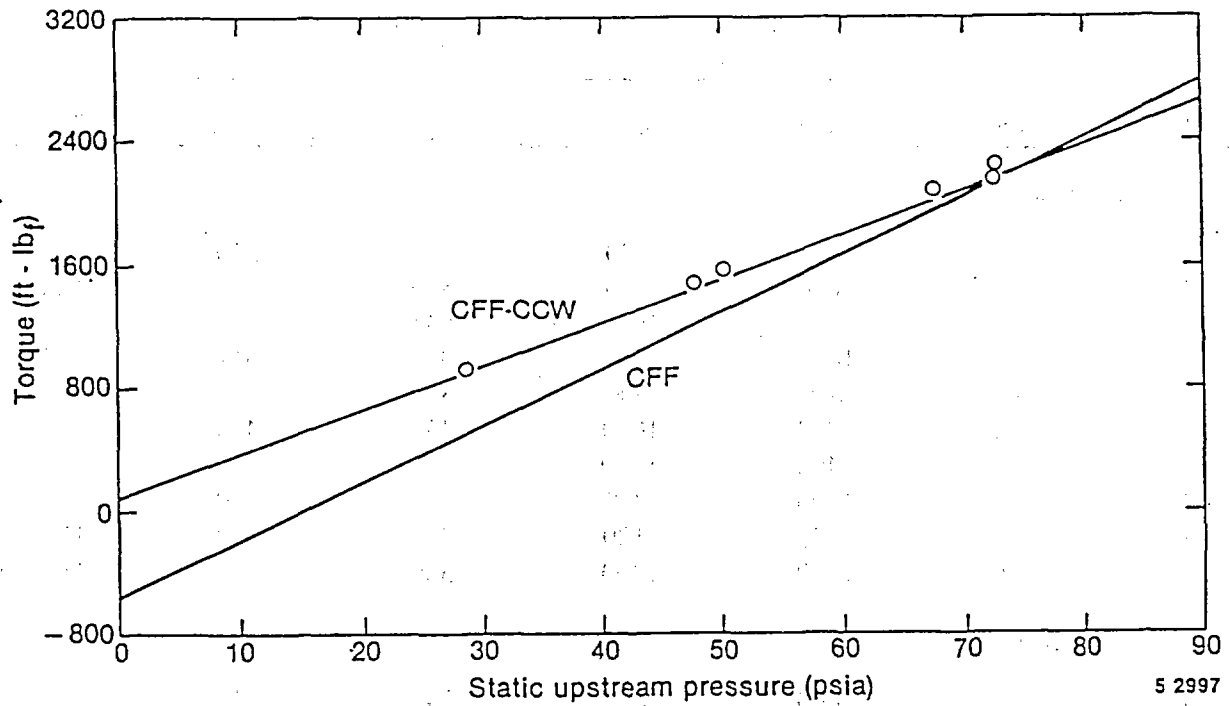


Figure 26. Peak torque versus static upstream pressure for Valve 3, the 24-in. butterfly valve, comparing the response of the peak torque with elbow and peak torque without elbow orientations.

Specific Observations

Table 3. Phase I gate valve flow interruption test temperatures and pressures.

Valve	Test	Pressure (psia)	Temperature (°F)	Test media
A	2	1000	530	Hot water
A	3	1000	480	Hot water
A	4	1000	400	Hot water
A	5	1400	580	Hot water
A	6	1400	530	Hot water
A	7	1400	450	Hot water
A	8	600	480	Hot water
A	9	600	430	Hot water
A	10	600	350	Hot water
A	11	1000	530	Hot water
B	2	1000	530	Hot water
B	3	1400	580	Hot water
B	4	600	480	Hot water
B	5	1000	530	Hot water

Table 4. Phase II gate valve flow interruption test temperatures and pressures.

Valve	Test	Pressure (psig)		Temperature (°F)		Test media
		Target	Actual	Target	Actual	
6-in. Valve Tests						
1	1	1000	900	530	520	Hot water
2	1	1000	950	530	520	Hot water
2	2	1000	1040	545	550	Steam
2	3	1000	750	<100	<100	Cold water
2	6a	600	600	300	450	Hot water
2	6b	1000	1000	430	470	Hot water
2	6c	1400	1300	480	520	Hot water
3	1	1000	920	530	520	Hot water
3	5	1200	1100	550	550	Hot water
3	7	1400	1300	580	570	Hot water
10-in. Valve Tests						
4	1	1000	750	545	510	Steam
5	1a	1000	800	545	520	Steam
5	1b	1400	1040	590	550	Steam
6	1a	1000	990	545	580	Steam
6	1b	1400	1400	590	590	Steam
6	1c	1200	1100	570	550	Steam

that was tested with two discs, performed in a manner we have called predictable. A predictable valve is one that does not exhibit evidence of internal damage during testing. In such valves, the highest stem forces occur when the disc is riding on the valve body seats just before wedging. Conversely, an unpredictable valve exhibits evidence of internal valve damage during testing, characterized by an erratic, sawtooth-shaped stem force response. In such valves, these high stem-force requirements typically occur while the disc is riding on the guides rather than just before wedging. Generally speaking, the results from testing unpredictable valves are not useful for the kind of evaluation described here. However, through selective analyses, we were able to include some of the results from two unpredictable valves, not while the disc was riding on the guides, but after the disc had transitioned to riding on the valve body seats.

We initially evaluated the test results with the standard industry gate-valve stem-force equation. Although some of the manufacturers modify the variables in these equations slightly, the application of the equations is basically the same.

$$F_{t, Industry} = \mu_d A_d \Delta P \pm A_s P + F_p \quad (3)$$

Later in the program after we developed the INEL correlation, the Nuclear Maintenance Assistance Center (NMAC) equation was released. We also evaluated that equation, which follows:

$$F_{t, NMAC} = \frac{F_w \pm F_p - A_s P \pm \frac{\mu A_{orifice} \Delta P}{\cos \theta \pm \mu \sin \theta} \pm F_s}{1 - \frac{\mu_t FS}{r_t}} \quad (4)$$

where

- F_t = stem force
- μ_d = disc factor
- A_d = orifice area

- ΔP = differential pressure across the valve
- A_s = area of the stem
- P = pressure upstream of the valve
- F_p = packing drag force
- F_w = disc and stem weight
- μ = dynamic coefficient of friction between disc and seat
- $A_{orifice}$ = disc area on which pressure acts
- θ = seat angle (degrees from stem axis)
- F_s = sealing force (wedging force only)
- μ_t = friction factor at torque reaction surface
- FS = stem factor
- r_t = distance to torque reaction surface.

For wedge-type gate valves, the industry has historically used a disc factor (μ_d) of 0.3; more recently, they sometimes specified a more conservative disc factor of 0.5. The disc factor acts in conjunction with the disc area and the differential pressure; the three multiplied together represent the largest component in the stem force equation. However, the disc area used in the area term is not uniformly applied throughout the industry. The area is based on the orifice diameter by some manufacturers, on the mean seat diameter by others, or even on the orifice diameter times one or more factors to artificially enlarge the area on which the differential pressure acts. We used a disc area based on the orifice diameter when we evaluated the standard industry stem force equation, because it represents the least conservative use of the term by the industry. This results in a lower estimate of required stem force than the other disc area terms.

Specific Observations

It is important to emphasize that the use of one disc factor over another, or the comparison of one disc factor to another, depends heavily on the disc area assumed. In other words, a disc factor developed empirically with the mean seat area will be lower and, thus, cannot be used to estimate the stem force using the orifice area. Likewise, the point in the closing cycle at which a disc factor is determined is also of great importance. A disc factor determined from the closing thrust history prior to total flow isolation will underestimate the isolation stem force if any extrapolation is necessary. The disc factor should be defined at flow isolation, just before wedging.

For the standard industry equation, the estimated stem force is always a positive value, and it is up to the analyst to differentiate between the force to open a valve and the force to close a valve. As a result, the stem rejection force must be represented as a positive value if the valve is closing and as a negative value if the valve is opening. This is because the stem rejection force always acts in an outward direction relative to the valve body, resisting valve closure and assisting valve opening. The packing force is always represented as a positive value because it always opposes motion. It is typically assumed to be constant for a given valve, but it varies from valve to valve, depending on the packing design and the packing gland nut torque.

For the NMAC equation, a dynamic coefficient of friction of 0.35 to 0.50 is recommended. More specific guidance is not given. At the time we initiated our study, the disc area term in the NMAC equation was labeled A_{orifice} and defined as the area on which pressure acts. The exact meaning of this term was not clear, but we initially used the orifice area in our assessment of the NMAC equation. Unlike the industry equation, however, the estimated stem force is represented as a negative value for closing and as a positive value for opening. The packing force, the force due to the differential pressure across the disc, and the sealing force can be either positive or negative, depending on whether the valve is opening or closing. The weight of the disc and stem acts in an inward direction relative to the valve body, so it is always positive. The stem

rejection force acts in an outward direction, so it is always negative.

Comparisons of the standard industry equation, Equation (3), with selected test results are shown in Figure 27. This figure presents the results of the same valve isolating a break at a common upstream pressure of approximately 1000 psig, but with the fluid at various degrees of subcooling. The subcooling ranges from none (steam) to approximately 400°F (cold water) with intermediate values of 10°F and 100°F. The recorded stem force is shown as a solid line; two calculations of the stem force history, using the industry equation and real time test data with standard industry disc factors of 0.3 and 0.5, are shown as dashed lines. This figure shows that, at flow isolation, each test required more force to close the valve than would be estimated using the standard industry disc factor of 0.3. In fact, for the tests shown on this figure, the more conservative industry disc factor of 0.5 ranges from acceptable (the steam test) to marginally acceptable (the 10°F subcooled fluid test) to unacceptable (the 100°F and the 400°F subcooled fluid tests). Note that, although the results of the industry equation are presented over the entire closure cycle, the equation represents a bounding estimate of the maximum stem force. Therefore, only the estimated stem force at the final horizontal line, just before wedging, is applicable. The results are presented for the entire closure to aid in identifying trends in the recorded stem force, not to assess the equation throughout the closure cycle. Note also that, although the same valve and operator were used for each test, the closure durations are different. Because of facility inventory limitations, some of the tests were initiated with the valve partially closed.

It is also interesting to note that the shape of the recorded stem force from flow initiation to flow isolation varies, depending on the degree of subcooling of the fluid. In tests with greater subcooling, the stem force during the initial portion of the closure is lower. In fact, during the test with cold water, the stem force trace was initially positive (i.e., the valve was self closing during this portion of the closure). However, just before

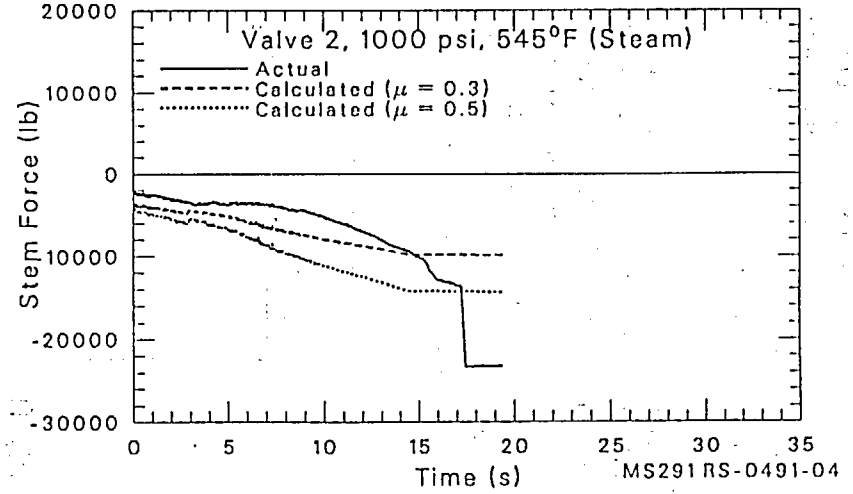
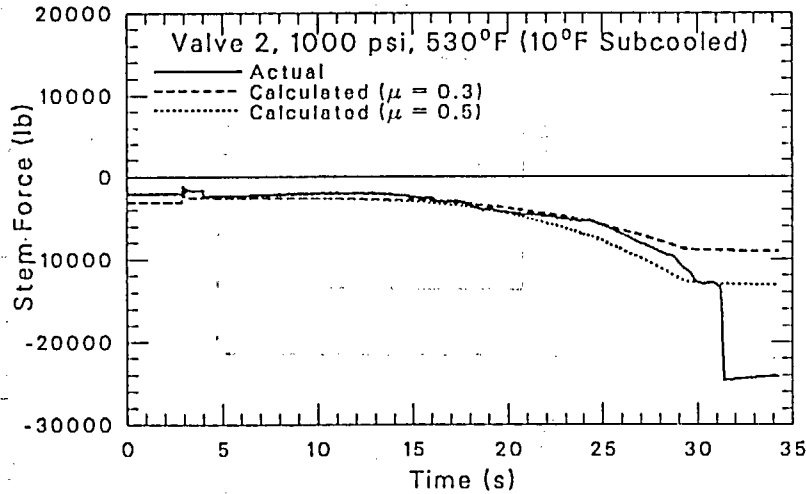
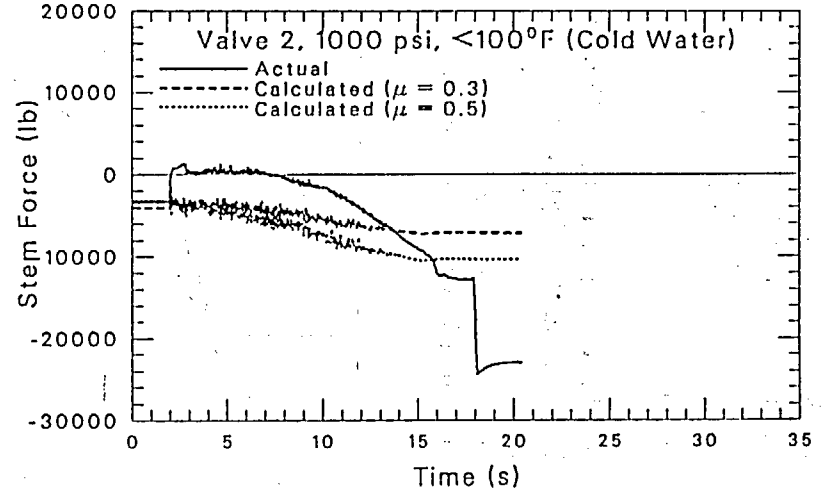
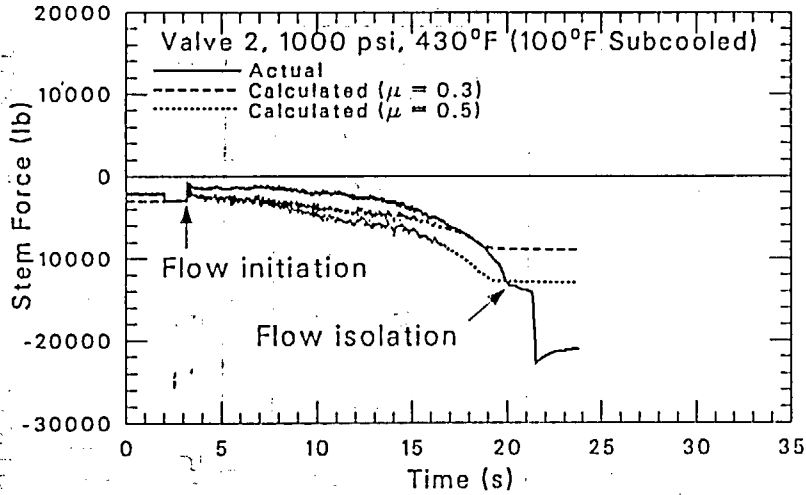


Figure 27. Comparison of the standard industry gate valve stem force equation with selected test results.

Specific Observations

wedging, the required stem force is generally higher in tests with greater subcooling of the fluid so that closure against cold water requires more force than closure against steam.

A comparison using the NMAC equation, Equation (4), is shown in Figure 28. In general, the estimated stem force using this equation is very similar to the estimated stem force using the industry equation. The trends in the stem force trace during a valve closure are also similar. As with the standard industry equation, the NMAC

equation represents a bounding estimate of the maximum stem force. The results of the NMAC equation were presented for the entire closure to aid in identifying trends in the recorded stem force, not to assess the equation throughout the closure cycle.

3.3.1 Assessment of the Disc Factor Term in the Industry Equation. As we studied the test results and analyzed the industry equation, it became increasingly evident that the disc factor or friction factor used in the equation was not well

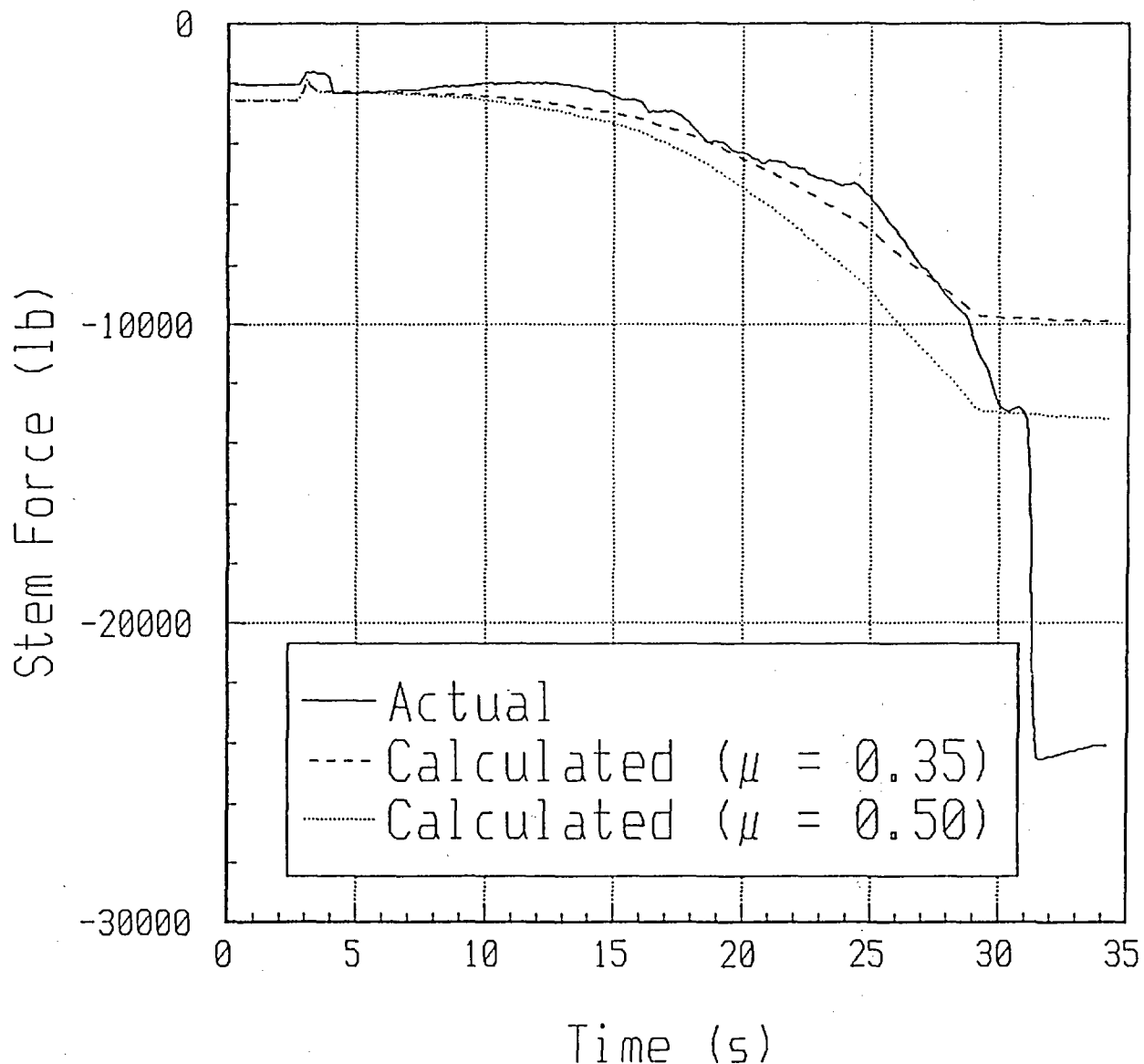


Figure 28. Comparison of the NMAC gate valve stem force equation with selected test results.

understood. It appeared that the disc factor depended on parameters not currently being accounted for, such as the subcooling of the fluid. Thus, we examined the equation in more detail, specifically the disc factor term as currently defined. To perform this evaluation, we used both the design-basis and applicable parametric testing to determine what influence pressure and fluid properties, such as subcooling, had on the required stem force of a valve.

If all of the parametric studies could have resulted in just one parameter being varied, then the tests could have been compared to each other to determine the effect of that one parameter (e.g., fluid properties). That was not the case, however. It was impossible to provide such precise temperature and pressure control at the valve. This, along with other facility limitations, such as the total system supply volume, resulted in tests that cannot be compared to one another without some type of normalization.

We normalized the test results using Equation (3) by solving for the disc factor. This was possible because we knew the stem force, the system pressure, and the valve differential pressure throughout the closure cycle. The resulting equation used in this evaluation was

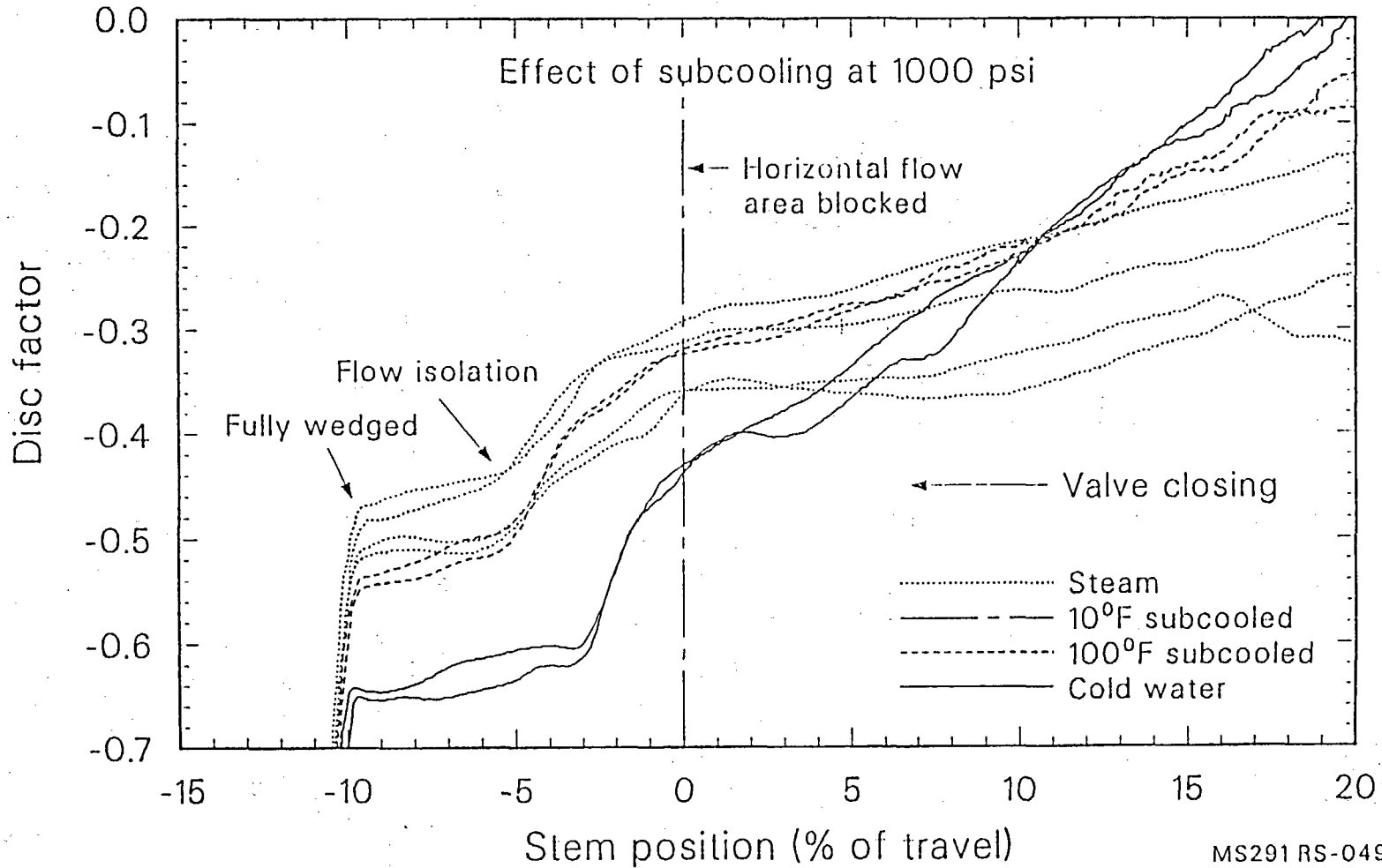
$$\mu_d = \frac{F_t - A_s P - F_p}{A_d \Delta P} \quad (5)$$

The results of a typical comparison are shown in Figure 29, where there are two closures at each fluid condition. The plot is read from right to left as the valve closes. As time increases, the disc factor increases in the negative convention (indicating valve closure) and is plotted against stem position. The zero stem position represents that point in the valve closure where the horizontal visual area is blocked. Recognize, however, that, although the visual area is blocked, fluid can still flow under the disc and through the valve. At this point, the disc area term in Equation (5) becomes constant. From the zero stem position to the minus 10% stem position, the stem travel involves full seat contact, flow isolation, and finally wedging. The forces maximize about the

-5% travel position. The slight slope on the plateau between -5% and the -9% stem travel is the result of valve inlet pressure increasing slightly with flow isolation. The plateau region represents the disc factor after flow isolation. Two observations can be made from Figure 29: (a) the absolute magnitude of the disc factor for any fluid condition exceeds a 0.3, and (b) the valve response is affected by fluid properties, steam having the lowest disc factor and cold water having the highest disc factor. The fluid-properties effect is evident throughout the closure cycle but is most pronounced on the plateau region, when the forces resisting closure have essentially stabilized. This effect is contrary to what was expected; one would expect water to be a better lubricant than steam. The industry equation and the NMAC equations do not contain terms for fluid properties effects.

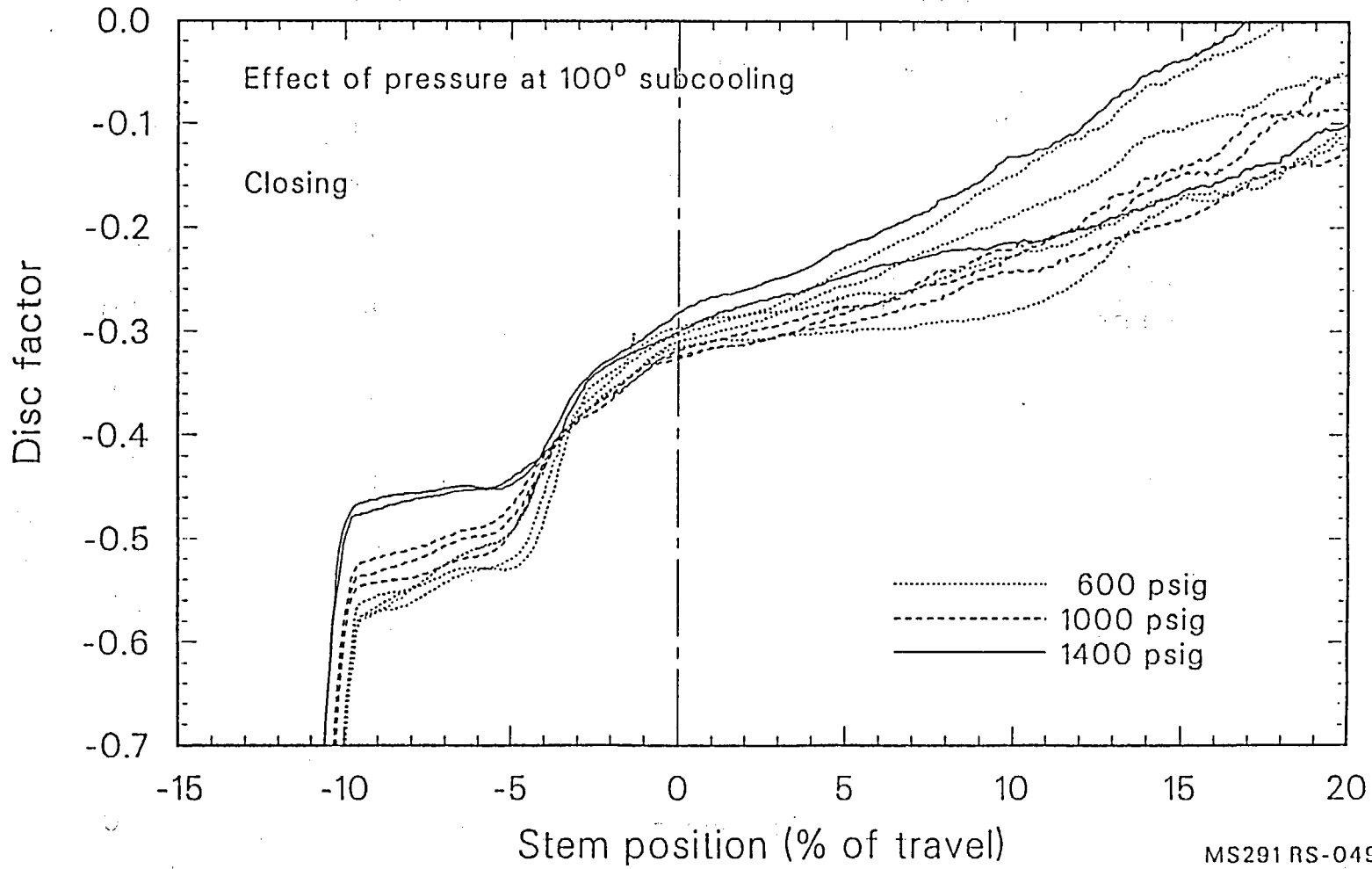
Our next effort was to determine if the disc factor was dependent on pressure. Figure 30 shows a comparison for Valve 2 using six parametric tests where the fluid properties remained constant but the pressure was varied. Although the disc factor did not exhibit a significant pressure dependency at the zero stem position, it did from the minus 5% to the minus 10% stem position, when the disc was riding on the seats just before wedging. The figure also indicates that the disc factor was lowest during the 1400 psig test and highest during the 600 psig test. This, too, is contrary to what was expected; one would expect a lightly loaded disc to have a thicker lubrication film and therefore a lower coefficient of friction than a heavily loaded disc.

Figure 31 depicts the effect of pressure in the opening direction, further highlighting inconsistencies with Equation (3). This plot is read from left to right as the valve opens. Although the disc factor (a positive value because the valve is opening) did not exhibit a pressure dependency at the zero stem position, it did from the minus 5% to the minus 10% stem position. This trend is similar to what was observed in the closing direction. The figure also reaffirms our previous observations that the disc factor is lower during a high-pressure test and higher during a low-pressure test. The opening disc factor is also



MS291 RS-0491-06

Figure 29. Disc factor for Gate Valve 2 closing on line break flow, effect of subcooling at 1000 psig.



MS291 RS-0491-09

Figure 30. Disc factor for Gate Valve 2 closing on line break flow, effect of pressure at 100°F subcooling.

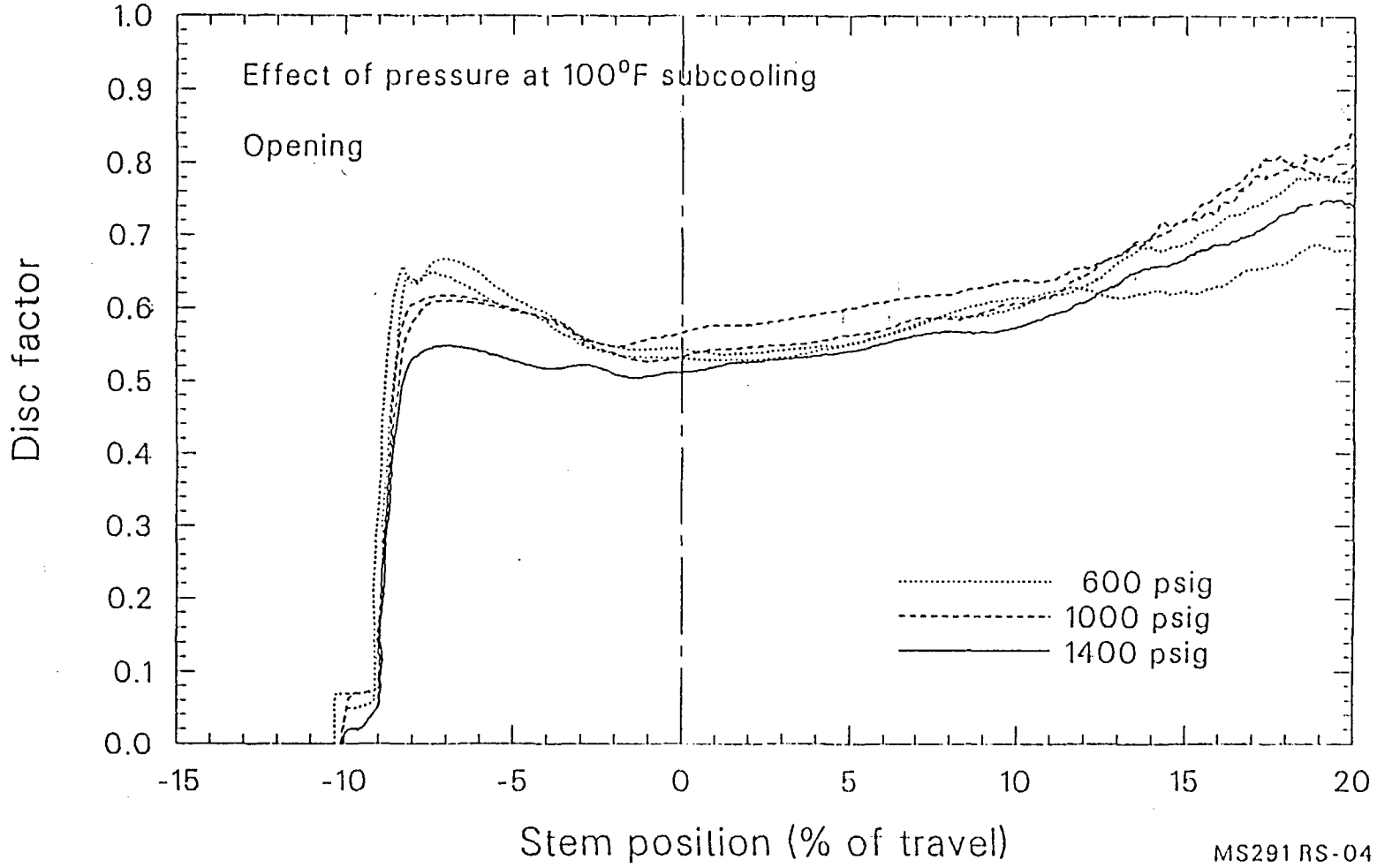


Figure 31. Disc factor for Gate Valve 2 opening on line break flow, effect of pressure at 100°F subcooling.

observed to be higher than the closing disc factor at its peak, non-wedging value.

The previously unaccounted influence of fluid subcooling and pressure on the disc factor is very evident. This influence is also contrary to what one might expect in terms of the effectiveness of a lubricant. However, what was expected is based on a lubrication that separates the load-bearing surfaces with a relatively thick film of lubricant to minimize metal-to-metal contact. This type of lubrication is known as thick-film lubrication. The condition resulting from too little lubrication is known as thin-film lubrication. The deficiencies of this thin-film lubrication can be aggravated by valve sliding surface areas that are too small to carry the maximum load.

When metal-to-metal contact exists, any condition that increases the ability of the lubricant to penetrate the bearing region will decrease the friction between the two surfaces. For instance, the higher the differential pressure across a bearing region, the more likely a given lubricant will be forced into this region, thus lowering the friction between the surfaces. Likewise, a lubricant in a vapor state is more likely than the same lubricant in a liquid state to penetrate the bearing region, thus lowering the friction between the surfaces. Other researchers have noticed these same phenomena; however, they attribute this sensitivity to changes in the temperature of the fluid and metal. We are still trying to isolate the reason, but the effect is real and must be accounted for.

From the results discussed above and from similar results for the other valves evaluated, it is apparent that Equation (3) is incomplete and fails to identify and predict the increasing stem force due to fluid properties. Equation (4), evaluated after development of the INEL correlation, is more complete and can bound the results, depending on the friction factor used; however, there is little guidance to selecting a friction factor other than a range of 0.35 to 0.50. In addition, the fluid subcooling and pressure dependencies of the disc factor or friction factor are inconsistent with past assumptions inherent in the industry's application of their equation. Thus, we concluded

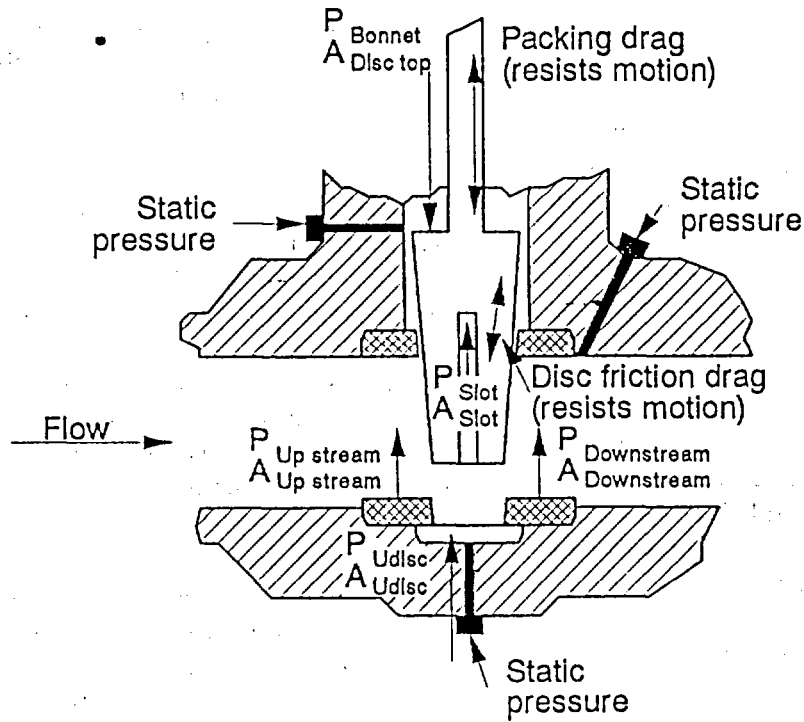
that the industry equations failed to consider parameters that have an important effect on the observed responses of the valves.

In response to the above conclusion, we directed our efforts toward investigating the flow phenomena through a flexwedge gate valve and the effect that pressures throughout the valve had on the resultant stem force. That investigation eventually yielded a correlation that bounds the required stem force during closure with more reliability than the standard industry equation with either a 0.3 or a 0.5 disc factor, or than the NMAC equation with a friction factor of 0.35 to 0.50.

Figure 32 shows a cross section of a typical flexwedge gate valve and identifies those areas on the disc and stem where the various pressure forces can act. This figure also shows where we drilled three pressure measurement ports into each of the valve bodies before the Phase II testing, to assist in the internal pressure distribution study. Figure 33 shows a typical pressure distribution observed during our testing. The pressures in both the bonnet region of the valve and under the disc are lower than the upstream pressure during most of the valve closure cycle. This reduction in pressure is due to the Bernoulli effect, the result of fluid accelerating through a valve in response to a reduction in the flow area. This phenomenon depends on the pressure and subcooling of the fluid and on the magnitude of the reduction in flow area through the valve. Thus, the Bernoulli effect will be system and fluid dependent. The bonnet area also shows a lower pressure because of the split in the disc and because of the gap between the disc and the valve body seats; these structural features provide a path so that the pressure in the bonnet region can more closely follow the pressure in the region under the disc.

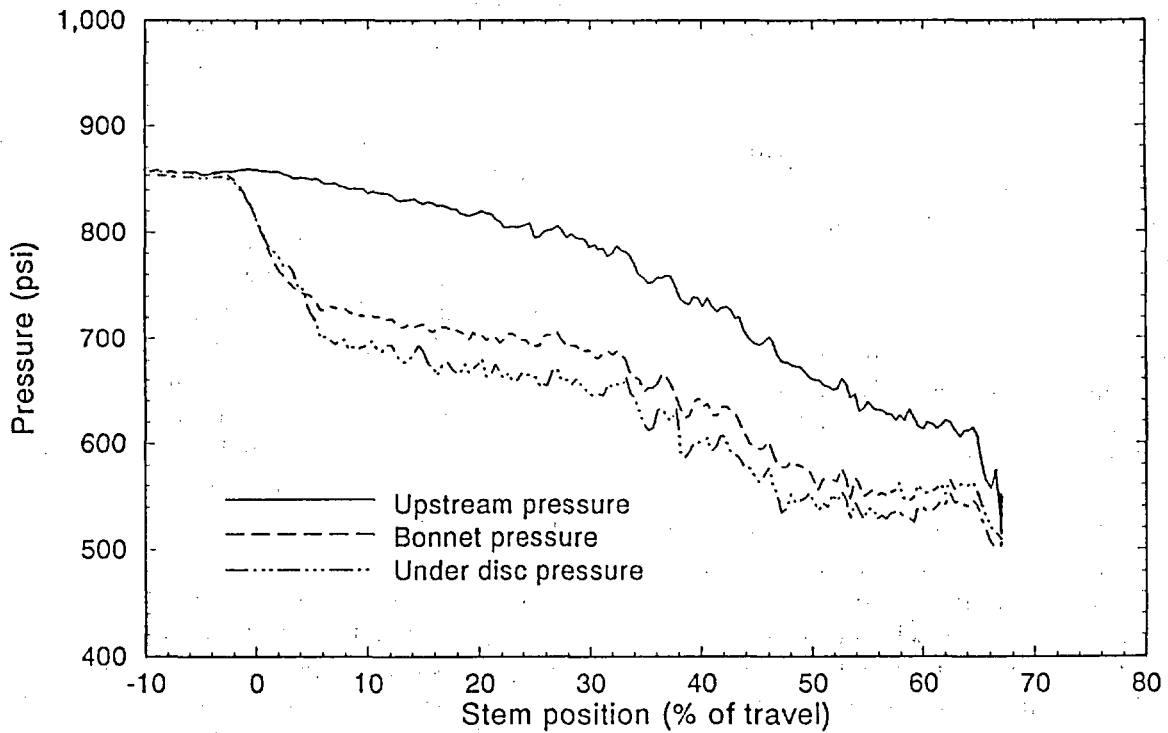
However, from the minus 3% to the minus 10% stem position during this test, the pressures converge. During this portion of the valve stroke, flow has been isolated and the disc is riding on the valve body seats; however, wedging of the disc has not yet begun. It is also during this portion of the valve stroke that predictable valves exhibit the

Specific Observations



M291 rs-0491-07

Figure 32. Gate valve disc cross section showing pressure forces and measurement locations.



M291 rs-0491-11

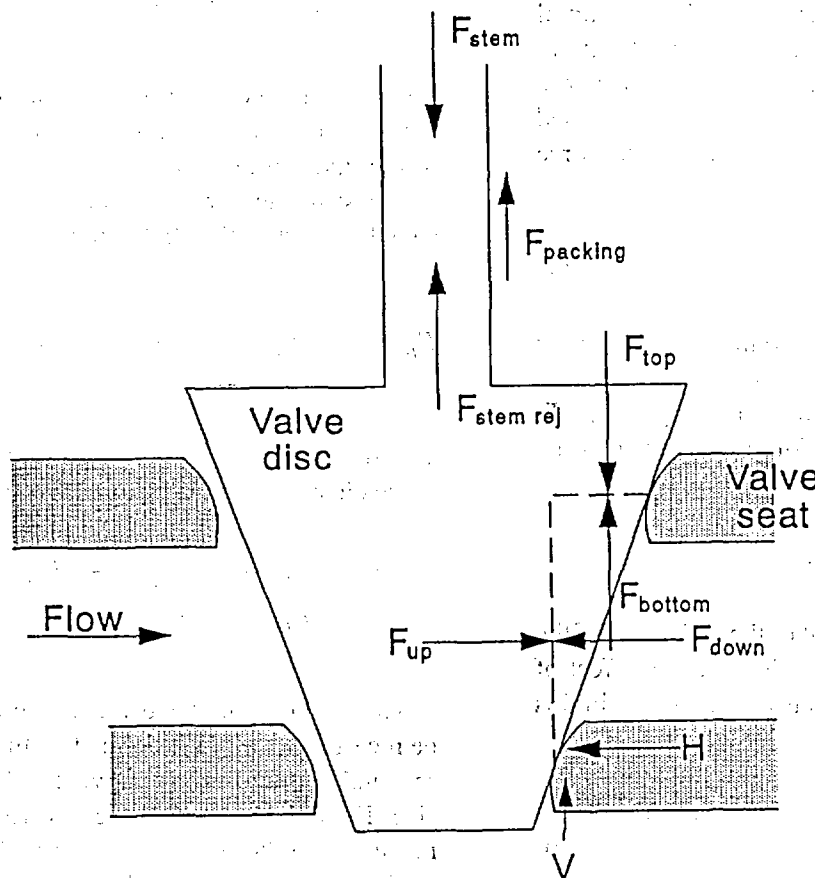
Figure 33. Gate valve internal pressure distribution.

largest stem force. Thus, we concentrated our efforts on this segment of the valve closure cycle. Wedging forces were not considered because these forces are not the result of fluid dynamic and frictional effects, but instead depend on the force capabilities of a given operator and on the structural stiffness characteristics of a specific disc and valve body.

3.3.2 Development of a Correlation to Bound the Stem Force on a Gate Valve during Closure. Our first effort was to develop a relatively detailed free body diagram of the disc while it is moving in the closing direction (after the flow has been isolated but before wedging), with the hope of better understanding the pressure and area terms that affect the stem force. Figure 34 presents the results of this effort and

identifies all the nonsymmetrical forces acting on the disc. Note that, according to the free body diagram, the forces acting on the disc ultimately react through the valve body seats, which are at a slight angle (for a flexwedge gate valve) relative to the horizontal and vertical valve coordinate system. To account for this slight seat angle so the forces are expressed in values consistent with the definition of a traditional friction factor, we found it necessary to transform the horizontal and vertical forces into a coordinate system that is normal and tangent to the valve body seating surfaces.

Following this logic, we theorized the existence of two horizontal forces acting on the disc. The first horizontal force (F_{up}) is a result of the upstream pressure (P_{up}) acting on that area of the disc defined by the mean diameter of the downstream seating surface. This surface presents a



M291 rs-0491-12

Figure 34. Gate valve disc cross section showing unbalanced forces just before wedging.

Specific Observations

circular profile in the horizontal plane. The mean seat diameter was selected because it best approximates that area of the disc in contact with the crown of the downstream seating surface over which the various pressure forces act. F_{up} is defined as

$$F_{up} = P_{up} \left(\frac{\pi D_{mean}^2}{4} \right) \quad (6)$$

Resisting this force (F_{up}) is a horizontal force (F_{down}) from the downstream pressure (P_{down}), also acting on that area of the disc defined by the mean diameter of the downstream seating surface

$$F_{down} = P_{down} \left(\frac{\pi D_{mean}^2}{4} \right) \quad (7)$$

These two forces represent the only horizontal forces acting on the disc and provide a far more realistic estimate of the horizontal force component than the orifice area term often used in the industry equation. The net horizontal force component (H) can be expressed as

$$H = F_{up} - F_{down} \quad (8)$$

The free body diagram also indicates that there are actually five vertical forces acting on the disc. The first vertical force is due to the operator and represents the net stem force delivered to the valve,

$$F_{stem} = \text{stem load} \quad (9)$$

The second force is a result of the resistance of the packing while the valve is closing. The effect of the disc and stem weights is also included in this term,

$$F_{packing} = \text{packing drag} - \text{disc and stem weights} \quad (10)$$

The third force represents the stem rejection force, the result of the pressure under the disc (P_{up} , once the flow has been isolated) trying to expel the stem,

$$F_{stem\ rej} = P_{up} \left(\frac{\pi D_{stem}^2}{4} \right) \quad (11)$$

The fourth force is a result of the pressure in the bonnet region of the valve (P_{up} once the flow has been isolated) acting on the area of the disc defined by the mean diameter of the seat cast in the vertical direction. This area term is the result of the slight angle of the seat in a flexwedge type gate valve (nominally a 5-degree angle) and results in an elliptical area over which the pressure acts. The major diameter is equal to the mean diameter of the seat; the minor diameter is equal to the mean diameter of the seat times the tangent of the angle the seat makes with the vertical axis of the valve.

$$F_{top} = P_{up} \left(\frac{\pi D_{mean}^2}{4} \right) \tan \alpha \quad (12)$$

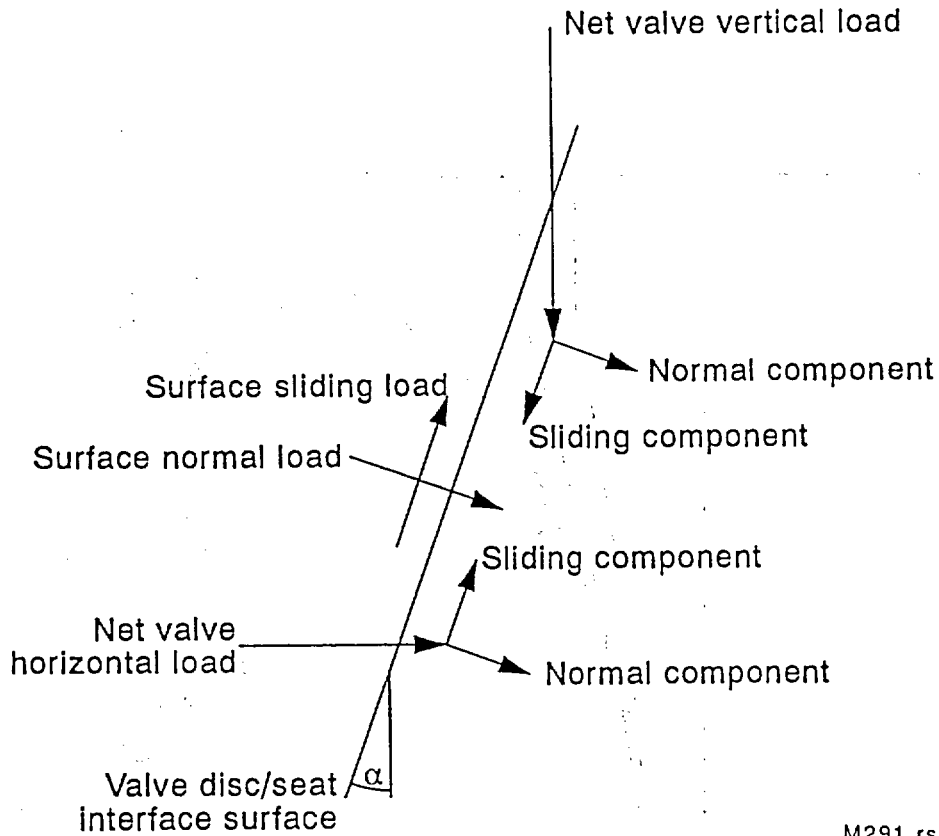
Resisting this is a fifth force resulting from the downstream pressure (P_{down}) acting on the area of the disc defined by the mean diameter of the seat cast in the vertical direction. This force is also the result of the slight angle of the seat.

$$F_{bottom} = P_{down} \left(\frac{\pi D_{mean}^2}{4} \right) \tan \alpha \quad (13)$$

The net vertical force component (V) during valve closure can thus be expressed as

$$V = F_{stem} - F_{packing} - F_{stem\ rej} + F_{top} - F_{bottom} \quad (14)$$

The net horizontal and vertical forces can now be recast into the plane defined by the valve body seat and normalized to remove the effect of valve size. Figure 35 shows these two forces and the resolution of these into forces normal and tangent to the seats. Note that the two normal forces resulting from this transformation act in the same direction, whereas the two tangent or sliding forces oppose each other. These can be expressed as follows for the normalized normal force (F_n)



M291 rs-0491-08

Figure 35. Resolution of horizontal and vertical gate valve disc forces into surface normal and sliding forces.

and the normalized sliding force (F_s), respectively:

$$F_n = \frac{H \cos \alpha + V \sin \alpha}{\left(\frac{\pi D_{mean}^2}{4}\right)} \quad (15)$$

$$F_s = \frac{H \sin \alpha - V \cos \alpha}{\left(\frac{\pi D_{mean}^2}{4}\right)} \quad (16)$$

The analysis described above allows us to better characterize the normal and sliding forces acting on a flexwedge gate valve disc just before wedging. Our next effort was to determine if the Phase I and Phase II flexwedge gate valve test data supported a relationship between these forces. From our data base, we extracted the test results of all predictable valves during the closure cycle when the disc was riding on the seats. We did not include the results of any testing if severe internal damage was evident, such as shown in

Figure 36. However, if the valve exhibited evidence of internal damage while the disc was riding on the guides but showed no evidence of such behavior while the disc was riding on the valve body seats, as shown in Figure 37, we included the results.

The Phase II data extraction included testing with three valves representing two valve sizes (6-in. and 10-in.). The full-flow isolation tests and normal operating flow isolation tests were used; upstream pressures ranged from 600 psig to 1400 psig, and fluid conditions ranged from steam to 400°F subcooled water. However, the results of tests when the differential pressure was less than 20% of the upstream pressure, or when both the differential pressure and the stem force were increasing very rapidly while the disc was riding on the valve seat, were not included. This is because the magnitude and trends of the resulting forces are obscured by relatively low loadings on

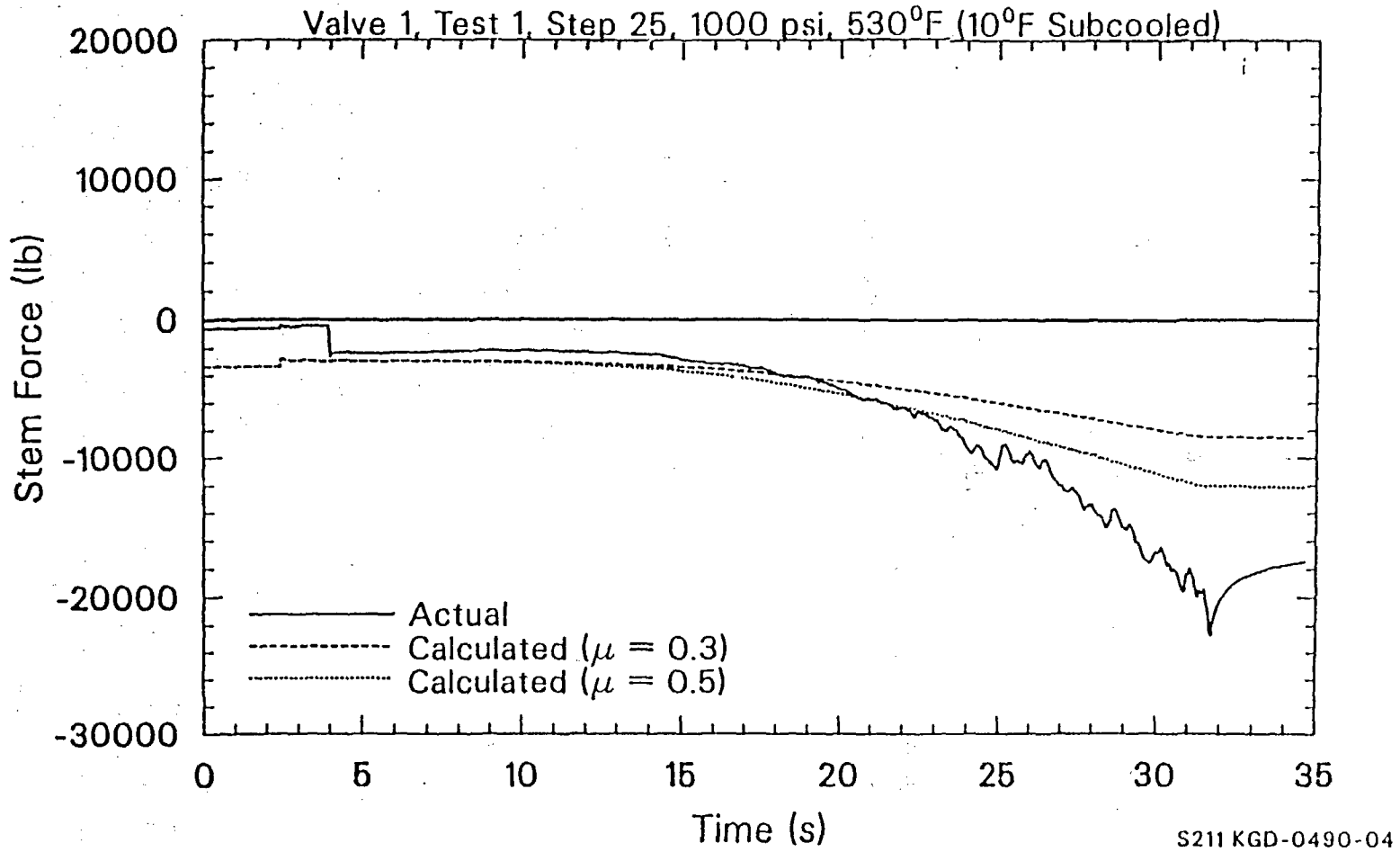
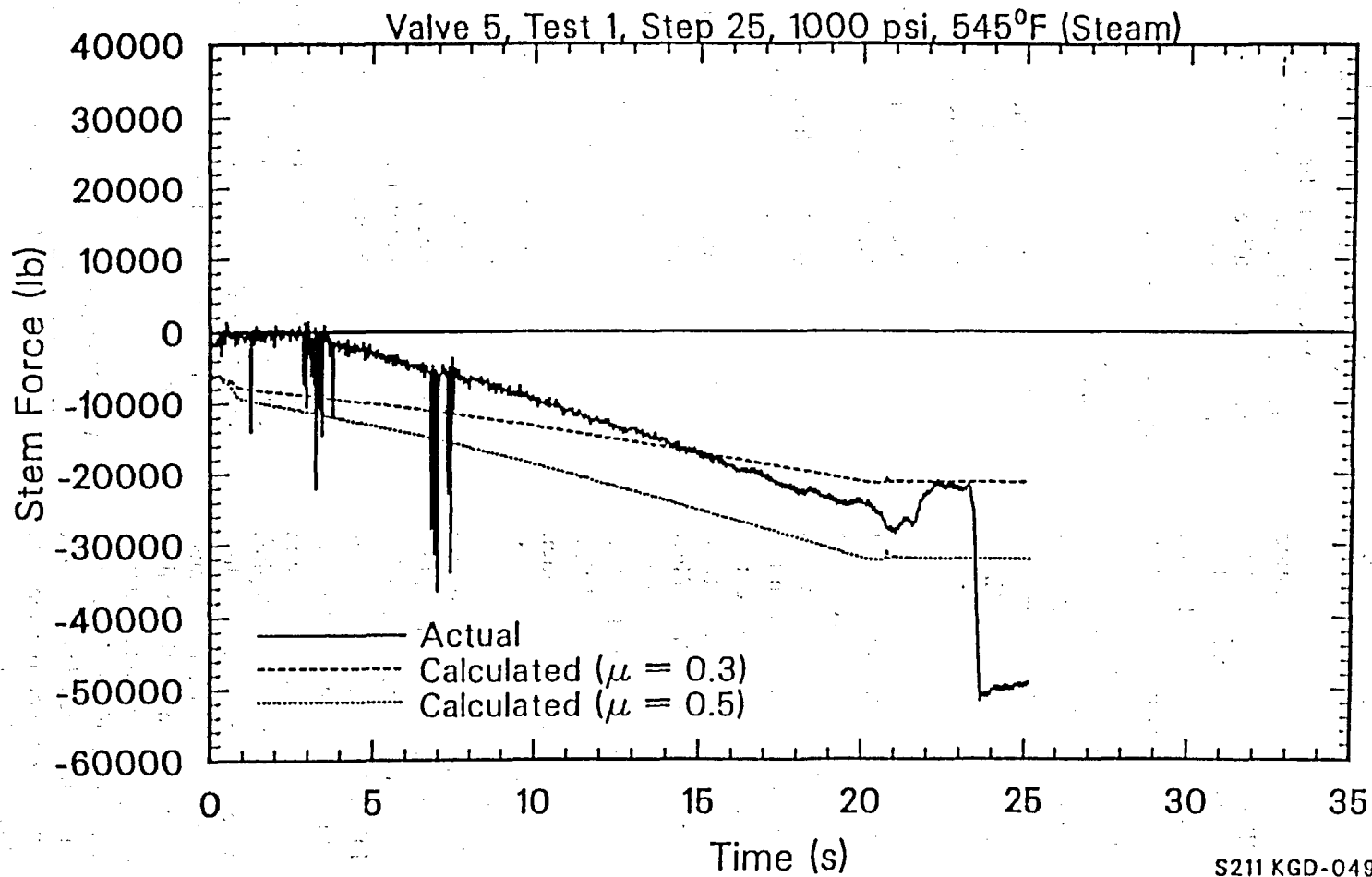


Figure 36. Gate-valve stem-force history, indicating severe damage to the guides.



S211 KGD-0490-10

Figure 37. Gate-valve stem-force history, indicating damage to the guides but not to the seats.

Specific Observations

the valve disc (which affect the transition from thick-film lubrication to thin-film lubrication), and by rapid changes in both the stem force and the differential pressure. This extraction yielded data from 30 tests, which are listed in Table 5.

The Phase I data extraction included testing with two valves representing a single valve size (6-in.). By way of comparison, these valves were nearly the same as Valves 1 and 2 in the Phase II testing. Only design-basis flow isolation tests were used from the Phase I testing. Upstream pressures ranged from 400 psig to 1400 psig, and fluid conditions ranged from 10°F subcooled to 140°F subcooled water. This extraction yielded data from 12 tests, which are listed in Table 6.

The results of both data extractions were used in the force balance developed as described above and presented in Figures 38 and 39. The results reveal two linear relationships between the normal force on a seat (F_n) and the tangent or sliding force (F_s) necessary to induce motion. One is representative of a fluid subcooling of less than 70°F, while the other is representative of a fluid subcooling of 70°F or greater. The two dashed lines on either side of the solid line represent the limits of the observed data scatter. The tight grouping of the data scatter lends confidence that not only can we bound the force requirements of a flexwedge gate valve, but we can also devise a method where the results of low differential pressure flexwedge gate valve testing can be verified and then the design-basis conditions used to bound the maximum stem force. Note also that the dashed lines do not extend below a normalized normal force of 400 lb_f/in^2 . Because of the limited low pressure and low differential pressure data available, and because of the postulated friction mechanism, the applicability of the INEL correlation is currently limited to normalized normal forces of 400 lb_f/in^2 and above. We are working with selected utilities that have proven diagnostic equipment to extend the applicability of the INEL correlation.

3.3.3 A Correlation to Bound the Stem Force on a Gate Valve during Closure.

We can now rearrange the previously developed force balance and solve for the stem force, based on a linear relationship between the normalized normal and sliding forces. Using Figures 38 and 39, the slope of the solid line (the friction factor between the disc and the seat) can be used to relate the normalized normal force (F_n) to the normalized sliding force (F_s) as

$$F_s = -f F_n \pm C \quad (17)$$

where

f = friction factor, the slope of line that relates the normal force to the sliding force and is equal to

0.400, if the fluid is less than 70°F subcooled

0.500, if the fluid is 70°F, or greater, subcooled

C = offset bounding term reflecting the scatter in the observed data and is equal to

0 for no offset

50 lb_f/in^2 to bound the data provided a normalized normal force of 400 lb_f/in^2 , or greater, exists according to Equation (15) (shown as the dashed lines in Figures 38 and 39).

Substituting the horizontal and vertical components of the normal force [Equation (15)] and the horizontal and vertical components of the sliding force [Equation (16)] into the above relationship yields

$$V = \frac{H (f \cos \alpha + \sin \alpha) \pm C \left(\frac{\pi D_{mean}^2}{4} \right)}{(\cos \alpha - f \sin \alpha)} \quad (18)$$

Table 5. Phase II gate valve test data supporting extrapolation.

Valve	Test number	Step	Stem position	Force (lbf)			Pressure (psig)		Subcooled fluid (°F)
				Stem	Normal	Sliding	Up	Delta	
2	1	25	-7.34	12929	987	-424	959.6	948.5	11.5
2	1	26	-7.38	13578	1021	-447	1002.4	980.3	16.3
2	6b	18	-7.10	10477	571	-332	887.5	540.6	95.9
2	6b	25	-7.26	12173	888	-404	856.4	851.3	36.2
2	6b	26	-7.08	12453	953	-409	922.4	915.8	36.0
2	6b1	26	-7.22	13654	1031	-451	990.6	989.6	48.4
2	6a	18	-7.54	7880	413	-254	601.7	389.7	91.9
2	6a	25	-7.37	7859	550	-260	525.5	526.5	18.8
2	6a	26	-7.14	7703	548	-254	524.7	524.5	10.9
2	6a1	25	-7.07	8688	609	-288	585.7	582.8	42.5
2	6a1	26	-7.35	8866	633	-294	603.1	606.7	39.0
2	6c	13	-7.13	15626	952	-490	1414.6	907.9	124.4
2	6c	18	-7.08	15046	970	-464	1431.2	927.8	115.4
2	6c	25	-7.29	15798	1315	-510	1276.3	1268.3	47.0
2	6c	26	-7.39	16452	1359	-533	1317.7	1310.8	39.7
2	2	18	-7.46	16083	1234	-528	1215.7	1186.4	9.5
2	2	25	-7.06	13096	1091	-422	1056.1	1052.5	9.0
2	2	26	-7.12	13079	1063	-424	1027.6	1024.3	8.4
2	3	25	-7.10	12751	793	-438	746.4	753.2	371.7
2	3	26	-7.27	14512	936	-496	886.7	890.8	388.6
3	1	25	-7.13	4355	247	-113	1012.0	237.0	17.2
3	1	26	-7.30	8628	887	-298	856.1	861.0	5.9
3	1a	25	-7.17	10804	942	-386	915.1	909.1	7.5
3	1a	26	-7.33	11032	928	-396	894.4	893.8	7.1
3	5	25	-7.18	12235	1144	-435	1117.4	1106.8	7.3
3	5	26	-7.23	13281	1177	-477	1140.4	1136.2	11.0
5	1	25	-7.47	24756	904	-336	879.9	876.8	9.6
5	1	26	-7.28	22547	835	-304	813.0	810.9	6.9
5	1a	25	-7.21	30474	1055	-421	1026.3	1021.3	5.6
5	1a	26	-7.33	29045	1013	-400	985.7	981.2	7.7

Specific Observations

Table 6. Phase I gate valve test data supporting extrapolation.

Valve	Test number	Step	Force (lbf)			Pressure (psig)		Subcooled fluid (°F)
			Stem	Normal	Sliding	Up	Delta	
A	2	5	11550	996	-413	959.3	— ^a	10
A	3	5	5347	472	-170	456.3	— ^a	60
A	4	5	12884	1040	-470	998.4	— ^a	140
A	5	5	17460	1573	-637	1516.3	— ^a	10
A	6	5	6183	416	-213	397.3	— ^a	60
A	7	5	15491	1378	-563	1328.0	— ^a	140
A	8	5	7406	557	-258	534.6	— ^a	10
A	9	5	7735	593	-270	569.5	— ^a	60
A	10	5	8183	616	-289	591.1	— ^a	140
A	11	5	11743	1047	-417	1009.9	— ^a	10
B	2	5	13833	978	-389	938.6	— ^a	10
B	4	5	8500	602	-206	580.5	— ^a	10

a. Full differential pressure tests were performed; a differential pressure equal to the upstream pressure was used.

Now, substituting the horizontal and vertical force components [Equations (8) and (14)] into Equation (18), limiting the final result to bound the maximum stem force, and rearranging yields

$$F_{stem} = F_v + \frac{\theta_1 F_h + 50 \left(\frac{\pi D_{mean}^2}{4} \right)}{\theta_2} \quad (19)$$

where

$$F_v = F_{packing} + F_{stem\ rej} - F_{top} + F_{bottom} \quad (20)$$

$$\theta_1 = f \cos \alpha + \sin \alpha \quad (21)$$

$$F_h = F_{up} - F_{down} \quad (22)$$

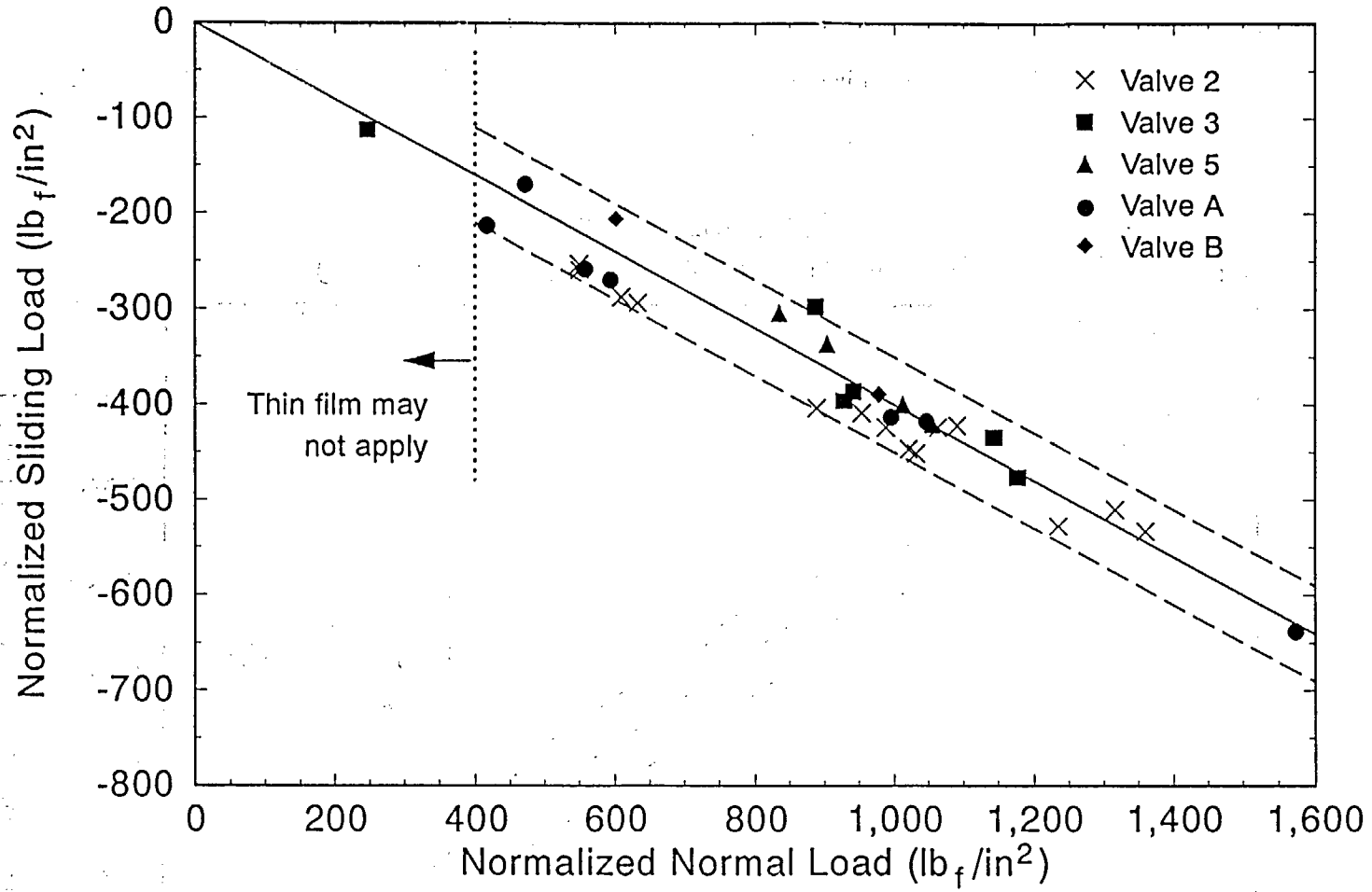
$$\theta_2 = \cos \alpha - f \sin \alpha \quad (23)$$

f = friction factor and is equal to

0.400 if the fluid is less than 70°F subcooled

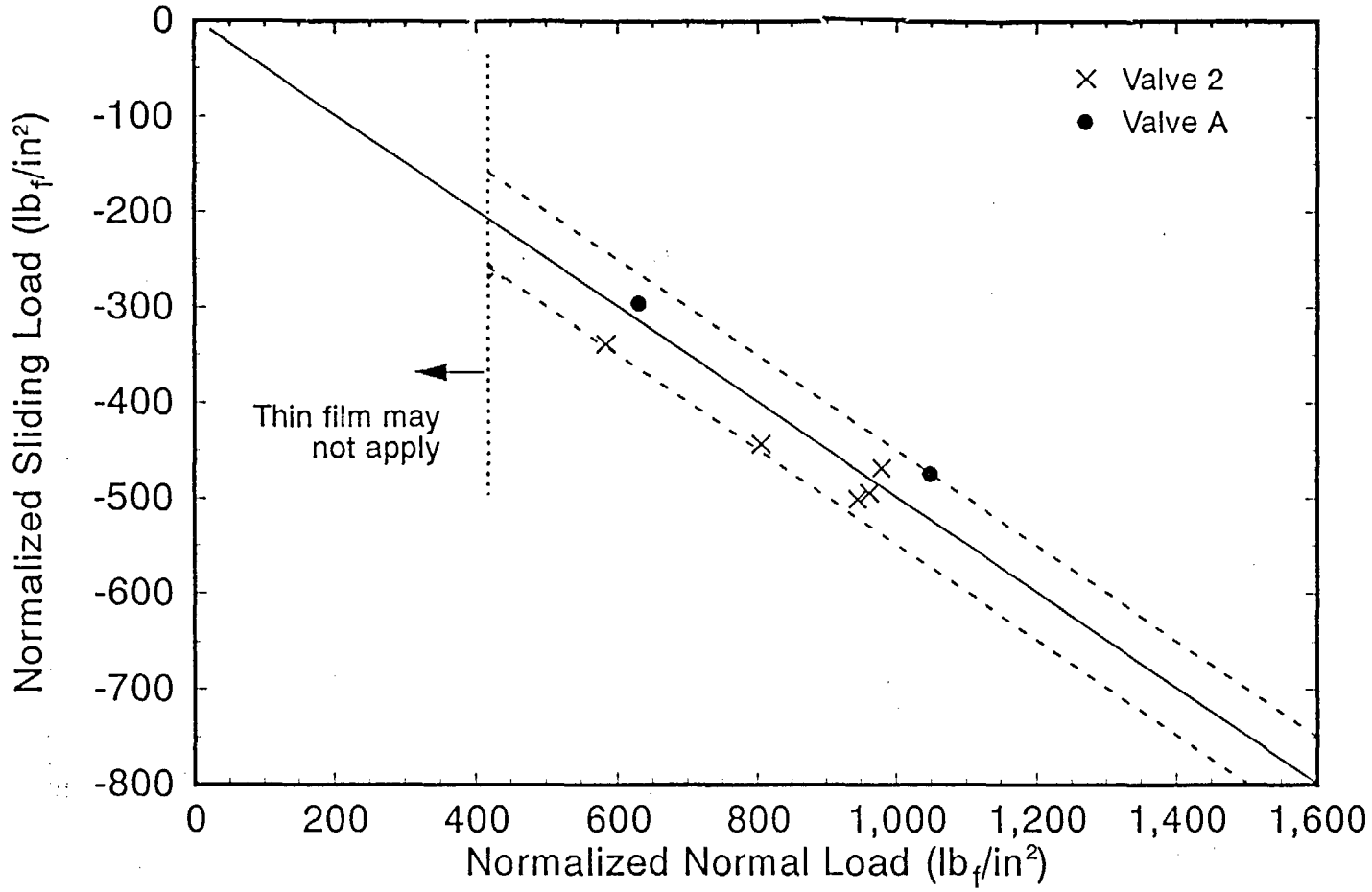
0.500 if the fluid is 70°F or greater subcooled.

Equation (19) provides a method that can be used to bound the maximum stem force requirements of a flexwedge gate valve closing against medium to high flows and whose operational characteristics have been demonstrated to be predictable at design-basis pressures and temperatures. This method will also provide the basis by which the results of in situ tests conducted on predictable valves at less than design-basis conditions can be verified and then the design-basis conditions used to bound the maximum stem force. Note that the correlation applies only



M455 kqd-1091-22

Figure 38. Normalized surface sliding force versus normalized surface normal force for gate valves closing against less than 70°F subcooled fluid.



M455 kgw-1091-23b

Figure 39. Normalized surface sliding force versus normalized surface normal force for gate valves closing against 70°F, or greater, subcooled fluid.

to flexwedge gate valve closure against medium to high flows, flows which will result in a normalized normal force of $400 \text{ lb}_f/\text{in}^2$ or greater, according to Equation (15). This correlation has not yet been validated for predicting the closing force requirements when the normalized normal loading is less, but we are working with selected utilities to extend the applicability of the INEL correlation.

The INEL correlation cannot be used in the opening direction. The following comparison best explains why. Figure 40 represents the stem force of a design-basis opening cycle of a smaller valve. The results are representative of a valve that experiences the highest stem force demands immediately after unseating and while the disc is still riding on the seats. A correlation similar to the one presented here may be applicable for such valves, subject to an assessment of the required friction factor. However, Figure 41 represents the stem force of a design-basis opening cycle of a larger valve and clearly shows a very different stem force response. Here, the highest stem force occurs when the valve is approximately 25 to 30% open. This is well outside the assumptions implicit in the INEL correlation, the NMAC equation, or the standard industry equation and dramatizes the influence fluid dynamic effects can have on valve response. The issue of bounding the maximum stem force to open a flexwedge gate valve will be investigated in the future.

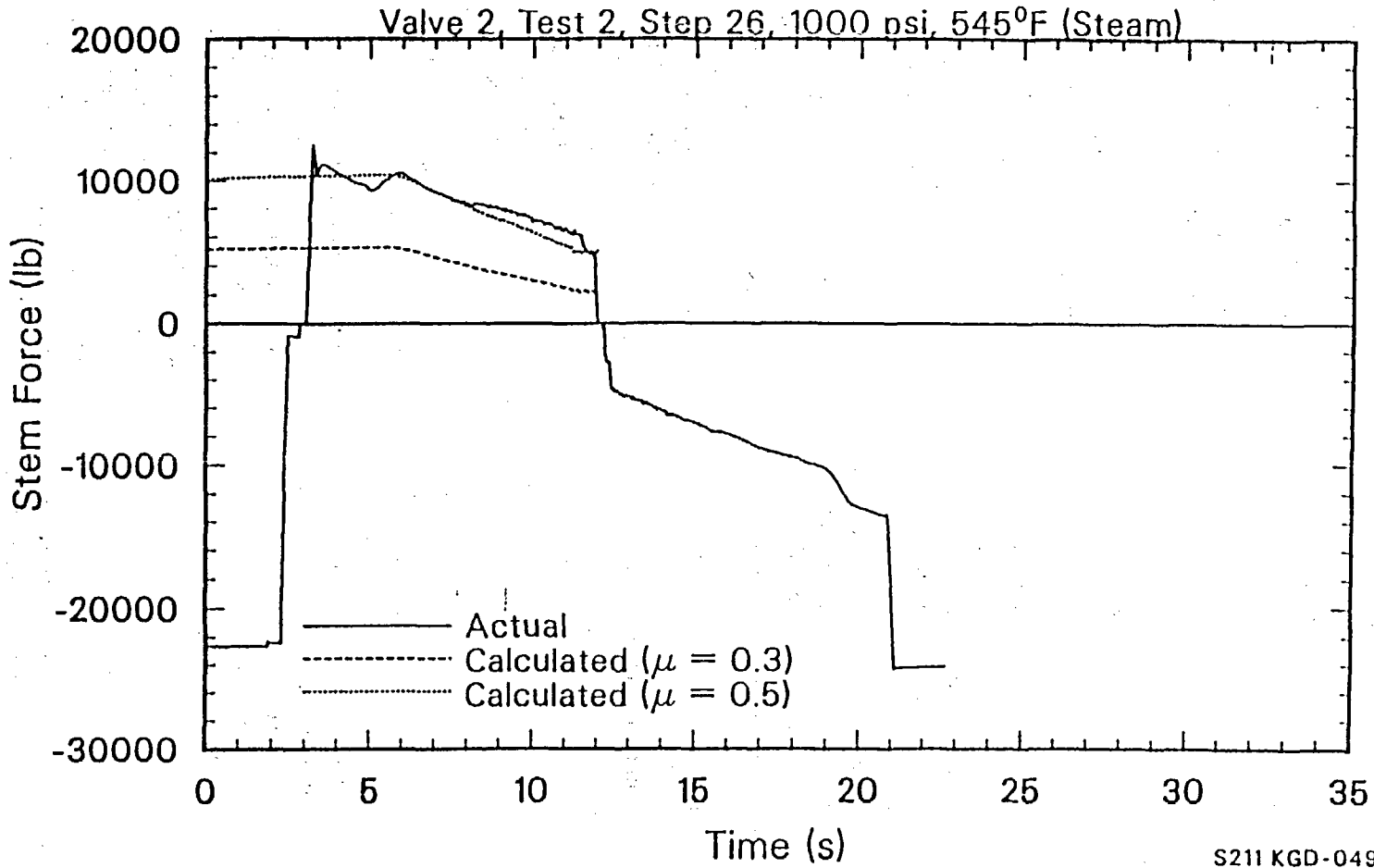
3.3.4 Use of the Correlation to Bound the Stem Force on a Gate Valve during Closure. To use the INEL correlation to bound the closing stem force requirements of a flexwedge gate valve, the analyst must first determine if the valve is of the type whose operational characteristics are considered to be predictable. If the valve is predictable, the following information can be used to bound the stem force:

- The mean diameter of the valve body seat (the average of the inside diameter and the outside diameter of the valve body seats measured in the plane perpendicular to the stem)

- The angle the valve body seat makes with the vertical or stem axis
- The outside diameter of the stem
- An estimate of the maximum packing drag expected, less the effects of the weight of the disc and stem
- The maximum upstream pressure that would exist after flow isolation but before wedging, typically the design-basis pressure
- The maximum differential pressure that would exist after flow isolation but before wedging, typically the design-basis differential pressure
- The subcooling of the fluid at design-basis conditions, either less than 70°F subcooled or 70°F or greater subcooled.

With this information, the net horizontal force (F_h) can be estimated with Equation (22) and Equations (6) and (7). The net vertical force (F_v) can then be estimated with Equation (20) and Equations (10) through (13). The angle between the seat and the vertical or stem axis can then be used with Equations (21) and (23) to estimate terms associated with transforming the horizontal forces into forces on the disc and seat and finally into a vertical force. Thus, all the terms in Equation (19) can be determined and the maximum stem force necessary to isolate flow at the specified pressure and differential pressure can be calculated.

By way of example, we will use the upstream pressure and differential pressure recorded after flow isolation, but before wedging during one of the Valve 2 tests, and will bound the stem force requirements of the valve using the INEL correlation. Similar estimates will also be made using the industry equation and either an orifice area or a mean seat area in conjunction with a standard industry disc factor of 0.3, as well as a more conservative industry disc factor of 0.5. The results of each estimate will then be compared with the actual stem force recorded during the test.



S211 KGD-0490-31

Figure 40. Stem-force history of a small gate valve during an opening test.

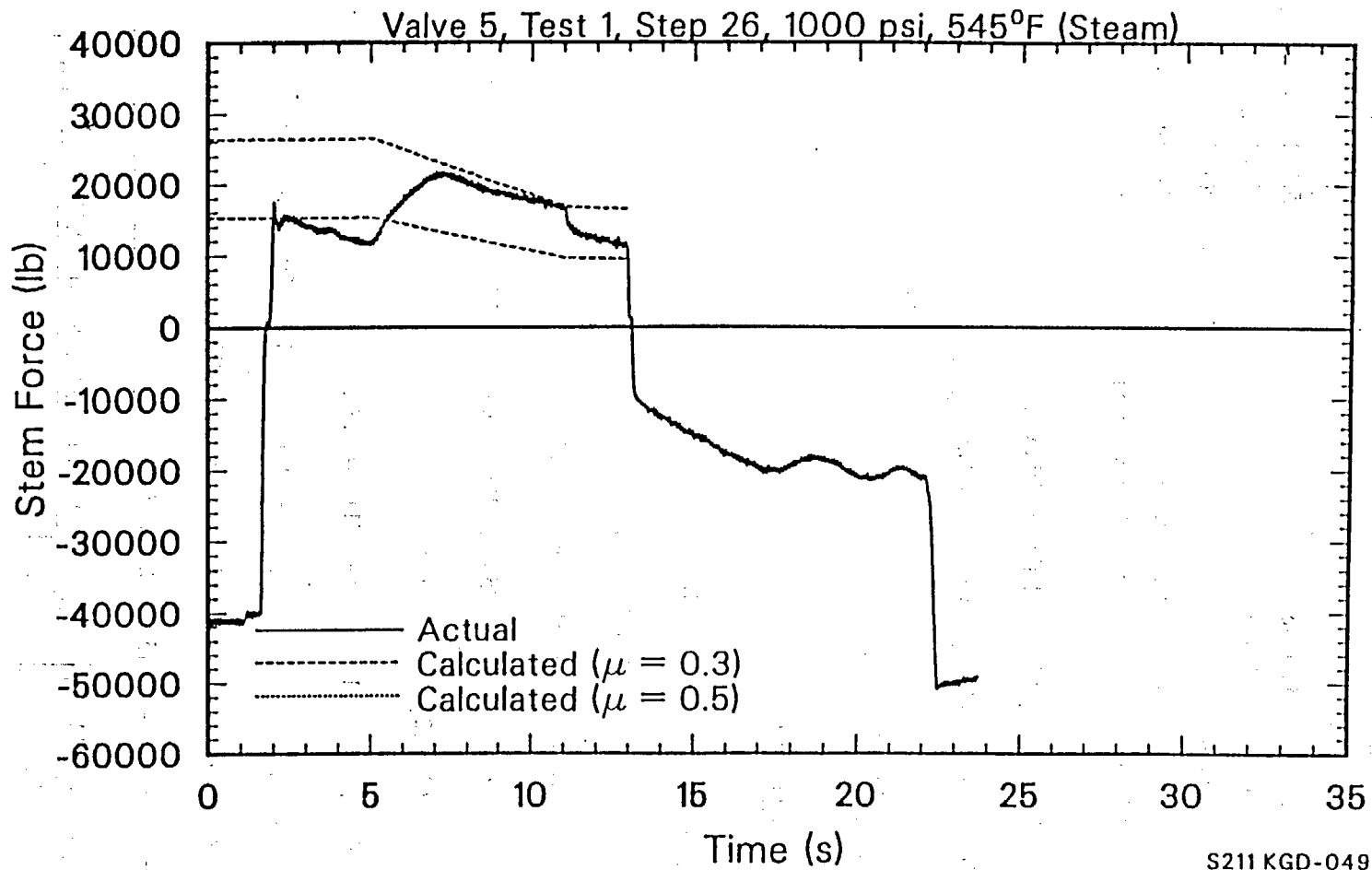


Figure 41. Stem-force history of a large gate valve during an opening test.

Specific Observations

The results from Valve 2, Test 3, Step 25 will be used for this comparison. Since this was a cold water test (400°F subcooled fluid), we will use the 70°F or greater subcooled friction factor in the INEL correlation. Pertinent valve information and the pressure and differential pressure recorded just before wedging are

Stem diameter	1.750 in.
Orifice diameter	5.187 in.
Seat inside diameter	5.192 in.
Seat outside diameter	5.945 in.
Packing drag	200 lb _f
Upstream pressure just before wedging	746 psig
Differential pressure just before wedging	753 psid

We can use this information in the INEL correlation as follows:

$$D_{mean} = \frac{(seat\ ID + seat\ OD)}{2} = \frac{(5.192 + 5.945)}{2} = 5.569$$

$$A_{mean} = \frac{\pi D_{mean}^2}{4} = \frac{\pi(5.569)^2}{4} = 24.358$$

$$A_{stem} = \frac{\pi D_{stem}^2}{4} = \frac{\pi(1.750)^2}{4} = 2.405$$

$$F_{up} = P_{up}A_{mean} = (746)(24.358) = 18,171$$

$$F_{down} = P_{down}A_{mean} = (746 - 753)(24.358) = -171$$

$$F_{top} = P_{up}A_{mean} \tan \alpha = (746)(24.358) \tan 5 = 1590$$

$$F_{bottom} = P_{down}A_{mean} \tan \alpha = (746 - 753)(24.358) \tan 5 = -15$$

$$F_{stem\ rej} = P_{up}A_{stem} = (746)(2.405) = 1794$$

$$F_h = F_{up} - F_{down} = 18,171 - (-171) = 18,342$$

$$F_v = P_{packing} + F_{stem\ rej} - F_{top} + F_{bottom} = 200 + 1794 - 1590 + (-15) = 389$$

$$\theta_1 = f \cos \alpha + \sin \alpha = 0.500 \cos 5 + \sin 5 = 0.585$$

$$\theta_2 = \cos \alpha - f \sin \alpha = \cos 5 - 0.500 \sin 5 = 0.953$$

$$F_{stem} = F_v + \left[\frac{\theta_1 F_h + 50A_{mean}}{\theta_2} \right] = 389 + \left[\frac{(0.585)(18,342) + (50)(24.358)}{0.953} \right] = 12,926.$$

We can also use this information with the industry equation as follows:

Industry equation with $\mu_d = 0.3$

$$A_{orifice} = \frac{\pi D_{orifice}^2}{4} = \frac{\pi(5.187)^2}{4} = 21.131$$

$$A_{stem} = \frac{\pi D_{stem}^2}{4} = \frac{\pi(1.750)^2}{4} = 2.405$$

$$\begin{aligned} F_t &= \mu_d A_{orifice} \Delta P + A_{stem} P_{up} + F_{packing} = 0.3(21.131)(753) + 2.405(746) + 200 \\ &= 4773 + 1794 + 200 = 6767 \end{aligned}$$

Industry equation with $\mu_d = 0.5$

$$\begin{aligned} F_t &= \mu_d A_{orifice} \Delta P + A_{stem} P_{up} + F_{packing} = 0.5(21.131)(753) \\ &+ 2.405(746) + 200 = 7956 + 1794 + 200 = 9950 \end{aligned}$$

During this test, the peak stem force recorded just before wedging was 12,787 lbf. Thus, the INEL correlation bounds the actual recorded stem force. The industry equation using either disc area term, with either the standard industry disc factor of 0.3 or the more conservative industry disc factor of 0.5, underpredicts the actual recorded stem force just before wedging. Additional comparisons are presented in Table 7 for each Phase II test evaluated. Examining these results indicates that the INEL correlation consistently bounds the maximum recorded stem force before wedging, whereas the industry equation, using either disc area term with either disc factor, typically underestimates the stem force, except with a disc factor of 0.5 and a mean seat area.

3.3.5 Identifying the Pressure Dependency Contributing to the Stem Force on a Gate Valve during Closure. Based on the results of our testing and data evaluation, we identified both a subcooled and differential pressure dependency on the disc or friction factor. The subcooled dependency has been previously shown; not so evident, however, is the differential pressure dependency of the correlation. Referring to either Figure 38 or 39, the INEL correlation follows the lower bounding curve, a higher resis-

tance for a given normal force, or a nominal friction factor plus an offset. This nominal friction factor plus an offset can also be reduced to a single load dependent friction factor. Figure 42 displays the friction factor and offset as shown in Figure 38. Also shown on this figure is the load-dependent friction factor at two normalized normal forces. The normalized normal force of 400 lbf/in² results in a load-dependent friction factor of 0.525. The normalized normal force of 1400 lbf/in² results in a load-dependent friction factor of 0.436. This effect is the result of the data offset or bounding term and its relative magnitude compared to the normal force component. Thus, embedded in the INEL correlation is the differential pressure dependency observed in our test data.

3.3.6 Low Differential Pressure Test Verification and Bounding of the Stem Force on a Gate Valve Closing against Design-Basis Flows. Utilities have numerous flexwedge gate valves in systems throughout a nuclear power plant; many of these valves must function in various design-basis events. The capability of these valves to operate at design-basis conditions usually cannot be verified with in situ testing, especially for valves where design-basis conditions include high pressures and medium to

Specific Observations

Table 7. Comparison of gate valve stem forces, estimates versus actual.

Test number	Step	Pressure (psig)		Stem force (lbf)					
		Up	Delta	Actual	INEL ^a	Industry equation			
						Orifice area		Mean seat area	
						$\mu=0.3$	$\mu=0.5$	$\mu=0.3$	$\mu=0.5$
Valve 2									
1	25	959.6	948.5	12929	13429	8525	12535	9444	14067
1	26	1002.4	980.3	13578	13845	8822	12964	9771	14545
6b	18	887.5	540.6	10477	10556 ^b	5765	8052	6289	8924
6b	25	856.4	851.3	12173	12182	7653	11250	8477	12623
6b	26	922.4	915.8	12453	13002	8224	12095	9111	13573
6b1	26	990.6	989.6	13654	13920	8859	13043	9818	14641
6a	18	601.7	389.7	7880	7930 ^b	4120	5768	4498	6398
6a	25	525.5	526.5	7859	8092	4806	7033	5316	7883
6a	26	524.7	524.5	7703	8070	4791	7010	5299	7857
6a1	25	585.7	582.8	8688	8806	5305	7769	5870	8710
6a1	26	603.1	606.7	8866	9091	5498	8063	6086	9043
6c	13	1414.6	907.9	15626	16558 ^b	9372	13218	10238	14662
6c	18	1431.2	927.8	15046	16827 ^b	9524	13446	10423	14944
6c	25	1276.3	1268.3	15798	17434	11307	16666	12535	18712
6c	26	1317.7	1310.8	16452	17975	11681	17221	12950	19336
2	18	1215.7	1186.4	16083	16455	10643	15655	11791	17569
2	25	1056.1	1052.5	13096	14718	9415	13865	10434	15564
2	26	1027.6	1024.3	13079	14355	9164	13494	10155	15144
3	25	746.4	753.2	12751	12934 ^b	6768	9950	7497	11165
3	26	886.7	890.8	14512	15044 ^b	7982	11747	8844	13185
Valve 3									
1	25	1012.0	237.0	4355	5249	3180	4205	3340	4472
1	26	856.1	861.0	8628	11283	7038	10762	7621	11734
1a	25	915.1	909.1	10804	11835	7421	11354	8037	12380
1a	26	894.4	893.8	11032	11649	7292	11155	7904	12175
5	25	1117.4	1106.8	12235	14058	8954	13743	9704	14993
5	26	1140.4	1136.2	13281	14376	9171	14085	9940	15367
Valve 5									
1	25	879.9	876.8	24756	29638	18260	27753	20133	30874
1	26	813.0	810.9	22547	27712	16951	25729	18683	28615
1a	25	1026.3	1021.3	30474	33839	21116	32167	23296	35801
1a	26	985.7	981.2	29045	32674	20325	30943	22419	34434

a. A friction factor (f) of 0.400 was used in the INEL correlation, except as noted.

b. 70°F or greater subcooled fluid test, a friction factor (f) of 0.500 was used.

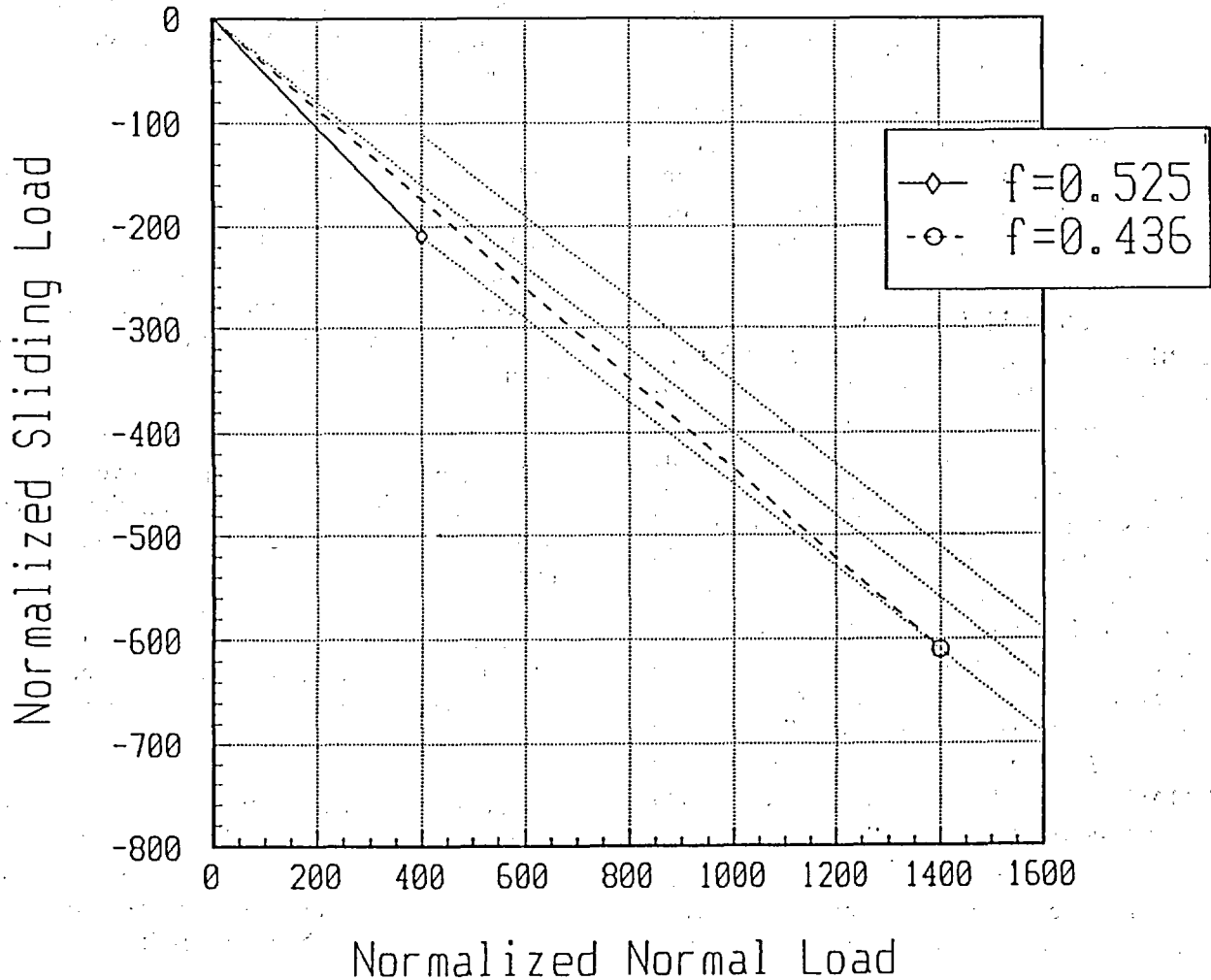


Figure 42. Gate valve load-dependent friction factor using the INEL correlation.

high flows. Usually, only low flow and low differential pressure conditions can be developed near valve closure under in situ conditions. When such valves are determined to be predictable by other means, the INEL correlation offers a method that can be used to bound the stem force requirements of the candidate flexwedge gate valve at design-basis conditions. This can be accomplished as follows:

Step 1: Perform a differential pressure test. Use the results of the testing to estimate the normalized normal and sliding loads for the valve, according to Equations (15) and (16). The valve is considered to be representative of the valves tested by the INEL if (a) the upstream pressure

and differential pressure while the disc is riding on the seats result in a normalized normal force of not less than 400 lb_f/in^2 , and (b) the resulting forces fall within the upper and lower bounds expected for valves of this design (see Figures 38 and 39). If the resulting loads do not fall within the expected band, the results of our testing are not representative of the valve being tested and the INEL correlation may not be applicable.

Step 2: If the results of Step 1 fall within the expected band, use the actual design-basis conditions in the INEL correlation to bound the stem force requirement of

Specific Observations

the valve being tested. Then use this maximum stem force estimate, along with the other necessary motor operator sizing calculations, to verify the size of the operator and the setting of the torque switch, and thus ensure that sufficient stem force is available to operate the valve at design-basis conditions.

3.3.7 Nuclear Maintenance Application Center (NMAC) Gate Valve Stem Force Equation. The current NMAC gate-valve stem-force equation is mathematically equivalent to the best-estimate portion of the INEL math. Like the INEL correlation, it is based on a first-principles analysis, but it does not provide the additional empirical derived guidance that is contained in the INEL correlation. The NMAC guide provides a range of dynamic coefficients of friction that might be encountered in gate valves. Suggested values range from 0.35 to 0.50, but more specific guidance is left to others. Our immediate concern is with the following footnote, presented in the NMAC guide, addressing the applicability and use of a coefficient of friction:

“Extensive testing . . . using Stellite 21 found no statistically significant variation

between static and dynamic friction. This testing also found that temperature, fluid type, and contact pressure had no statistically significant effect on friction.”

Our data assessment to date has not addressed the issue of static versus dynamic friction; however, we have clearly shown that fluid type (subcooling) and differential pressure have a significant effect on the friction factor. We suggest that this statement be reviewed in light of the INEL test results.

The NMAC guide also presents their equation as being applicable for estimating valve opening stem forces. One of the basic assumptions stated in the guide regarding the use of their equations is that

“The limiting thrust occurs at or near the seat, during seating or unseating, and no additional dynamic flow effects contribute to the required stem thrust.”

As mentioned earlier in this report, INEL test results indicate that some valves experience their highest stem forces when the valve is 25 to 30% open. Thus, this statement, too, should be reviewed in light of INEL test results.

4. UNDERSTANDING DIAGNOSTICS AND DIAGNOSTIC TESTING OF MOTOR-OPERATED VALVES

4.1 Overview

Recent recommendations made by the NRC in Generic Letter 89-10 suggest that licensees develop programs for MOV inspection, maintenance, and testing under pressure and flow conditions to ensure that the valves will function when subjected to design-basis conditions. Development of the licensees' MOV programs is underway, but in our opinion, it is obvious that MOV diagnostic testing will play a large part in these programs. Diagnostic test equipment and methodologies are continuing to be developed by both the diagnostic industry and by selected utilities. Over the years, we have developed a very sophisticated diagnostic capability to aid in our MOV research. Admittedly, some of this capability is needed from a researcher's standpoint and is not necessary for diagnostic in situ testing. However, we have identified from this larger capability what we believe to be the minimum diagnostic capability necessary for thorough in situ testing of rising-stem MOVs. This section of the report presents our thoughts on measuring and assessing the performance of MOVs during diagnostic testing and then relates that performance to design requirements. Because MOV diagnostic test equipment is still being developed, some of the judgments made in this section are based on the capability of equipment that was commercially available when this report was written.

MOV diagnostic systems should serve the following purposes: (a) to identify deterioration or faulty adjustment in the valve and operator, (b) to maintain assurance of design-basis capability that has been established previously for a particular MOV, and (c) to provide information to establish design-basis capability based on low-pressure and low-flow tests and/or from prototype tests. MOV diagnostic equipment is used in conjunction with one of two types of tests: unloaded static testing or testing under flow and pressure loads (dynamic testing). Both position-controlled and torque-controlled valves will be discussed.

Unloaded static testing of position-controlled and torque-controlled valves provides measurements of the packing drag and stroke time. For torque-controlled valves, the static test also provides measurements of torque and stem force at torque switch trip. However, the direct determination of the capability of an operator at design-basis conditions from an unloaded test of either a position-controlled or a torque-controlled valve is highly suspect. These data can be used for trending the MOV.

Flow and pressure testing provide much more information on both torque-controlled and position-controlled valves than does no-load static testing. It is well known that some valves cannot be design-basis tested in the plant, but the higher the in situ test loading, the more in-depth information the analyst will have to determine the performance of the valve and the margins available in each of the MOV components. Again, more information will come from the torque-controlled valves than from the position-controlled valves. For critical position-controlled valves that cannot be significantly loaded in situ, it may be necessary to consider dynamometer testing of the motor operator.

The thoughts presented here are a product of our experience in the four full-scale test programs discussed in Section 1. The recommendations are also based on the results of special effects testing being conducted at the INEL on the Motor-Operated Valve Load Simulator (MOVLS), described in Section 4.3. Our research to date indicates that, for rising-stem MOVs, ideally a diagnostic system should be able to accurately measure the following parameters as a minimum: position of the motor operator switch (for limit switches and torque switches), motor current and voltage, motor operator torque, and valve stem force. The following discussion explores each of the recommended measurements and explains its value to the analyst.

4.2 Understanding MOV Diagnostic Testing

4.2.1 Motor Operator Switch Position.

4.2.1.1 Limit Switches. For ac- and dc-powered position-controlled valves (including those valves that close on torque but open on limit), the analyst can determine valve stroke time and stem position in either a static test or a dynamic test. The point in time when the switch is activated provides the basis for analyzing many of the other diagnostic measurements. Figure 43 shows typical dc limit switch histories.

4.2.1.2 Torque Switches. Torque switch trip (for torque-controlled valves) establishes a timing point to assess the output of the operator. The stem force at torque switch trip will typically be lower than the peak force produced after torque switch trip, when the motor controller dropout time and the motor and operator momentum result in further compression of the stem. The motor controller dropout time for both ac- and dc-powered MOVs is small, but its effects are real; the length of the dropout time is further influenced by the state of the ac cycle when the torque switch trips. Momentum effects are conspicuous in static tests, but they can be absorbed by the higher loadings in dynamic tests. In addition, if the torque switch trips before the disc is fully seated in a dynamic test, then the momentum does not produce the additional stem force that would have been produced in a static test. Figure 44 is a torque switch history showing a typical ac-powered motor controller torque switch trip.

For a torque-controlled valve operating in the closing direction, the exact trip time (for ac-controlled circuits this must be interpreted from the motor controller holding coil ac sine wave) is important for analysis of all the other quantitative measurements. It is important that the data acquisition system have a sample rate that is fast enough to allow the analyst to correctly determine the time of torque switch trip and all other data with respect to this time. The faster the sample rate, the less conservatism the analyst will have to add to the measurements to account for time errors. We have found that a sample rate of

1000 samples/second is usually sufficient; it provides a resolution that is faster than most of the sensor responses.

4.2.2 Motor Current.

4.2.2.1 Torque-Controlled Alternating Current Motor Operators. The margin of an electric motor can be estimated from a motor current history. The concern is that the output from an ac motor can change quickly when the motor is operating too close to stall current, where a large increase in required current and a large decrease in motor speed correspond with only a small increase in torque (in some cases, no increase at all). To determine if the electric motor may have problems, compare the peak motor current just before torque switch trip with the motor torque/speed curve for the specific electric motor to help estimate electric motor margins. By way of example, Figure 45 is a current history for a valve closing against a design-basis load; Figure 46 is the ac motor torque speed curve for the operator motor. Comparing the current drawn in Figure 45 with the motor torque speed curve, even though the current transducer is nearly saturated on this stroke, we see that the motor is operating well out on the knee of the motor torque speed curve. Figure 47 shows the motor current during the next valve closure against a design-basis flow load. During this second test, which was performed within five minutes of the test shown in Figure 45, the motor went into a stall. [Careful examination of the motor current trace from the previous cycle (Figure 45) would have alerted the analyst to the impending problem.] Motor heat and voltage drop, in conjunction with a marginally sized electric motor, were the primary causes of the stall. If the analyst cannot obtain a motor torque speed curve for a specific motor, it may be necessary to conduct dynamometer testing to produce such a curve to determine motor margins.

4.2.2.2 Position-Controlled Alternating Current Motor Operators. The analyst must subject the position-controlled valve to its design-basis loading, by in situ or prototype testing, to make an analysis that is equivalent to that previously described for torque-controlled valves. Again, the analyst may want to consider dynamometer testing of the motor operator.

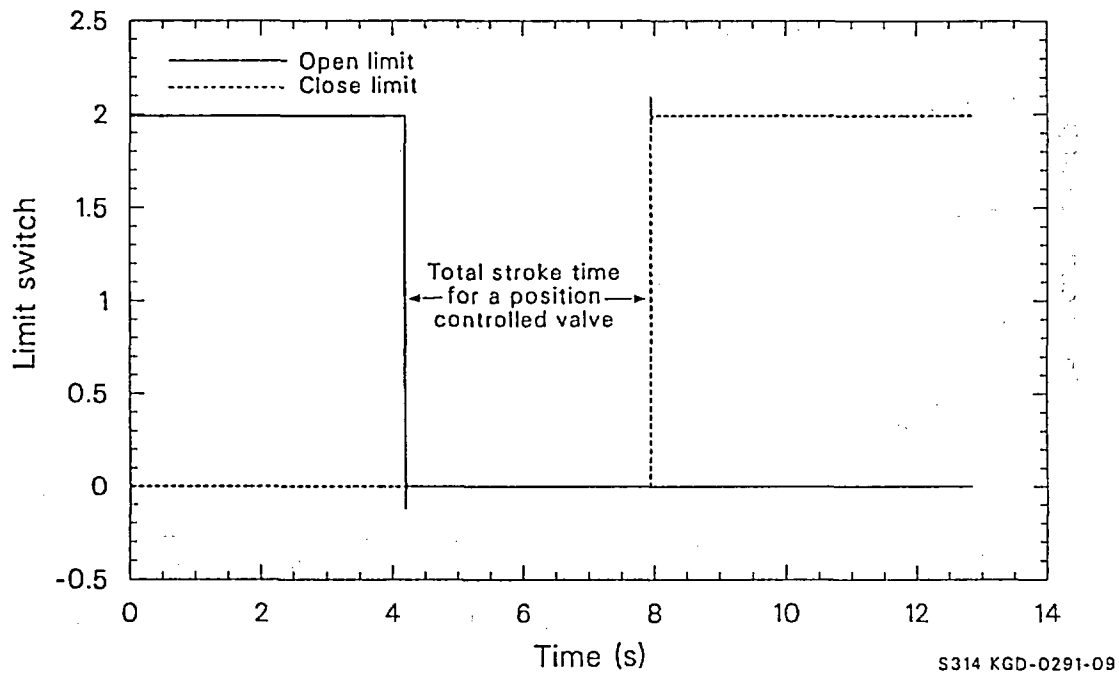


Figure 43. Limit switch history showing stroke time for a position-controlled valve. Limit switch actuation points are important when analyzing other data.

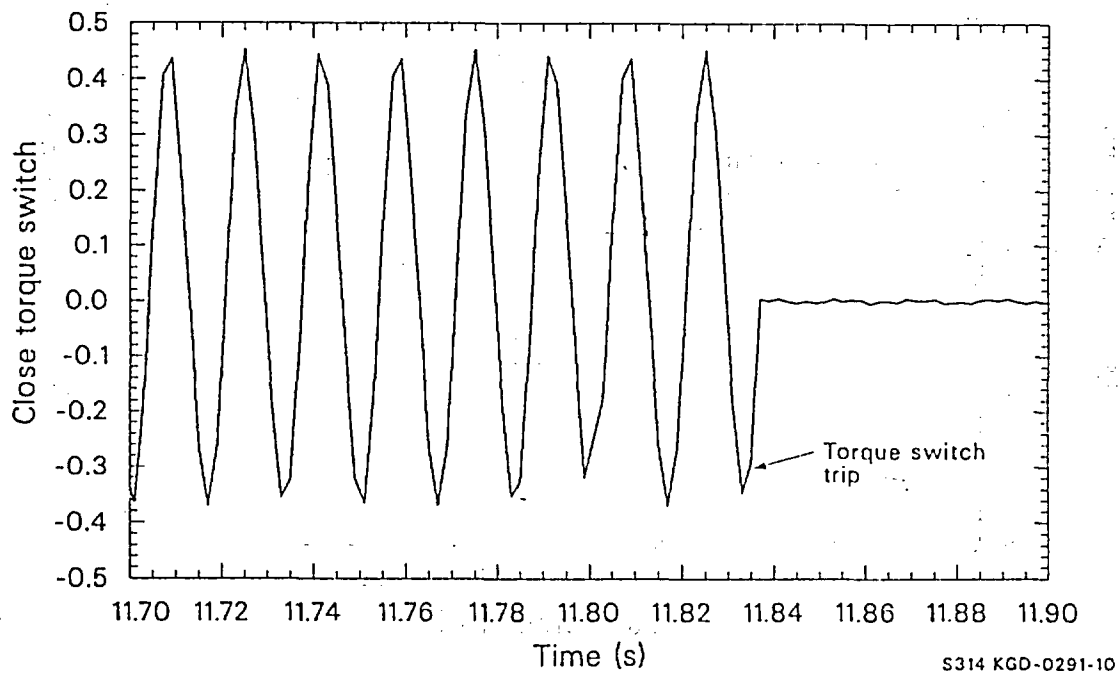


Figure 44. Torque switch history showing torque switch trip and the termination of current flow to the motor controller holding coil.

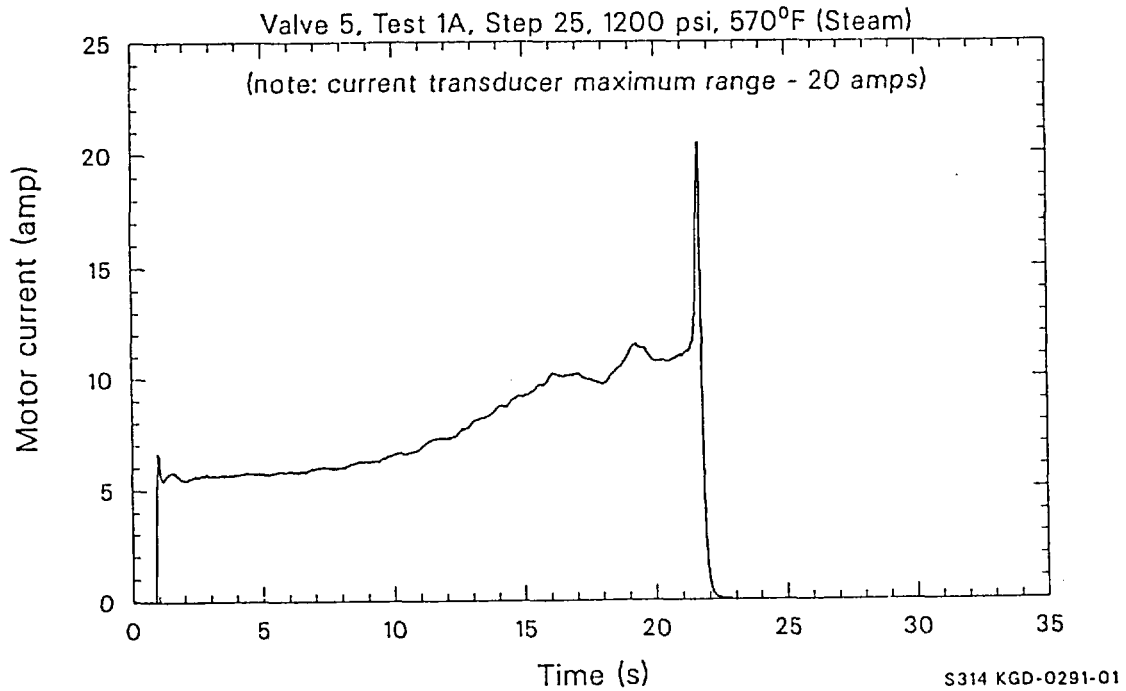


Figure 45. Current history from a design-basis test showing current increasing as the valve closes; the rapid increase in current indicates torque switch trip. The test began with the valve 75% open.

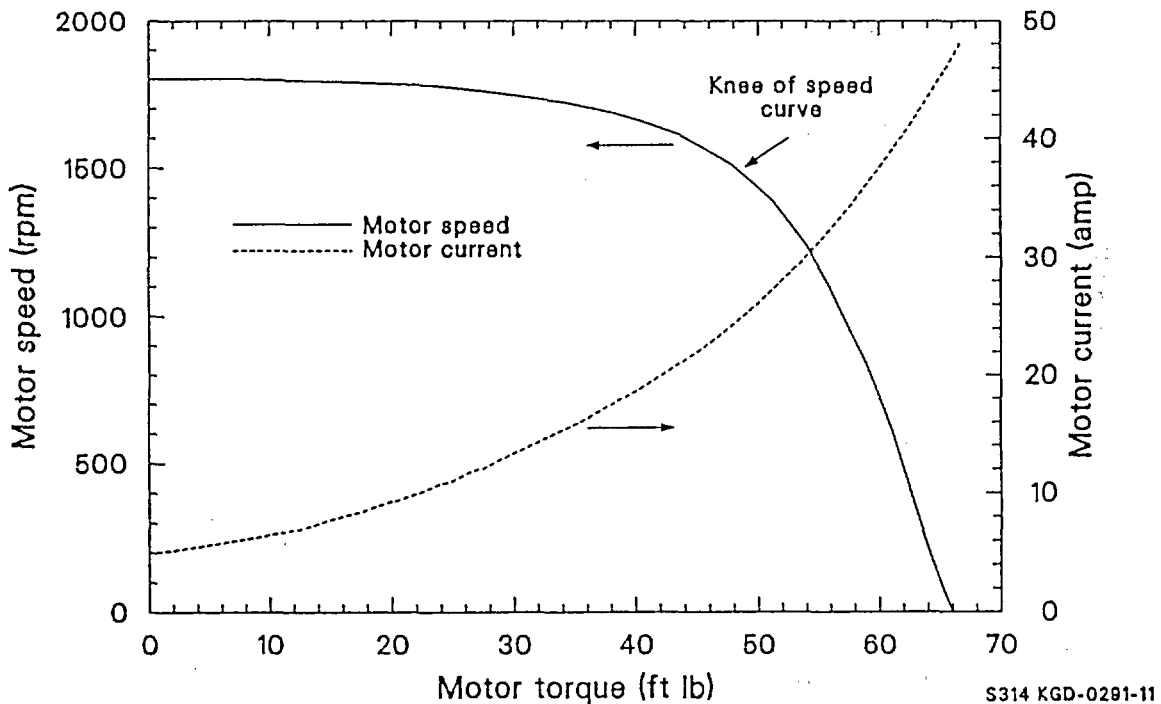


Figure 46. Motor torque-speed curve showing the speed-torque-current relationship for the ac motor test results shown in Figure 45. Beyond the knee of the curve, the torque increase is small in proportion to the speed loss and the current increase. For some motor configurations there is no increase; for some there is actually a decrease in torque beyond the knee of the speed curve. (Arrows indicate the applicable axis.)

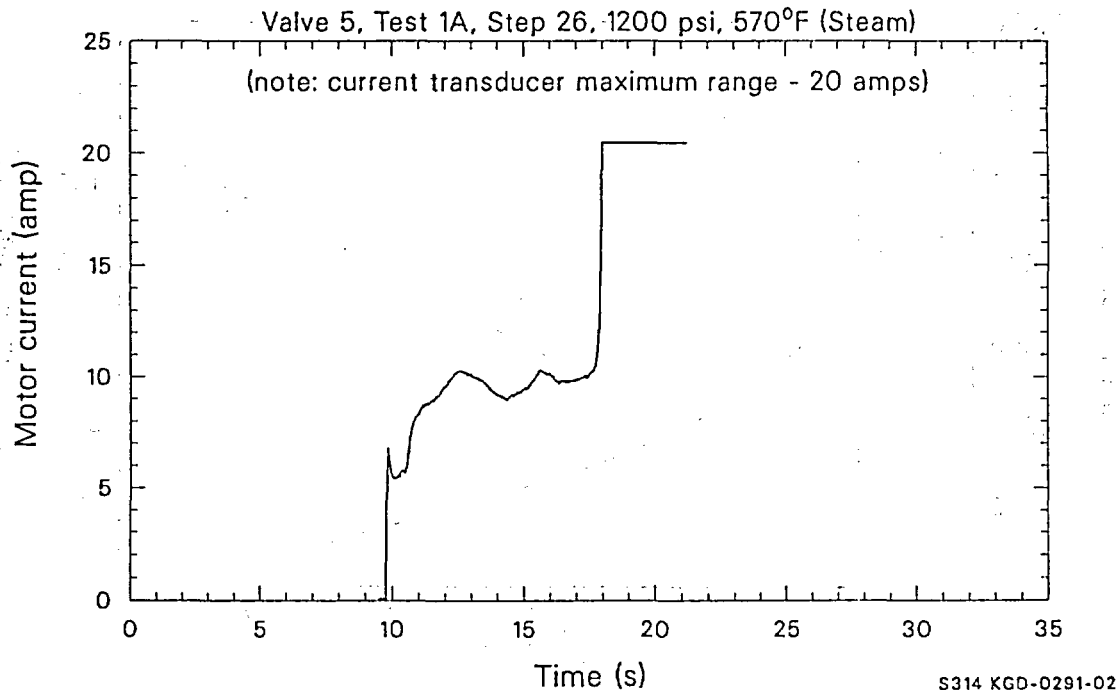


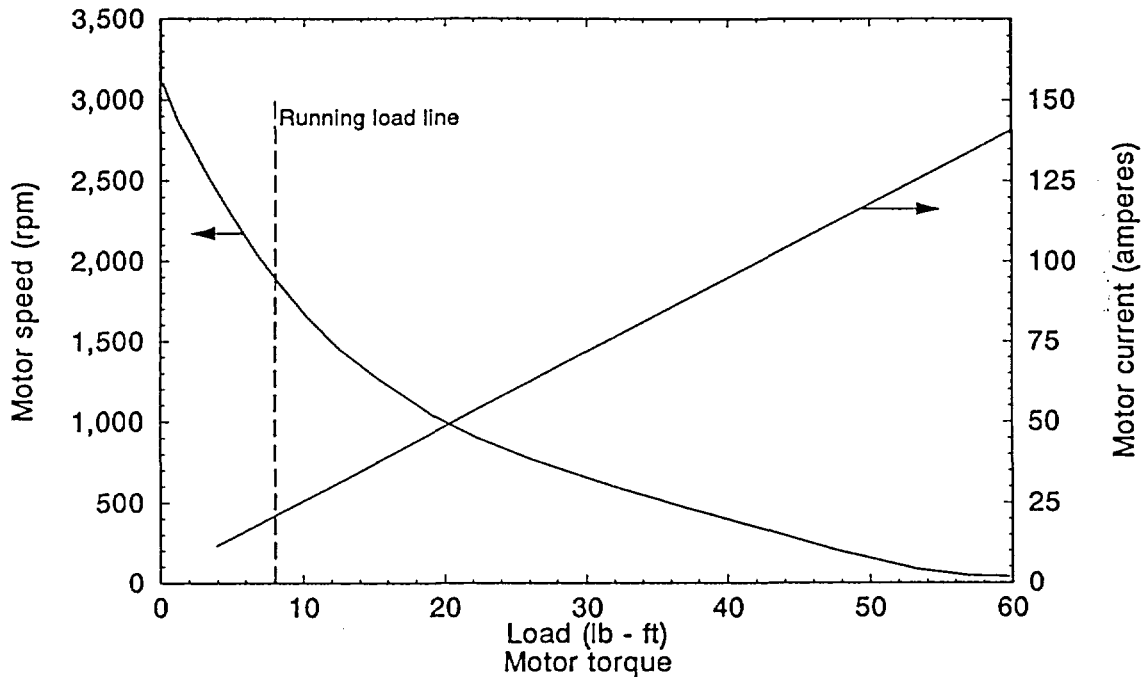
Figure 47. Current history from a design-basis test showing the motor going into a stall, saturating the current transducer. The test began with the valve 30% open.

NOTE: All other readings of motor current for both torque and position controlled valves are made for trending. Additionally complicating the subject, Limitorque has publicly informed the industry that ac motors of a given model operating under the same conditions can vary up to 20% in their output.

4.2.2.3 Direct Current Motor Operators. As in the previous analysis, the dc MOV must be loaded before torque or limit switch trip. The analyst can then compare the motor current to the motor torque speed curve to determine how far out on the curve the motor is operating. Figure 48 shows that, unlike ac motors, dc motors continue to produce torque linearly even as they approach stall conditions; however, at the lower motor speeds that accompany the higher operating currents, the effects of motor momentum are less. As a result, the lower motor speeds produced under high loads can affect the stroke time, as shown in Figure 49. In addition, dc motors operating at high loads can heat up very quickly, which in turn reduces their output torque. Figure 50 shows the drop in output torque over time for a 40 ft-lb dc

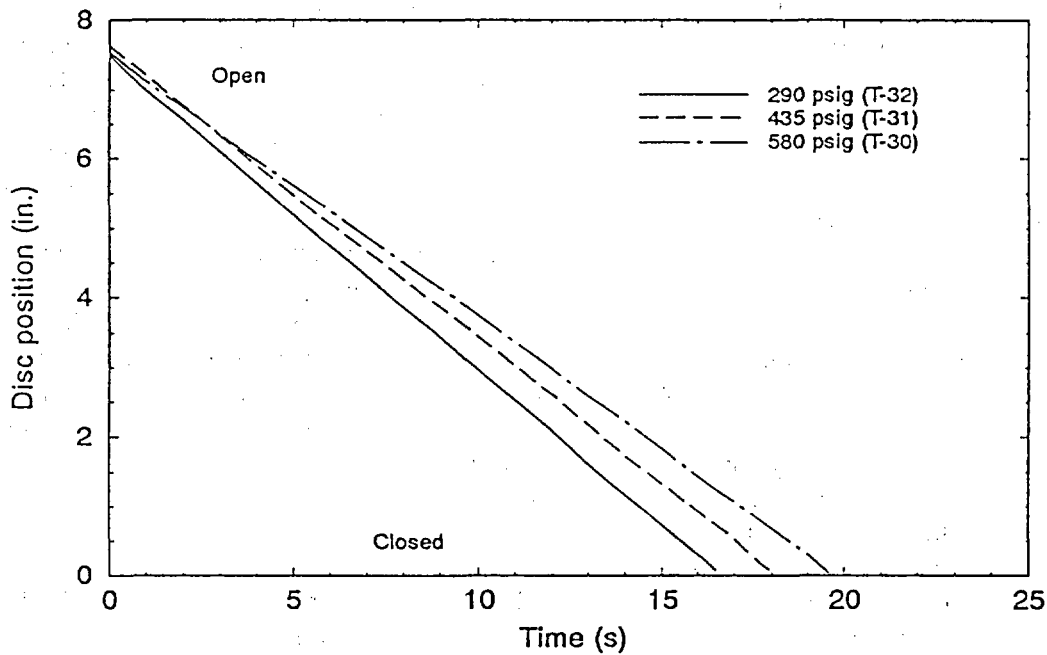
motor as it heated. Degraded voltage (because of line losses) can also reduce the output of the motor. As the motor turns at lower speeds, the overall efficiency of the operator is reduced. Figure 51 shows the results of these effects. The test at the lowest loadings closed the valve, and the motor tripped out on the torque switches. The tests at the next two higher loadings did not close the valve, but the motor was able to generate enough torque to trip the torque switch. However, the test at the highest load not only did not close the valve, but because of the efficiency losses in the motor circuit, it was also unable to generate enough torque to trip the torque switch and therefore stalled the unit. These factors, working separately or together, can thus produce motor stall and motor burnout.

4.2.3 Motor Voltage. Voltage drop under load can alert the analyst to undersized cables in the power circuit. It has been found on a number of occasions that some plant circuit designers did not realize that both ac and dc motors can operate at four to five times the running current stamped



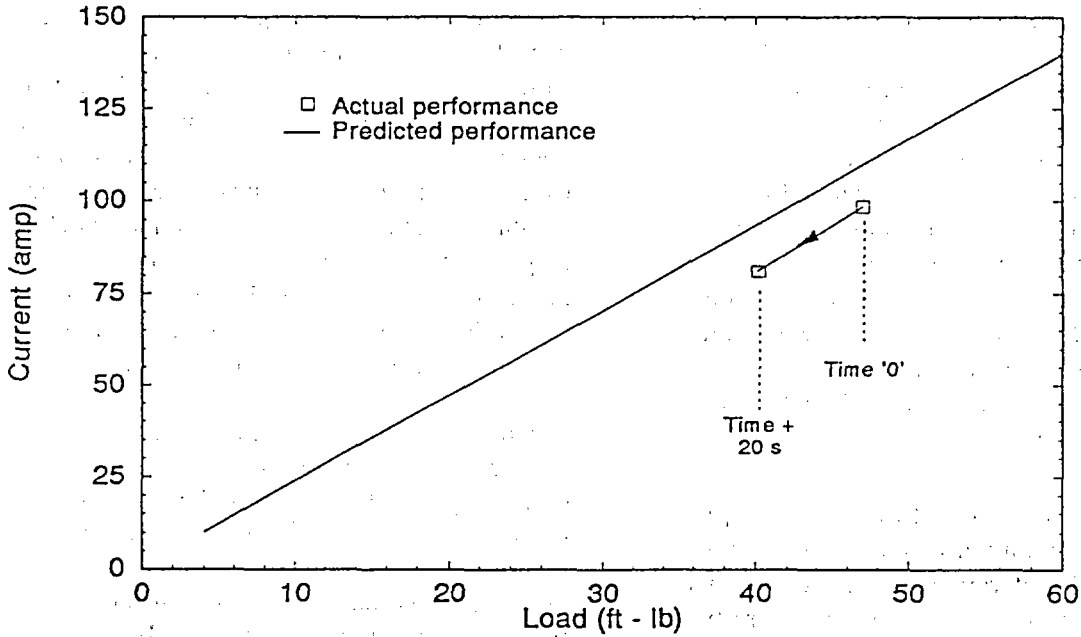
M611 kgd-0592-01

Figure 48. Motor torque-speed curve showing the speed-torque-current relationship for a dc motor. The torque (load) continues to increase as the speed drops and the current increases. (Arrows indicate the applicable axis.)



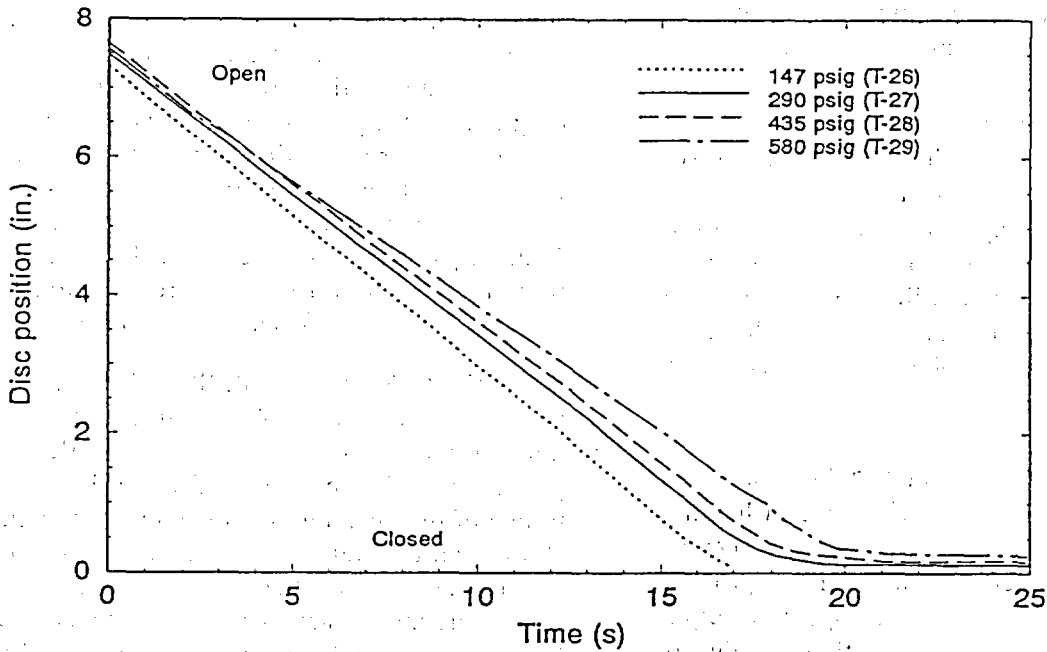
M248 kgd-0291-02

Figure 49. Disc position histories from three dc-powered closing tests showing that the stroke time is longer with higher loads.



M248 kgd-0391-05

Figure 50. Motor heating under load caused the current demand of this dc motor to decrease at a rate of 1 amp per second during the 20-second test, resulting in a decrease in the output torque of approximately 1 ft-lb every 2 seconds.



M248 kgd-0291-03

Figure 51. Disc position histories from four dc-powered MOV closing tests, showing that the stroke time is longer with higher loads. Three of the tests did not fully seat the valve, and the test at the highest load stalled the motor.

on the motor nameplate, and therefore specified less than adequately sized power cables. Not long ago, a utility traced several burned out dc motors to this undersized-cable problem. Limitorque has publicly stated on a number of occasions that, for the small number of dc motor-operated valves in the industry (compared to the large number of ac motor-operated valves), the percentage of replaced dc motors far exceeds that of ac motors. This increased incidence is probably a result of the lower dc voltages and the associated higher current to perform the same work as the higher voltage, lower current ac motor.

It should also be noted that in the typical Limitorque dc motor wiring circuit, it is impossible to accurately determine the voltage drop in the circuit from one measurement. There are typically four wires that conduct the motor current and interconnect the motor controller and the motor. Two of the wires interconnect the armature and the series field; this interconnection provides the ability to reverse the direction of the motor. Since the resistance of each wire contributes to the voltage drop, any single measurement of motor voltage will be contaminated by a voltage drop caused by a minimum of two wires.

Previously unexplained motor burnouts may be the result of excessive voltage drop in the power circuit; a voltage check at the highest valve loading possible may provide the explanation. The voltage check will also aid the analyst who needs to know the actual line losses at normal voltage conditions so that the additional losses at design-basis degraded voltage conditions can be calculated.

4.2.4 Motor Operator Torque. Load-sensitive motor-operated valve behavior (rate of loading explained in Section 4.3) and the need to establish individual valve performance margins provide the incentive to measure motor operator output torque. Some of the new-generation transducers measure motor operator output/stem torque directly. Where these new transducers are not available, special-effects testing at the INEL is providing an increasing data base showing that the relationship between spring pack force or

deflection and output torque is very constant and not affected by the loading on the operator. Figures 52 through 54 show that the ratio of spring force divided by stem torque (the torque applied to the stem by the stem nut) does not vary over a wide range of loadings. Figure 52 is from a lightly loaded test with a low torque switch setting. Figures 53 and 54 are from tests with higher loads and with a high torque switch setting. (The stem force histories from those two tests are shown in Figures 55 and 56.)

Motor operator torque measurements are used in determining the stem factor (operator torque divided by stem force) part of the margins assessment for a specific valve and provides a second reference for the indirect- or direct-force measurements made with some of today's stem force measurement transducers. To reduce the potential errors in indirect torque measurements, the analyst should obtain detailed calculations for spring pack force or deflection versus operator torque. The spring pack should be calibrated to determine any offset from the published Limitorque spring constant for each spring pack assembly. Figure 57 shows a spring pack calibration. Using this kind of information and the specific operator moment arm, the analyst can obtain reliable values for the operator output torque from many of the commercially available spring force or deflection transducers. Torque determined from static testing will not provide useful information for stem factor determination. Both torque- and position-controlled valves need to be tested with a flow and pressure load to properly load the stem-stem nut interface.

4.2.5 Valve Stem Force. Stem force in both position- and torque-controlled valves can best be determined from measurements. While it is possible to estimate the stem force if the output torque of the operator is known, our experience shows that the stem factor varies significantly with load. However, if the analyst knows the operator torque and the stem force, the stem factor can be determined by the operator torque divided by the stem force. Note that the operator torque and stem force measurements must be obtained just before the valve hard seats; after the valve starts wedging, there is almost no motion between the stem nut and the stem, so no useful value can be

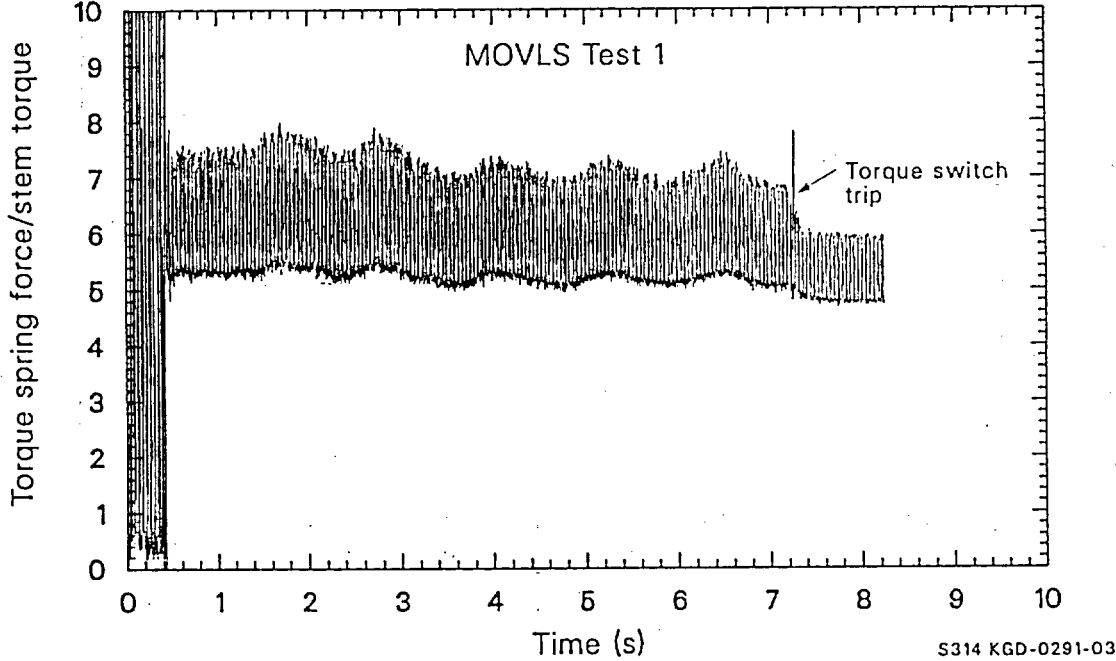


Figure 52. Ratio of torque spring force to stem torque from MOVLS Test 1, with a small stem force.

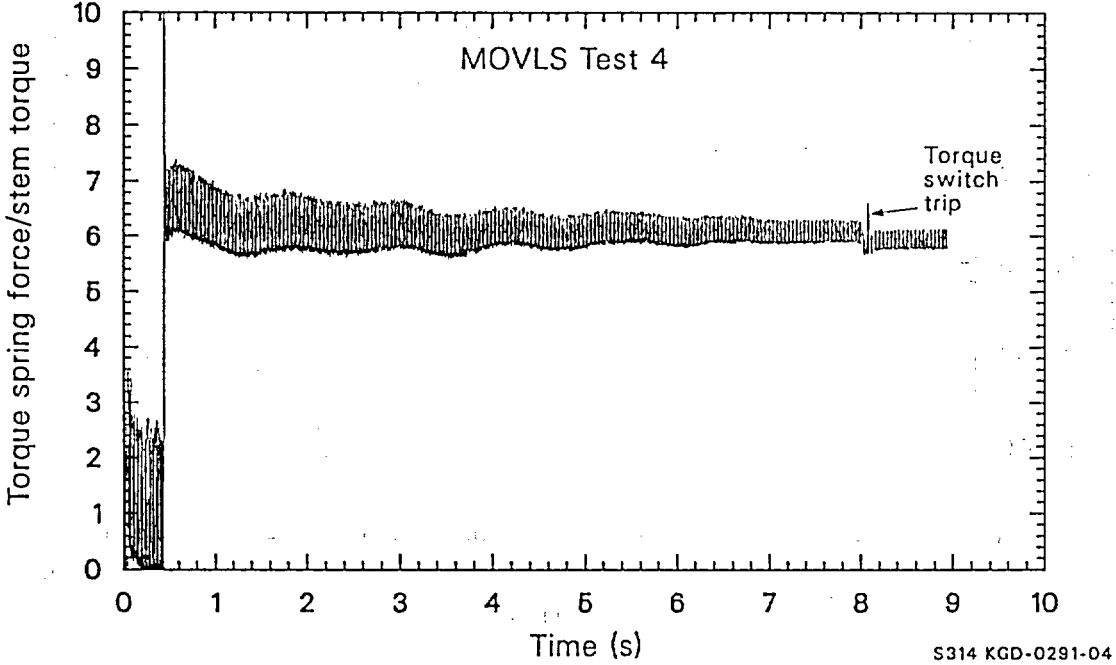


Figure 53. Ratio of torque spring force to stem torque from MOVLS Test 4 at a higher stem force.

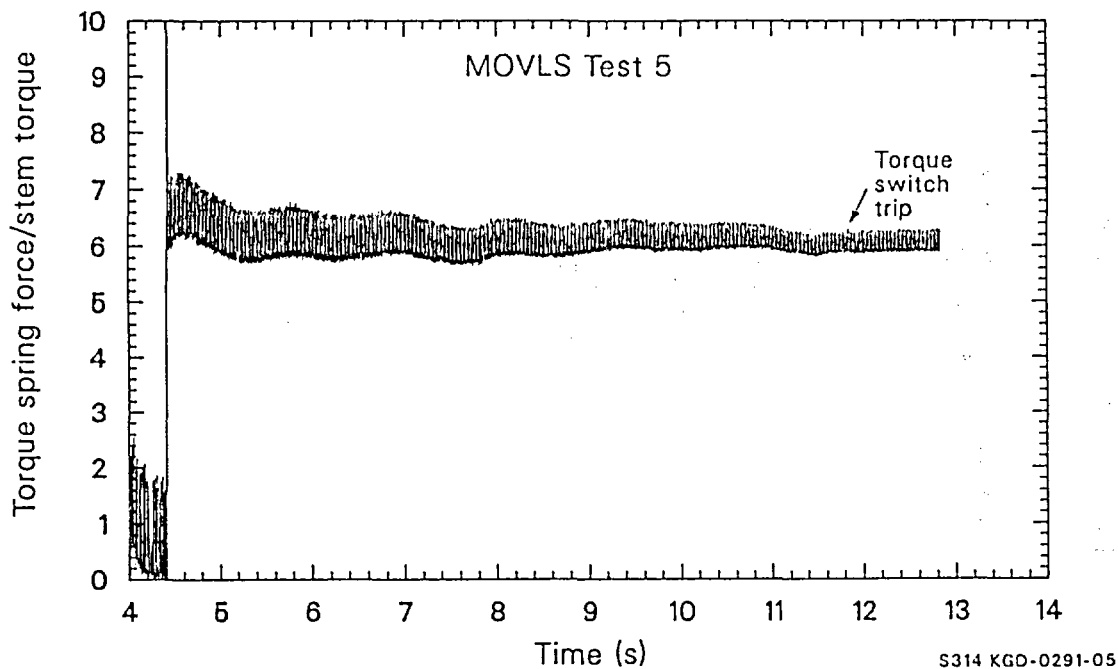


Figure 54. Ratio of torque spring force to stem torque from MOVLS Test 5, at a high stem force, in which final seating was not achieved, showing that the average torque spring force to stem torque ratio was not influenced by the load on the operator.

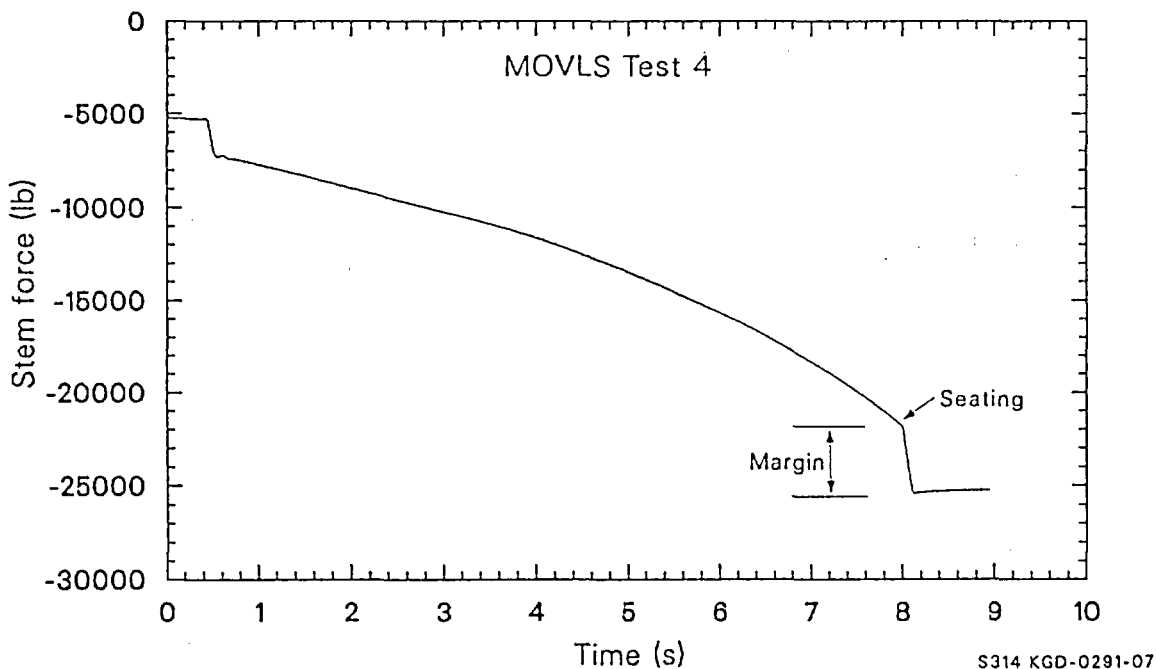


Figure 55. Stem force history from MOVLS Test 4, showing a 3000 lb_f margin between the peak stem force and the stem force at final seating.

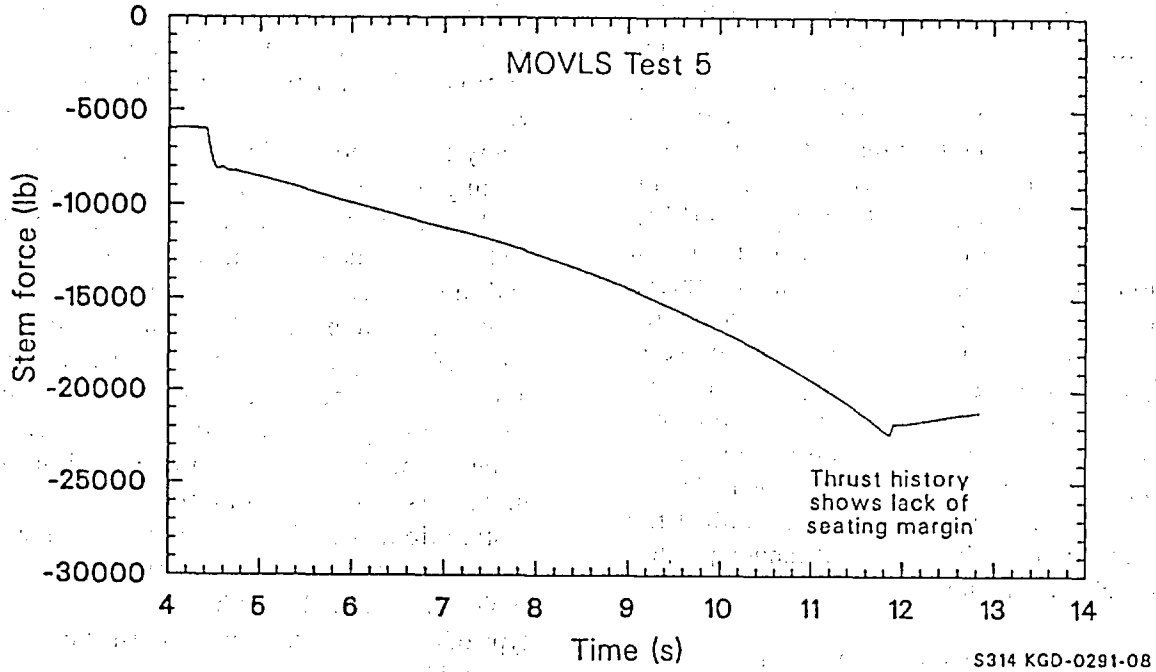


Figure 56. Stem force history from MOVLS Test 5, showing that a 1000 lb_f increase in the initial stem force eliminated the 3000 lb_f final seating stem force margin observed in MOVLS Test 4.

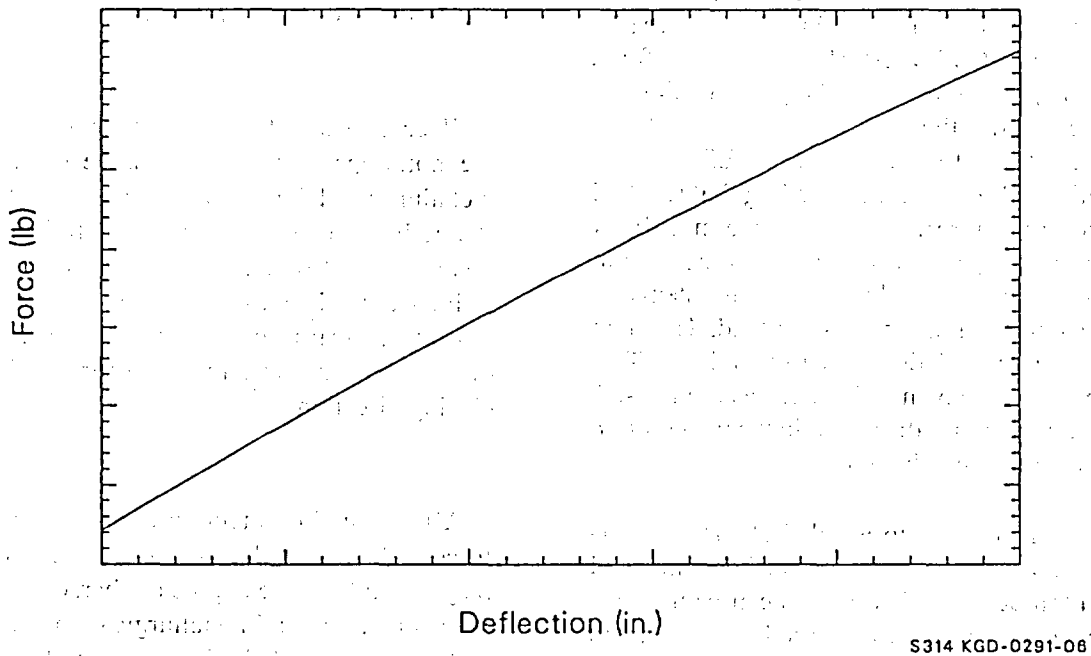


Figure 57. Typical torque spring calibration plot shows the initial force offset at zero deflection. This figure also confirms that for this spring, the spring force to deflection relationship is linear. The actual values are omitted from this figure because the data are proprietary until the MOV diagnostic equipment validation is complete.

obtained for the stem factor. After the analyst has determined the stem factor and how well the conversion of operator torque to stem force is taking place, extremely good or bad stem factors can alert the analyst to either faulty torque or force measurements or to problems at the stem-to-stem-nut interface. Limitorque selection guides (SEL) provide stem factors at several coefficients of friction for most popular stem diameter, thread pitch, and lead combinations. Accurate stem force measurements can also alert the analyst to excessively high packing loads. Packing loads that are higher than allowed by the design calculations can adversely affect the valve's ability to function when pressure and flow loads are added. Current and torque measurements can also alert the analyst to high packing loads, but cannot quantify the actual packing drag.

For torque- and position-controlled valves, the stem force measurement also can be used to determine the available stem force margin if the valve is tested at design-basis flow and pressure loads. Stem force values obtained from less than fully loaded tests cannot be used to establish fully loaded stem force margins. Figures 55 and 56 show why this is so. Figure 55 is a stem force history from an MOVLS test, showing a stem force margin of approximately 3000 lb_f (see Section 4.3 for a discussion of the MOVLS). Figure 56 shows the stem force history from an MOVLS test with an additional 1000 lb_f initial loading that resulted in no seating margin. A stem force margin of 3000 lb_f was wiped out by a 1000 lb_f increase in the initial stem force loading because the stem factor increased with the increase in load. The stem factor increased 6% during the second test. This phenomenon is known in industry as the rate-of-loading effect, and is discussed in the next section as a load-sensitive behavior.

Although not useful to establish stem force margins, stem force measurement data from unloaded tests on torque-controlled valves can be used for trending. Changes in the measured stem force can alert the analyst to problems with the valve or with the measurement system. Stem force measurements from unloaded position-controlled valves will provide the analyst with little useful information, as the only load in the stem is the packing load.

Inaccuracies in the stem force measurements do occur; this affects the reliability of data from testing either torque- or position-controlled valves. Valve stem force transducers come in many types and applications. The accuracy of strain gages depends on accurate characterization of the materials involved, the expertise of the installer, the quality of the installation technique, and in some cases the accuracy of the in-place calibration. Removing the stem from the valve and performing a calibration of the strain gages in a tensile machine can determine their accuracy. The accuracy of stem collar transducers also depends on extensive characterization of the materials involved and the quality of the installation. All of these instruments measure very small reaction loads in materials that are typically specified only by type. Without some type of calibration, the analyst must choose either the middle of the material's properties range or a conservative high or low bound, depending on the calculation. All of these problems are magnified when the stem force measurement must be made in the threaded portion of the stem. Using strain gages installed on the yoke can result in a combination of these problems.

Placing load cells between the valve yoke and the motor operator requires that the attaching bolt metallurgy and the structural stiffness of the yoke flange be known. The structural stiffness of the yoke flange also affects the calibration, if strain bolts are used to attach the yoke to the motor operator. Strain bolts without other intrusive devices will measure the stem force only in the closing direction.

All of the above technologies measure stem force with varying degrees of accuracy; the accuracy depends on the degree of characterization of the geometrical and metallurgical considerations and the quality of the installation. The sensitivities and overall accuracies of all the current commercial diagnostic torque and thrust measuring systems will be better known after the NRC/Motor-Operated Valve Users Group completes its validation testing and evaluation.

4.3 Load-Sensitive Motor-Operated Valve Behavior

The MOVLS in its simplest configuration was built to help develop our field test instrumentation and data acquisition equipment. Following our Phase II gate valve testing, the MOVLS was improved to perform special effects testing. It was again improved for the diagnostic equipment validation program. Its current configuration, shown in Figure 58, consists of a Limitorque operator bolted to a valve yoke, which in turn is bolted to a hydraulic cylinder. The cylinder discharges to an accumulator, and the operator resistive loads are varied by controlling the initial fluid level and initial gas charge in the accumulator. The output thrust from the operator is transferred to the hydraulic cylinder through a valve stem, a thrust bearing, and a load cell. A torque arm is bolted to the valve stem and serves two purposes: it acts as an anti-rotation device and is instrumented to measure the torque in the stem.

Instrumentation used on the MOVLS includes 3-phase current (both rms and peak to peak), rms voltage, 3-phase power and power factor, motor speed, open and close limit switch positions, torque switch position and trip signals, spring pack position and force, and the stem force, torque, and position. The data acquisition system typically runs at 1000 Hz, resulting in a 1-ms time resolution. Loadings in the stem can be varied from a no-load condition to design-basis-type loads. Stem thrust histories obtained from our MOVLS compare very favorably with stem thrust histories obtained from full-scale valve tests we obtained in the field. The MOVLS provides an economical means of producing realistic valve loadings in the laboratory and allows us to study operator-related phenomena that we have observed in our full-scale valve tests.

Load-sensitive MOV behavior describes the phenomenon in which the maximum output thrust of a rising-stem MOV at torque switch trip decreases as the load on the stem increases. This

phenomenon has been observed throughout the industry and occurred on two occasions during our full-scale valve test programs. Although we lacked sufficient instrumentation and analyses to pinpoint all of the possible causes of this phenomenon at the time it occurred, we were able to determine that it occurred when the torque switch was not set high enough to fully seat the valve. Since then, we have been able to use the INEL MOVLS to perform the separate effects testing necessary to isolate the first-order cause of the phenomenon.

Using the MOVLS, we performed a series of 17 simulated valve closings. The first seven were setup tests and will not be part of this discussion. The 10 tests that will be discussed are shown in Figures 59 through 61, which show the thrust histories for each of these tests. Each of these tests had the same torque switch setting. The only variable from test to test was the stem load applied by the simulator. The first three tests shown in Figure 59 are low load closures, typical of what could be obtained during inplant testing while the valve is under pressure with no flow through it. These low load tests were followed by the four tests shown in Figure 60. During these tests, the closing load was increased before Test 11 and again before Test 12. Thereafter, the closing load was not increased. Test 11 is representative of a valve closing against a pressure and flow load and shows that increasing the stem load results in a small decrease in the thrust margin. The thrust margin is the difference between the thrust at the time the valve seats and the thrust at torque switch trip. During Test 12, the stem load is again increased and results in a larger decrease in the thrust margin. For comparison purposes, Test 12 is equivalent to slightly less than the design-basis loading of a typical predictable 6-in. BWR RWCU flexwedge gate valve.

Tests 13 and 14 represent two additional tests at the same stem loading as Test 12 and show that, with a constant load, the thrust margin continues to decrease. Test 13 has effectively no thrust margin and the simulator was just able to seat. Test 14 shows a negative thrust margin and the simulator does not seat. At the full design-basis loading, we have been able to create the

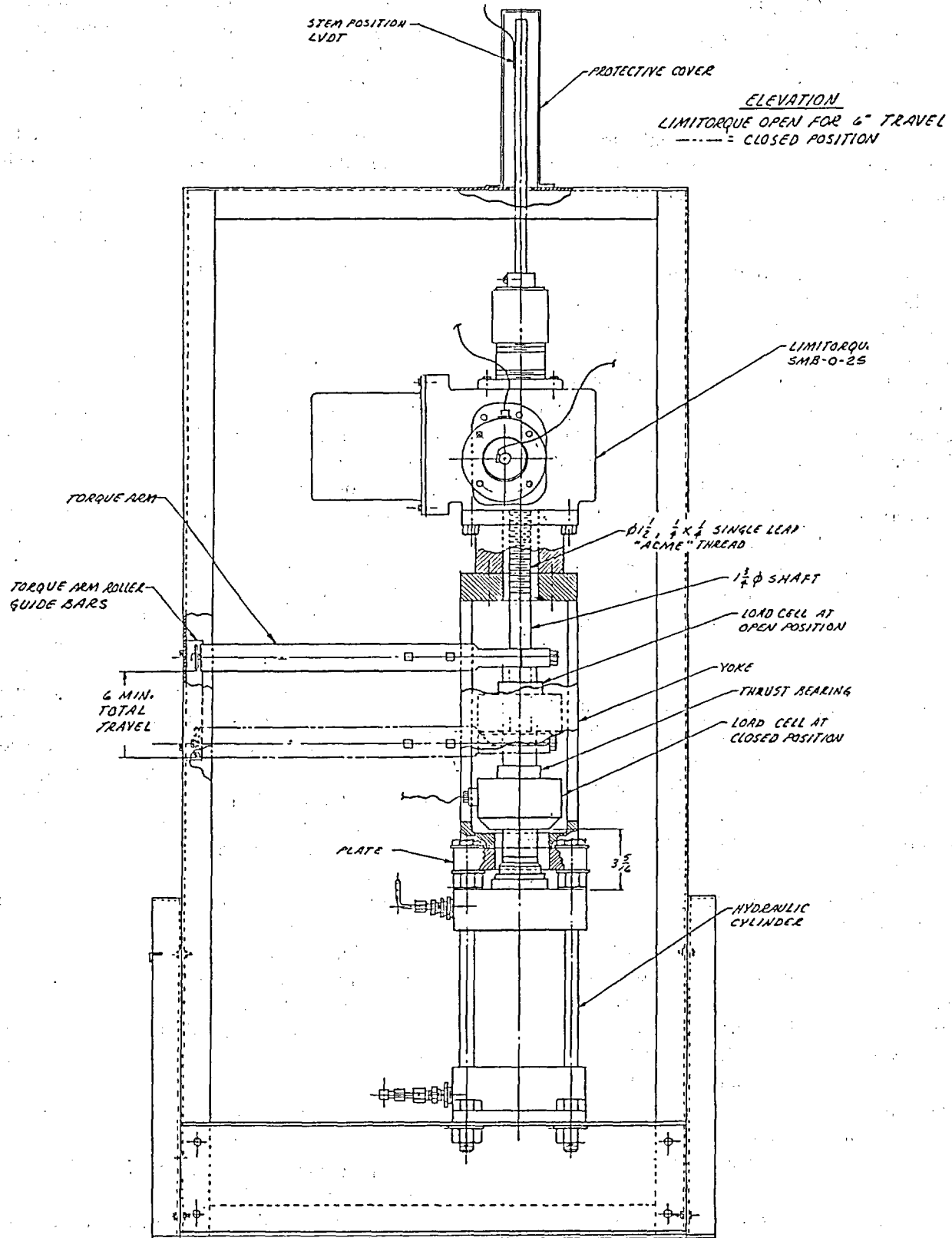
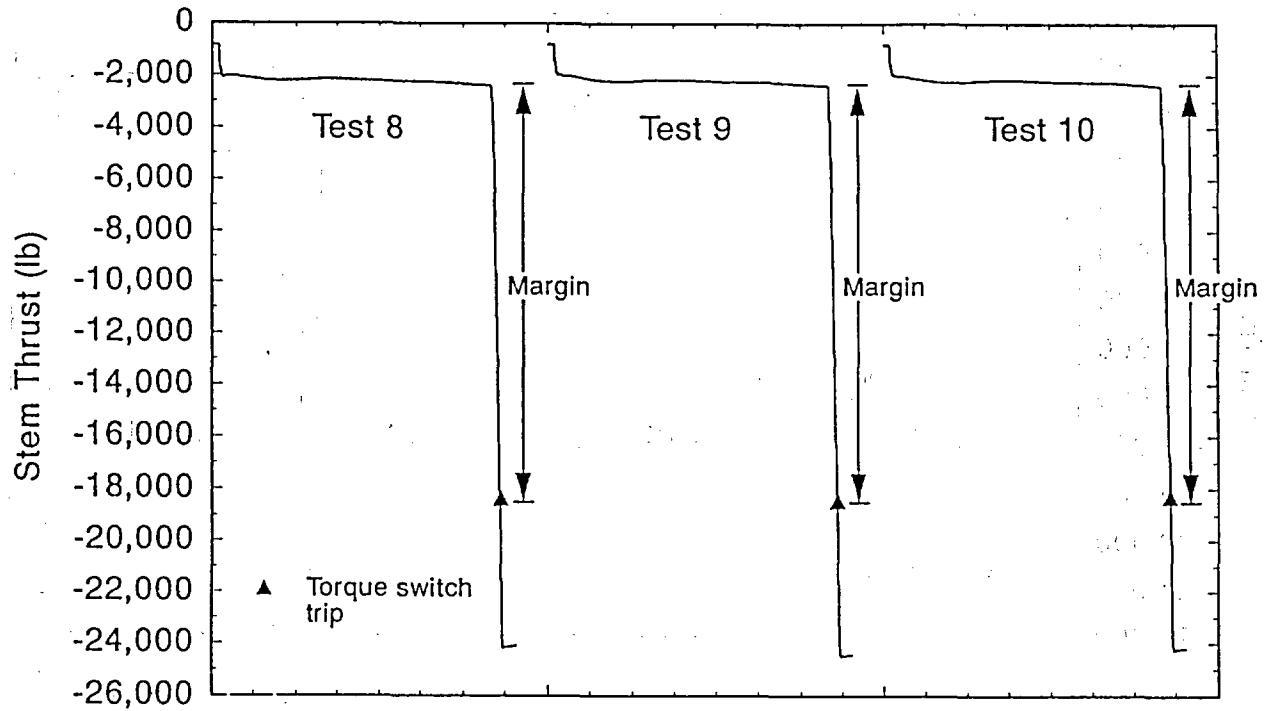
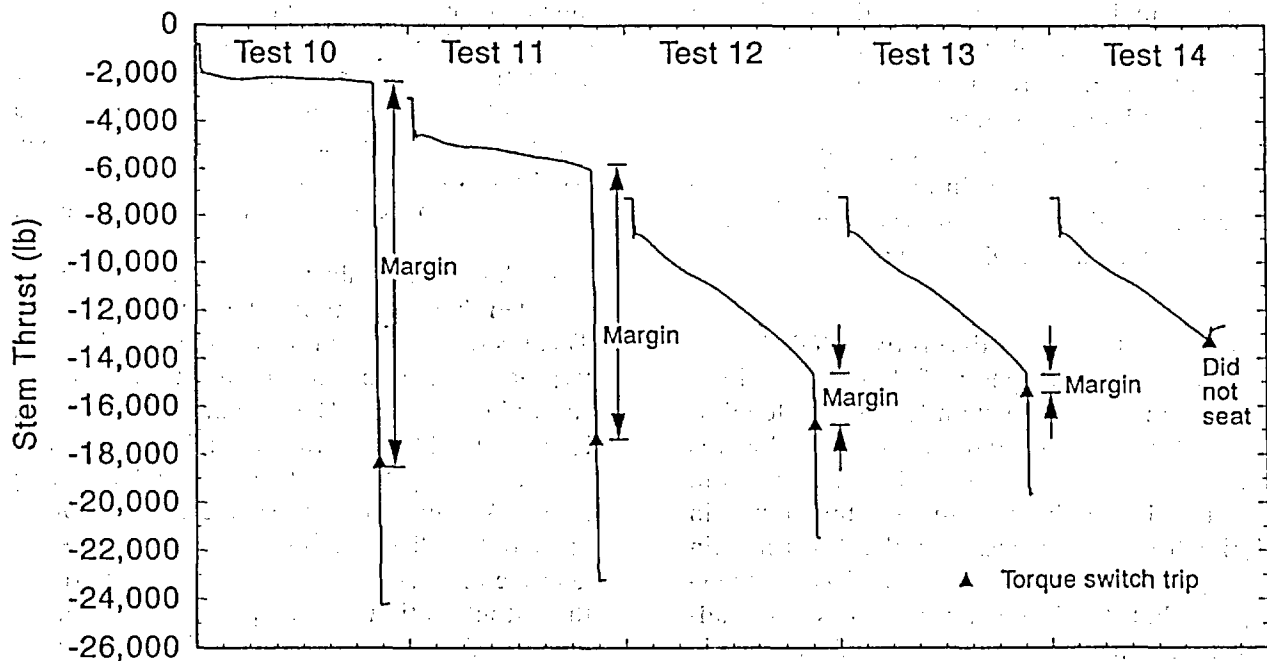


Figure 58. MOVLS layout drawing.



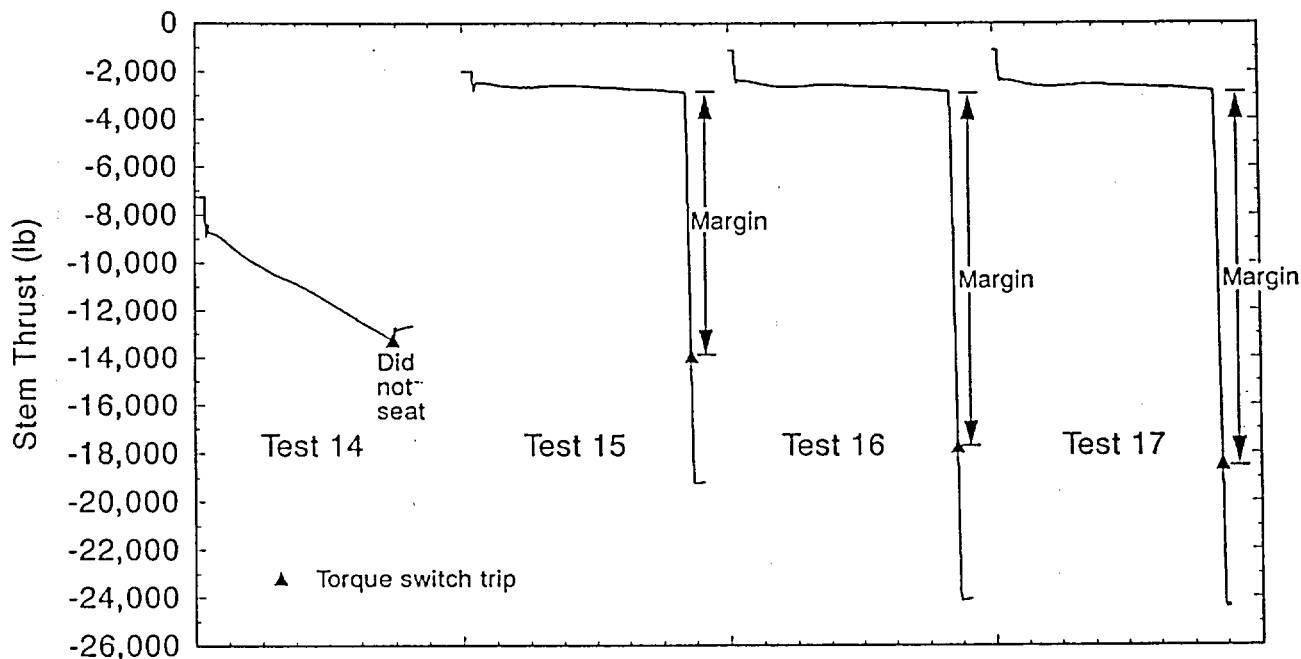
M450 rs-1091-09

Figure 59. Traces of thrust versus time for Tests 8 through 10 of the MOVLS test sequence. These are identical low-thrust tests.



M450 rs-1091-10

Figure 60. Traces of thrust versus time for Tests 10 through 14 of the MOVLS test sequence.



M450 rs-1091-11

Figure 61. Traces of thrust versus time for the final three tests of the MOVLS test sequence. Tests 12–14, which exhibit load-sensitive MOV behavior, were followed by a series of low-thrust tests (Tests 15–17), with resistance to closing much like the first three of the series.

Test 14 response in a single step following Test 11. However, we went through the transition from normal stem behavior to abnormal stem behavior so quickly that we were not positive of the root cause. Performing the test at a lower loading, and repeating it, provided further insight about the cause of load-sensitive MOV behavior, as we will discuss later in this section. We are aware that three near-design-basis closures back to back are not a normal design requirement.

We expected this load-sensitive MOV behavior, based on the setup tests. Following the above tests, we reduced the stem load to the level of Tests 8 through 10 and repeated the closures three times. Tests 15, 16, and 17 are shown in Figure 61. We observed that the thrust margin during Test 15 was less than the thrust margin during Tests 8, 9, 10, 16, and 17. This was unexpected, but it did indicate that the MOV load-sensitive behavior was the result of a change in some parameter that we should be able to isolate.

To better understand this phenomenon, and to be sure it was not a combination of causes, kinematic and kinetic evaluations of the motor-operated valve were performed. Based on these evaluations, we identified potential first-order causes of this phenomenon. Using measured data taken from the MOVLS testing discussed above, we then evaluated the likelihood of each contributing to the load sensitive MOV behavior.

The kinematic evaluation of the motor operator revealed that it functions like a planetary gear. There is one input path for motion, but there are two possible paths for the output motion, as shown in Figure 62. The motion input to the unit is the result of the electric motor; the two possible output motion paths are at the stem and the spring pack. Like any planetary gear, the geometry of the operator (the diameter of the gears, the number of gear teeth, etc.) does not completely determine the output motion of each path. Therefore, the kinetics of the operator were considered for more insight into the behavior of the unit. We learned

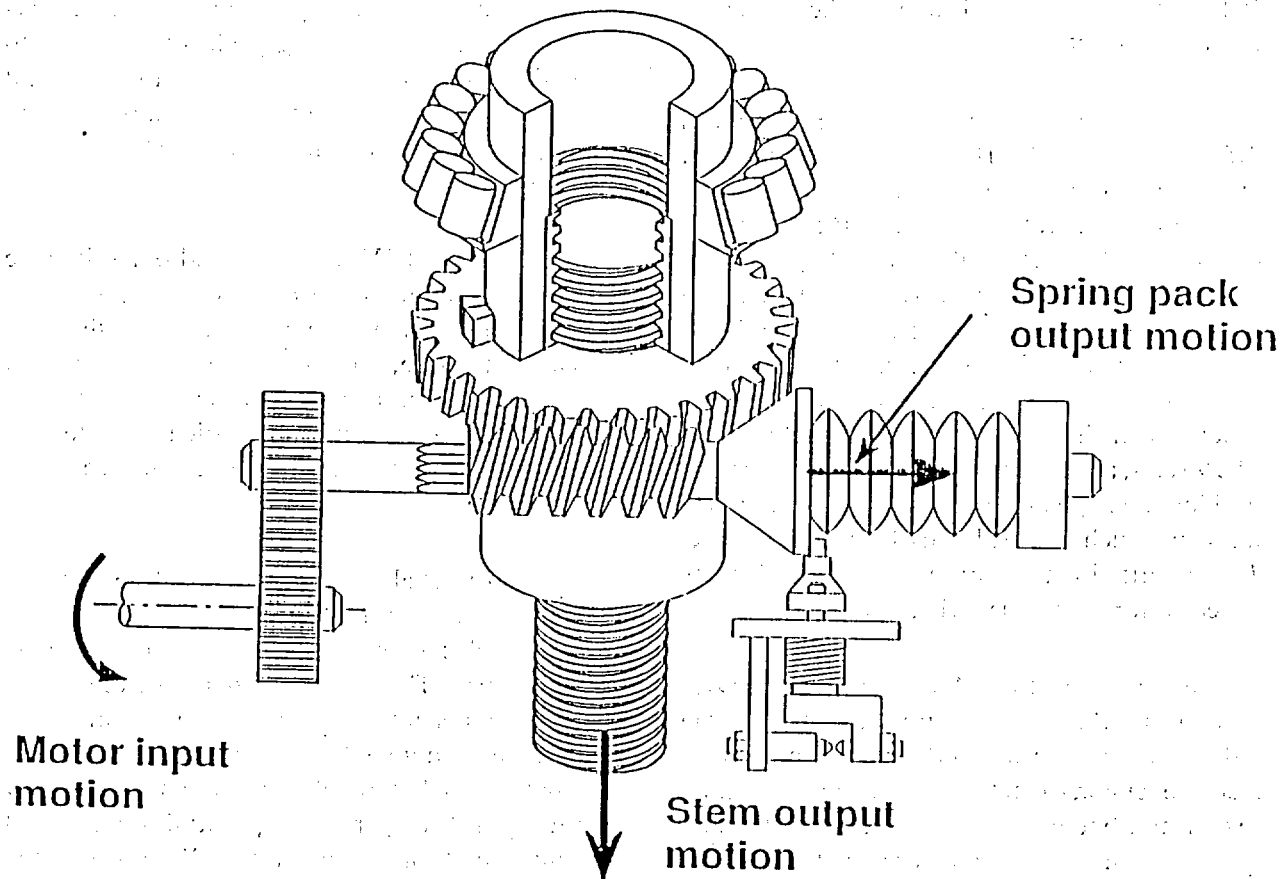


Figure 62. The design of the operator allows two potential output motion paths.

that the relative resistance to motion of each path at any given instant determines how the input motion is distributed between each of the possible output motion paths. At very low stem loads, the entire input motion is transferred to the stem. Motion of the spring pack does not occur until there is enough resistance to stem motion (observed as an increase in the stem thrust) to overcome the preload of the spring pack. Once the preload of the spring pack has been overcome, increasing the resistance to motion at the stem causes motion in both the spring pack and the stem. If the resistance to motion in the stem becomes too high (high valve closure loads or valve seating), then all the input motion will be transferred to the spring pack.

Perhaps this conversion of input motion to output motion can best be visualized with examples of a lightly loaded MOV (Test 8), a moderately loaded MOV (Test 11), and a heavily loaded

MOV (Tests 12-14). In a lightly loaded MOV, the two output motions occur, but they occur in series, one after the other. Prior to seating, the input motion to the worm drives the worm gear, resulting in motion of the stem but no motion in the spring pack. After the valve seats, motion can no longer occur in the stem, so all the input motion is transferred to the spring pack until the torque switch trips. In this situation, all the kinetic energy of the operator is transferred to the stem as the valve seats and results in operator torques and stem forces that exceed the values expected for the setting of the torque switch. Increases in stem thrusts after torque switch trip are the result of motor controller dropout time and post-torque switch trip kinetic behavior. The torque switch does not interrupt the electrical energy to the motor, it interrupts the power to the motor controller contact holding coil. Motor controller dropout time includes the collapse time of the coil

Understanding Diagnostics

field and the mechanical time for the springs to open the contacts.

The response of a moderately loaded MOV can differ significantly. If the resistance to stem motion is large enough, the increasing torque levels in the operator can overcome the spring pack preload before the valve seats. Output motion will then occur simultaneously in the stem and in the spring pack. Because there are now two simultaneous output motion paths, the increased frictional losses cause a slight reduction in the overall efficiency of the unit. As the moderately loaded MOV seats, the motor controller dropout time and the kinetic energy of the operator are transferred to the stem, much like the lightly loaded MOV case. This results in stem forces that exceed those expected for the torque switch setting.

The behavior of an MOV that is so heavily loaded that the torque switch trips before the valve seats is similar to that of a moderately loaded operator, except that the stem is not rigidly restrained because of valve seating. Consequently, the motor controller dropout time and the kinetic energy of the operator are dissipated because motion of the stem following torque switch trip and the high stem thrusts of a rigid body are not developed.

The above discussion of MOV behavior and careful analyses of the motor operator internals generated a number of potential candidates for the first-order cause of load-sensitive MOV behavior. These candidates represent one of two types of effects: frictional losses of the operator mechanism or inertial effects of the operator mechanism resulting from the stoppage of motion. We used the MOVLS-generated data to investigate each candidate and determine the single most likely cause of the observed load-sensitive behavior. To do so, we grouped each of the inertia and friction effects into one of four categories, based in part on their possible influence on motor operator behavior and in part on the type of data available from existing MOVLS instrumentation. The four categories are (a) effects that increase the load on the motor but do not influence the interaction between the torque switch and the stem, (b) effects that influence the

spring pack force at torque switch trip, (c) effects that influence the spring pack force needed to achieve the same level of stem nut torque, and (d) effects that influence the amount of stem nut torque necessary to achieve the same level of stem thrust.

Based on MOVLS testing and our full-scale valve test programs, load-sensitive MOV behavior was not observed to be associated with motor stall. Therefore, effects associated with the first category are not related to the load-sensitive behavior. Effects from the electric motor slowing down will be presented in the dc-powered MOV section.

Small inertial and large frictional possibilities are associated with the second category that could cause a change in the spring pack force at torque switch trip. These include inertia of the spring pack components and friction among them. Variations of spring pack force at torque switch trip would cascade through the mechanism and vary the operator output torque and stem thrust achieved at torque switch trip. We investigated this possibility.

Inertial and frictional effects associated with the third category could cause a change in the ratio of spring pack force to output torque. Input torque to the worm gear/drive sleeve/stem nut assembly is generated by application of the spring pack force at a moment arm distance from the stem centerline (see Figure 63). Elastic effects (worm shaft bending, for example) could change this distance a bit under varying spring pack force, resulting in a change in the ratio of spring pack force to output torque. Other effects in this category include friction between the worm shaft and worm, a component of the friction force between the worm and worm gear, and friction in the drive sleeve bearings. Inertial effects that fall into this category include those associated with acceleration of the worm or deceleration of the worm gear/drive sleeve/stem nut assembly. These additional effects are depicted in Figure 64. The summed result of all the third category effects would be an instantaneous difference between the torque input to the mechanism by the spring pack

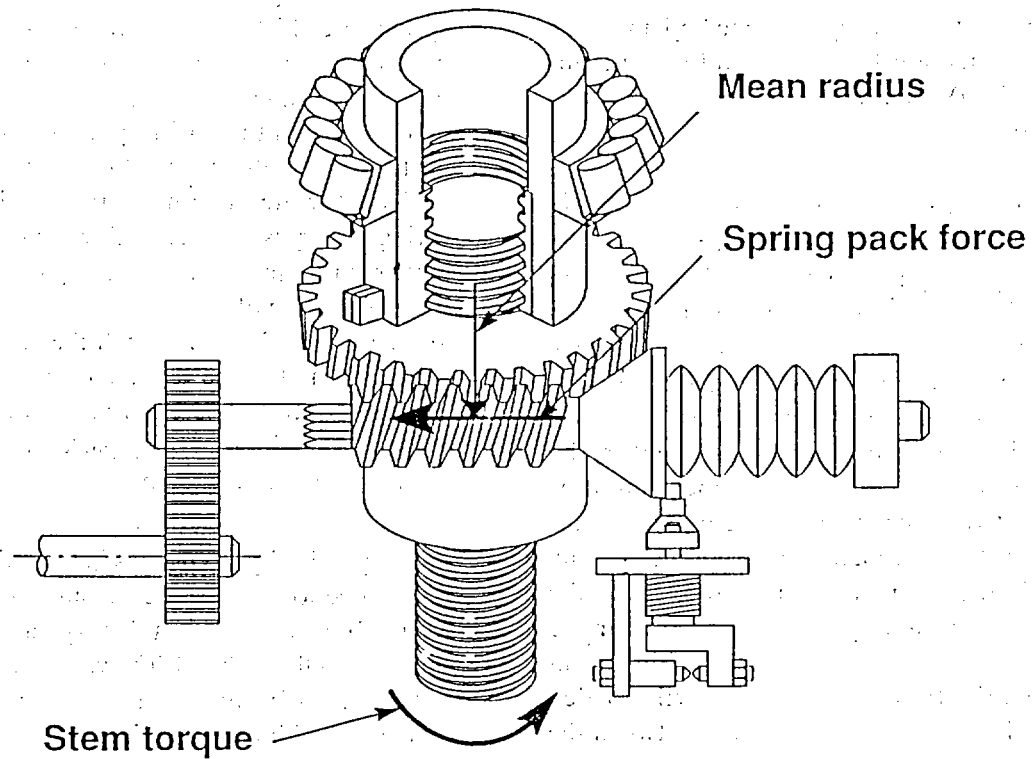


Figure 63. The application of spring pack force to the operator mechanism at an offset distance from the stem centerline generates the torque input to the mechanism.

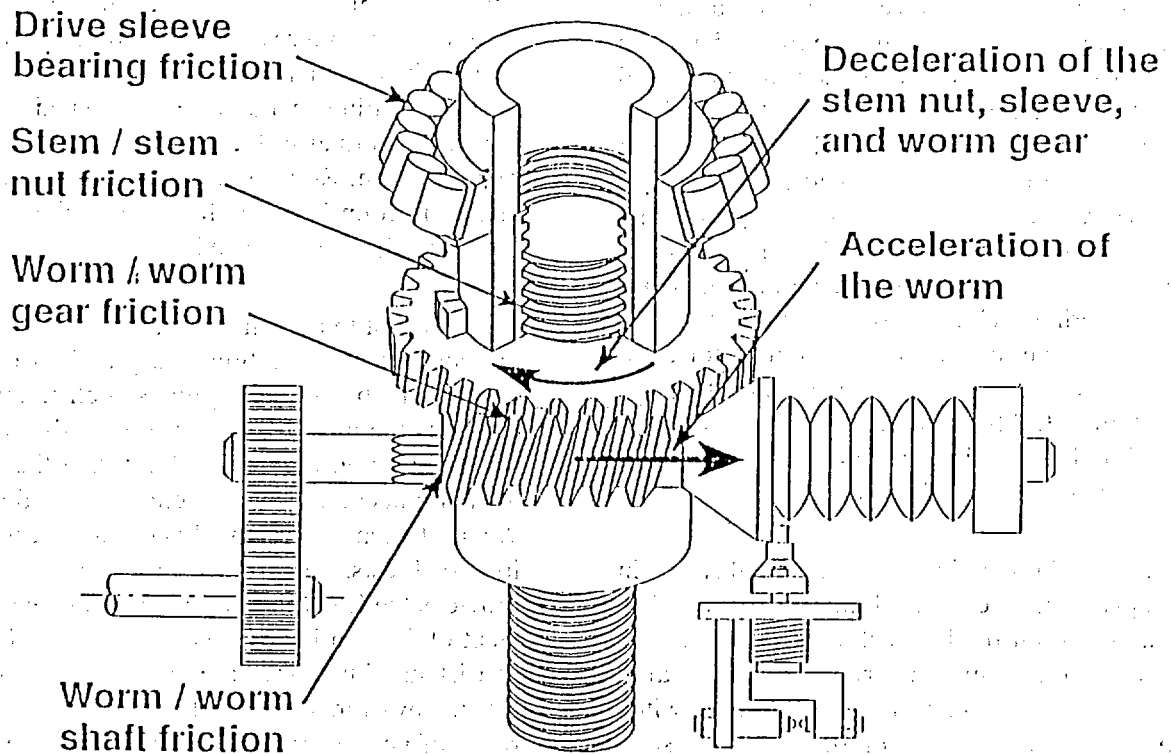


Figure 64. Potential causes of torque loss in the operator are identified.

force and that output by the mechanism to the stem nut. Such a difference could cause load-sensitive MOV behavior. We investigated this possibility.

There is only one inertial or frictional effect in the fourth category, an effect that increases the output torque required to achieve the same stem thrust. This effect would be seen in the stem factor, defined as the ratio of output stem torque to stem thrust. The industry uses the traditional power thread equation to estimate the stem factor: an equation based on the stem diameter, the thread pitch and lead, and the coefficient of friction between the stem and stem nut threads. This power thread equation does not include any inertial terms, and none are required. All of the parameters in the expression, except for the coefficient of friction, are obviously invariant between a lightly loaded and a heavily loaded MOV. This leaves only the friction between the stem and the stem nut threads as this category's possible cause of the load-sensitive behavior. We also investigated this possibility.

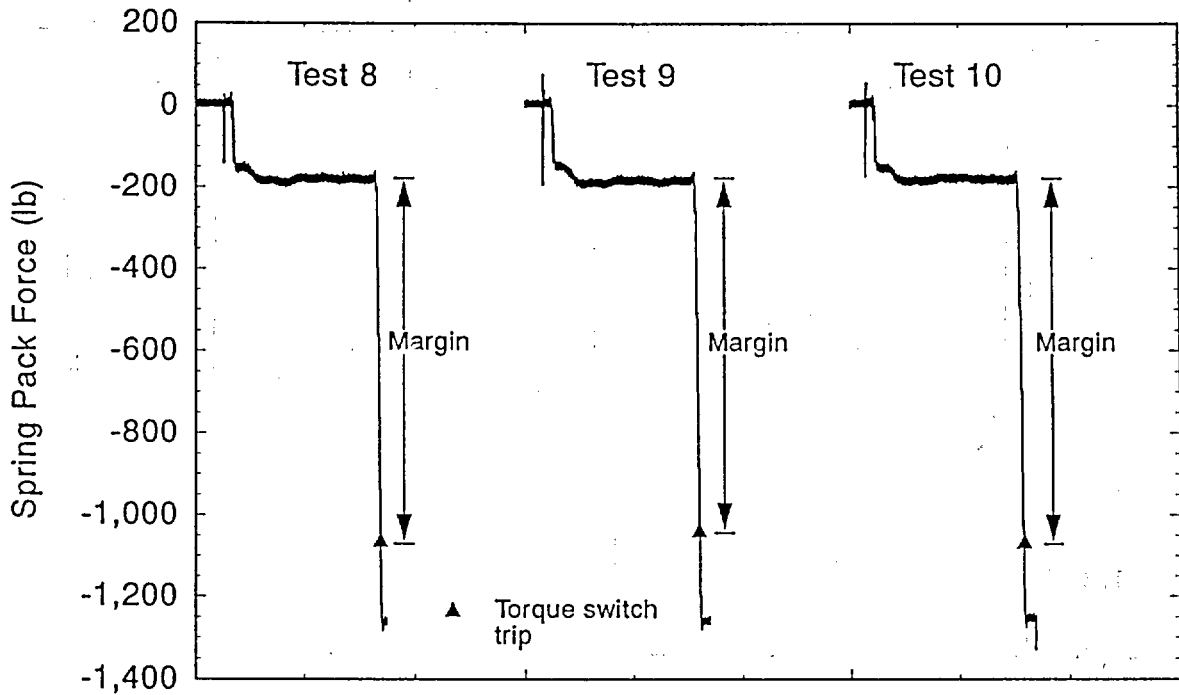
Up to this point, we have identified and categorized potential candidates for the first order cause of load-sensitive MOV behavior. We then used data from each of the MOVLS tests described earlier to evaluate the likelihood of each candidate causing the observed load-sensitive behavior. In addition to acquiring stem thrust data, spring pack force data, and stem torque data, we were also able to calculate an instantaneous ratio of spring pack force to stem torque, the ratio of stem torque to stem thrust (stem factor), and the coefficient of friction between the stem and the stem nut. All calculations were made on a real-time basis, using measured data and valve and operator design information.

The possibility of inertial or frictional effects in the spring pack causing load-sensitive MOV behavior is not likely, as shown in Figures 65 through 67. These figures show the same margins in the spring pack force at torque switch trip throughout the series of 10 tests as the stem force plots (Figures 58-60). Torque spring force margin is defined as the difference in the torque

spring force history between the point where the operator goes into single-path response and where the torque switch trips. There are observed differences in the spring pack force at torque switch trip, but these are within the 5% advertised by Limitorque. The most interesting torque spring history is from Test 15, which shows that a higher spring pack force was required during the running portion of the stroke than was required in Tests 16 and 17, even though the stem load was the same in all three tests. The stem nut coefficient of friction discussed later in this section caused the additional spring pack force during the running portion of Test 15.

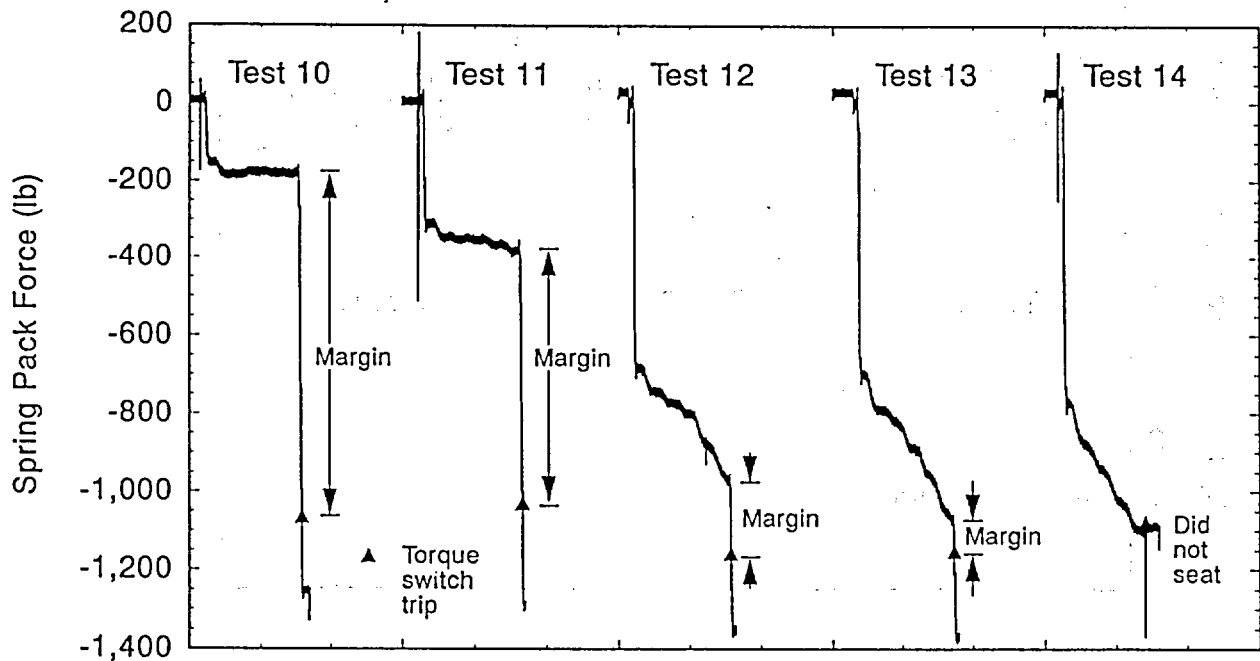
The possibility of changes in the ratio of spring pack force to stem torque causing load-sensitive MOV behavior is not likely, as shown in Figures 68 through 70. The variation of the ratio between individual tests was less than that associated with the worm interacting with different parts of the worm gear during the same test, as shown by the oscillations in the figures. Changes in the ratio indicate that the torque transfer efficiency of the motor operator mechanism actually improves somewhat with increasing load. Such an improvement could result from a small reduction in the coefficient of friction in the operator bearing gear surfaces associated with an increasing normal surface force, a known friction phenomenon. Regardless, an increase in efficiency is counter to the losses associated with load-sensitive MOV behavior.

In contrast to the other data, the stem-to-stem-nut coefficient of friction changed significantly and in a fashion that supports such frictional losses as the most likely cause of load-sensitive MOV behavior. Figure 71 shows that the stem-to-stem-nut coefficient of friction during Tests 8, 9, and 10 remains relatively constant during the low-load tests. Test 11, as shown in Figure 72, provides the first truly loaded test and the coefficient of friction is observed to decrease. This is consistent with an increase in the normal surface force. However, Tests 12, 13, and 14 are not the result of normal friction behavior; they are most likely the result of the lubricant being squeezed out of the stem-to-stem-nut interface. In other



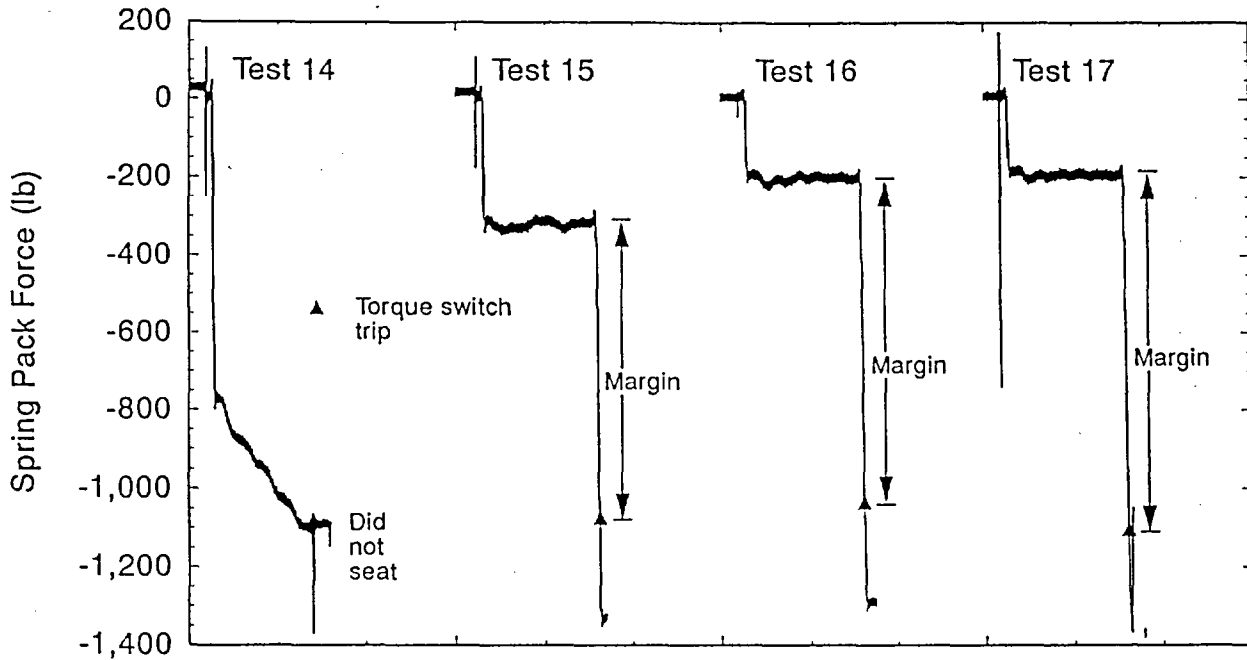
M450 rs-1091-06

Figure 65. Traces of spring pack force versus time for Tests 8 through 10 of the MOVLS test sequence. These traces correspond to the thrusts of Figure 59.



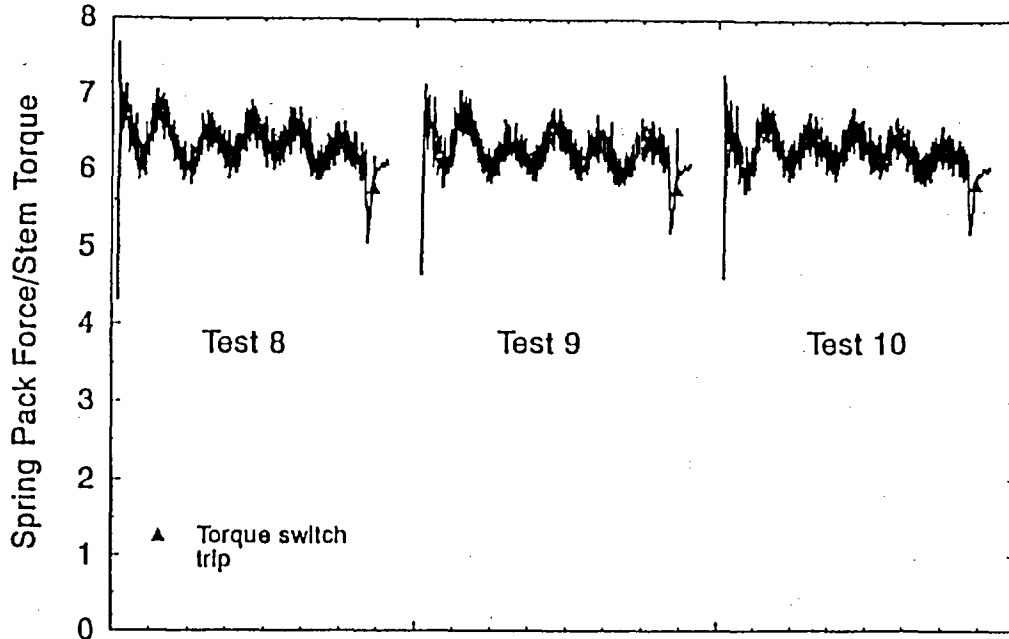
M450 rs-1091-07

Figure 66. Traces of spring pack force versus time for Tests 10 through 14 of the MOVLS test sequence. These traces correspond to the thrusts of Figure 60. Spring pack force does not change significantly from test to test.



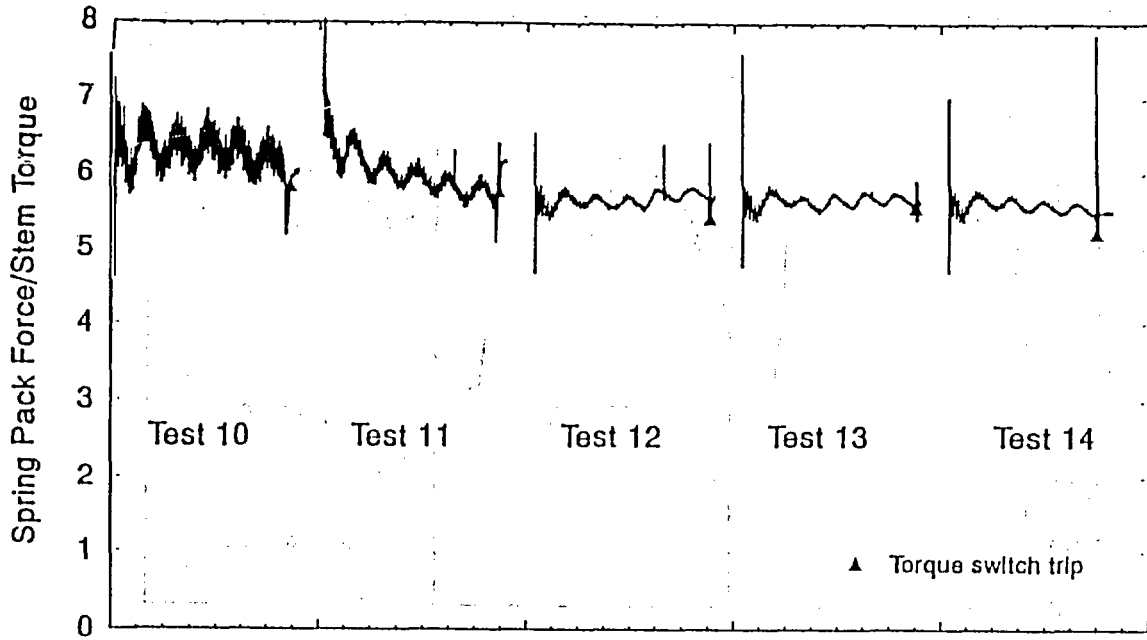
M450 rs-1091-08

Figure 67. Traces of spring pack force versus time for Tests 14 through 17 of the MOVLS test sequence. These traces correspond to the thrusts of Figure 61. Spring pack force does not change significantly from test to test.



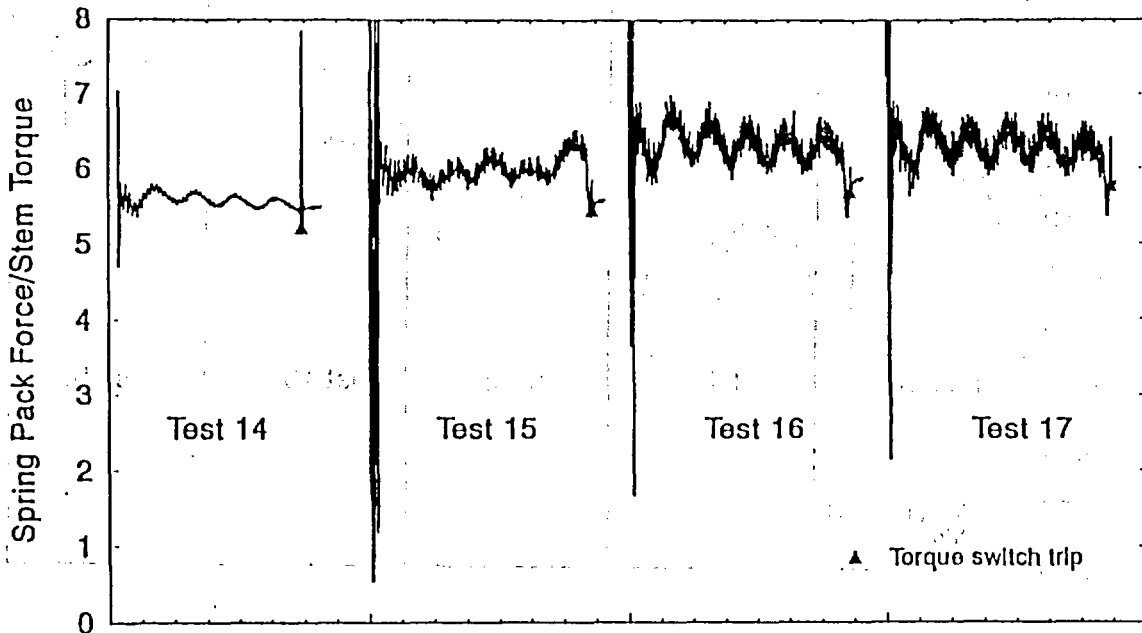
M359 kgd-0791-19

Figure 68. The ratio of spring pack force to stem torque for Tests 8 through 10 of the MOVLS test sequence. These traces correspond to the thrusts of Figure 59.



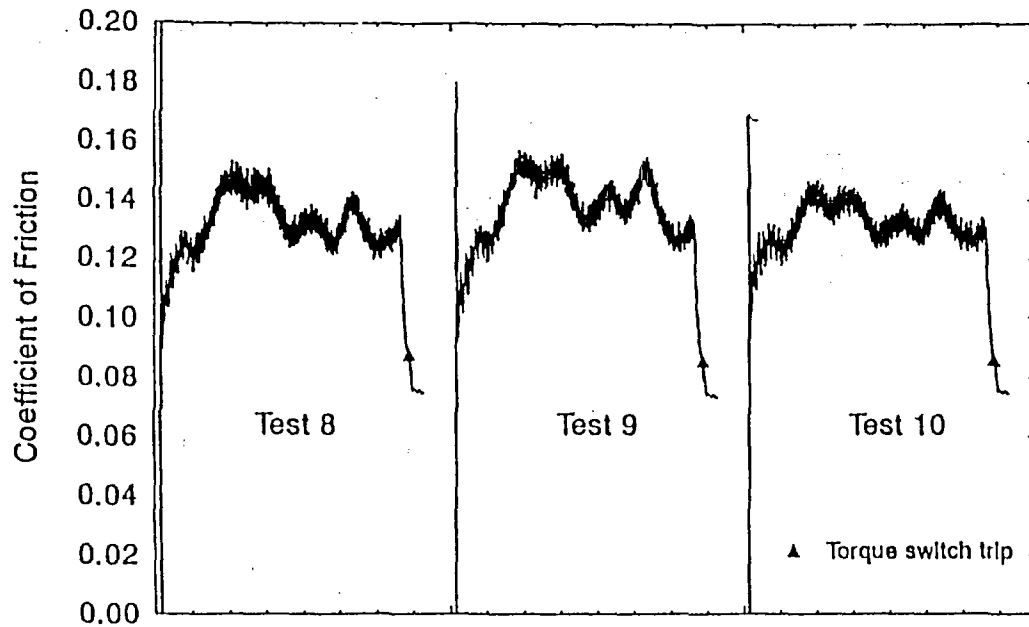
M350 kgd-0701-20

Figure 69. The ratio of spring pack force to stem torque for Tests 10 through 14 of the MOVLS test sequence. These traces correspond to the thrusts of Figure 60.



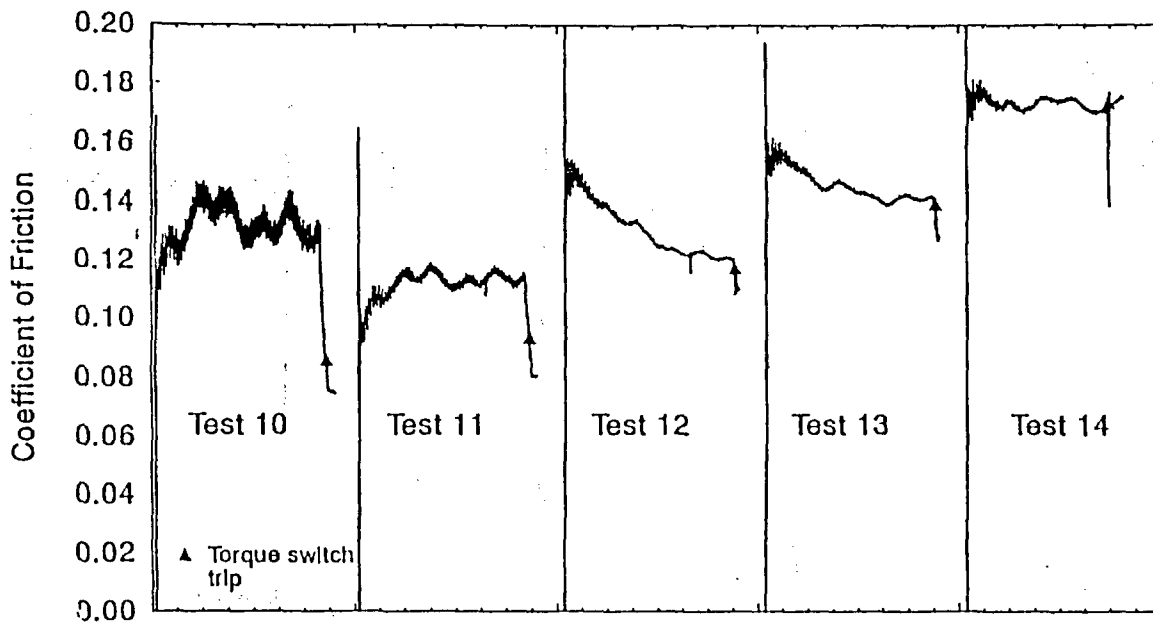
M359 kgd-0701-21

Figure 70. The ratio of spring pack force to stem torque for Tests 14 through 17 of the MOVLS test sequence. These traces correspond to the thrusts of Figure 61. Spring pack force does not change significantly from test to test.



M359 kgd-0791-27

Figure 71. Traces of coefficient of friction in the stem nut versus time for the first three tests of the MOVLS test sequence. Very little change in coefficient of friction is observed at the low thrust levels of these tests.



M359 kgd-0791-28

Figure 72. Traces of coefficient of friction in the stem nut versus time for Tests 10 through 14 of the MOVLS test sequence. A steady increase in coefficient of friction is evident in these tests. Coefficient of friction is highest during Test 14, the test exhibiting load-sensitive MOV behavior.

words, the stem-to-stem-nut interface goes from a thick-film lubricated surface to near metal-to-metal contact. This hypothesis is further substantiated by Test 15, as shown in Figure 73, where the coefficient of friction remains high during the first unloaded test following the highly loaded tests. During this test, the stem-to-stem-nut interface is relubricating itself. During subsequent Tests 16 and 17, the lubrication returns to thick-film lubrication.

This behavior has been observed with two stem and stem nut combinations in the same operator. Other stem and stem nut combinations in other operators must be evaluated before any definitive statements can be made, but if additional research confirms the hypothesis, this provides an additional concern in bounding load-sensitive MOV behavior. The coefficient of friction of a lightly loaded stem varies with stem-to-stem-nut combinations. We have observed values from 0.08 to 0.18; however, they all increase when the load on the stem increases. In fact, we have observed that the coefficient of friction can increase from 20 to 50%. A typical in situ test is a static no-load test, or at best a low-load test similar to those shown in Figure 59. During these no-load static or low-load valve tests, the stem and disc slide into the valve seat basically unloaded and with little or no pressure on the lubricated surfaces of the stem-to-stem-nut interface. Consequently, the unloaded test fails to generate the load necessary to evaluate the stem-to-stem-nut coefficient of friction that will exist when the MOV is highly loaded. Therefore, additional margin must exist to ensure closure against a high stem load. Means to conservatively establish such an acceptable margin still need to be developed.

Once an MOV has been tested, the no-load relationships can be baselined and monitored for degradation. However, it is important to recognize that valves that experience load-sensitive MOV behavior at torque switch trip are not as fully seated as those that do not.

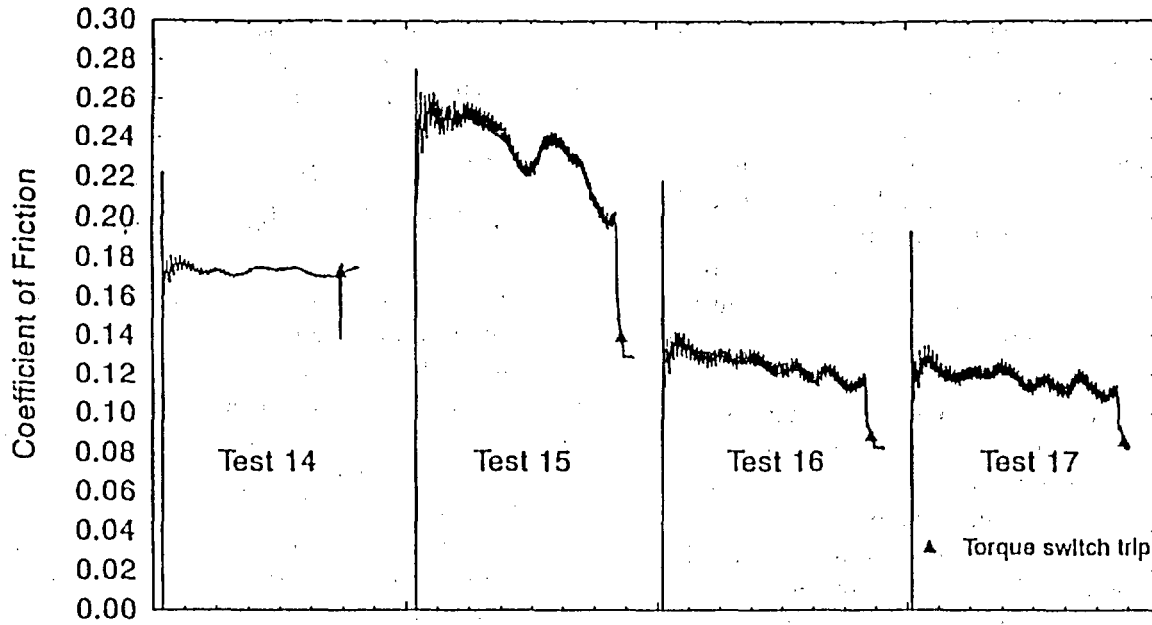
These valves are operating in the margin between successful and unsuccessful closure. When possible, increasing the torque switch set-

ting enough to fully seat the valve at design-basis loadings will reduce or eliminate the effects of load-sensitive MOV behavior.

4.4 Direct Current Powered Motor Operators

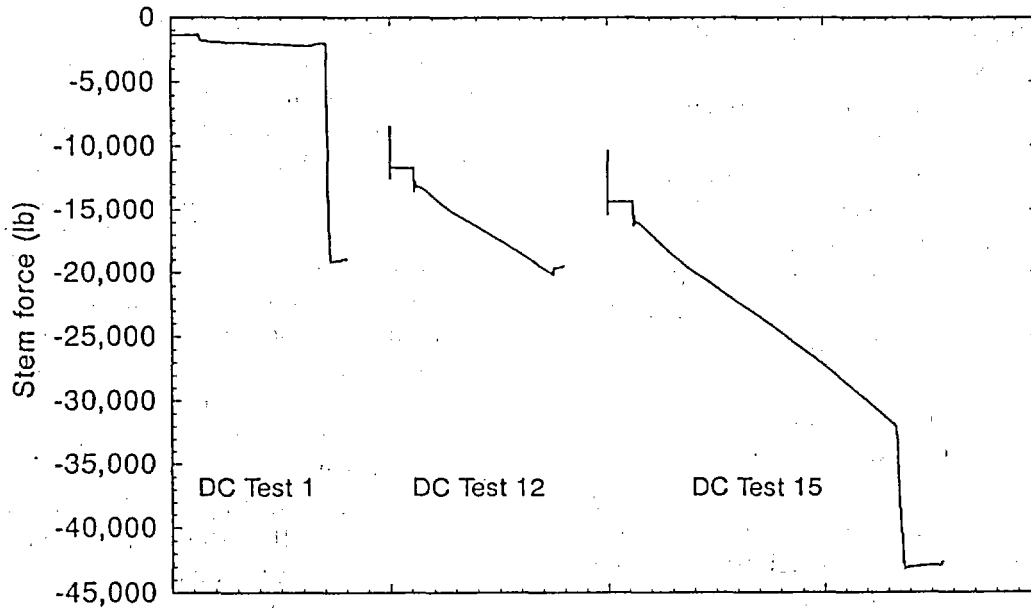
Some of the differences in ac- and dc-powered motor operators have been discussed in other sections of this report. This section deals with dc-powered motor operators with respect to Generic Issue (GI)-87 concerns. In most BWRs, one valve out of each pair of GI-87 isolation valves is dc powered. As part of our GI-87 research, we looked at dc-powered motor operator performance. The results of the work show that if the dc motor operator is correctly sized for the valve application and the power cables are large enough, the dc-powered motor operator will probably equal or exceed the performance of an equally sized ac-powered motor operator.

These results were determined from MOVLS testing and earlier work performed in the field. The MOVLS is described in Section 4.3 of this report. The changes to the MOVLS for this testing included removing the ac motor and installing a 125 Vdc, 40 ft-lb dc motor, and running the dc motor controller field coil current through the torque and open limit switches. Appropriate dc instrumentation was also substituted for ac instrumentation such as voltage and current. The dc testing used the same Limitorque SMB-0 motor operator that had previously been used in the motor-operated, load-sensitive behavior study cited earlier in this report. This ensured that the operator would not influence the results. After a series of check-out tests, the motor operator was subjected to a 15-cycle test series. Figure 74 represents typical thrust histories from these tests. Simulated valve loadings included no-load tests (Test 1) to tests that bypassed the torque switch and nearly stalled the motor (Test 15). As expected from previous field experience, the stroke time increased as the motor operator load increased. The MOVLS monitored motor speed through a monopole pickup that counts the teeth on the worm shaft gear. In the highest loaded test (Test 15), the motor speed was reduced from an



M359 kpd-0791-29

Figure 73. Traces of coefficient of friction in the stem nut versus time for the last four tests of the MOVLS test sequence. A full opening/closing low-thrust cycle (Test 15) is needed following the test exhibiting load-sensitive MOV behavior (Test 14) before the coefficient of friction returns to the levels recorded for the initial low-thrust level tests.



M450 rs-1091-01

Figure 74. Typical stem thrust histories from the dc-powered MOVLS tests.

unloaded speed of 1900 rpm to below 400 rpm, at which time the current was manually interrupted. The stroke time, of course, increased dramatically, going from an unloaded stroke time of 6.0 seconds (Test 1) to a fully loaded stroke time of 12.5 seconds (Test 15 of Figure 74). One of our concerns before testing a dc-powered motor operator was the effect of the lower stem nut speed.

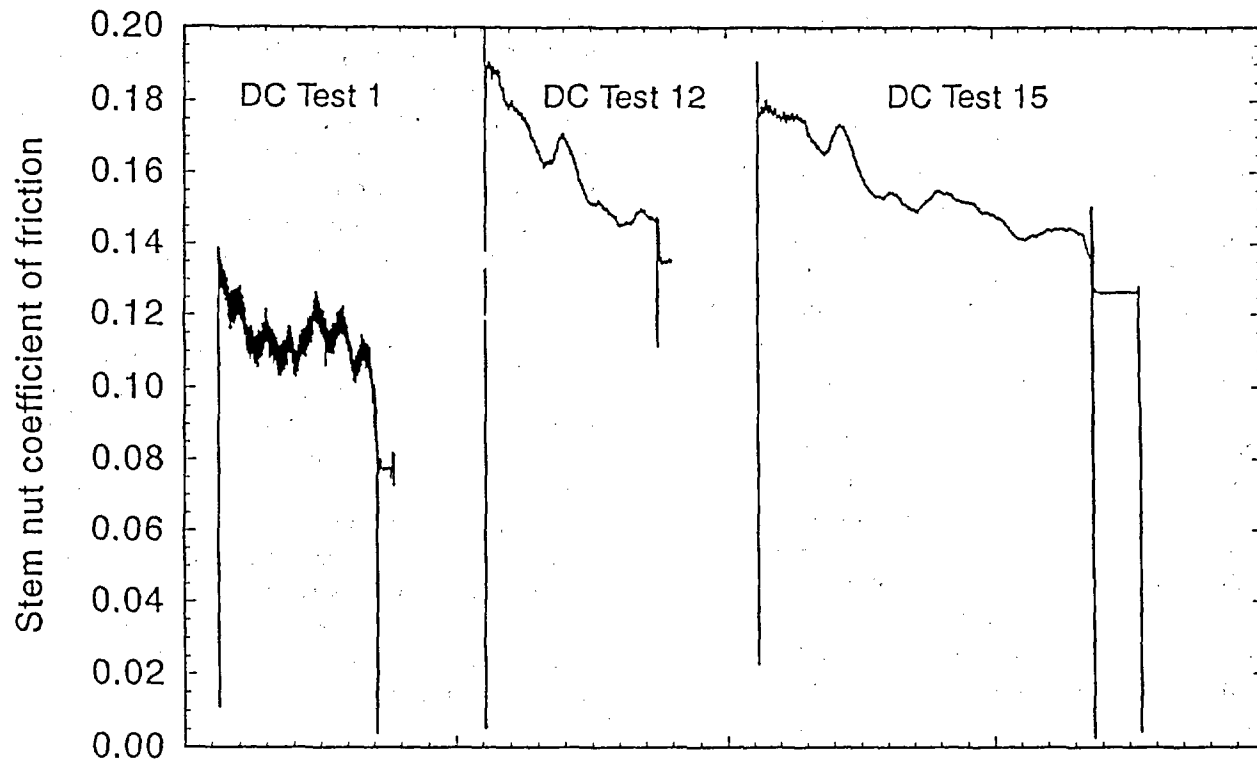
As the dc motor slows down and increases the time the stem nut is highly loaded, it may increase the load-sensitive behavior of the motor operator (rate-of-loading effect). This was not the case. Figure 75 compares an unloaded coefficient of friction history, Test 1 with Test 12, which shows the increase in friction from a heavily loaded operator, and with Test 15, which represents the coefficient of friction resulting from an operator that was subjected to twice the load used in Test 12. The increase in the stem nut coefficient of friction appears to have stabilized between Tests 12 and 15 in spite of the increasing load. This offers the possibility that the increase in the stem nut coefficient of friction under load can be bounded. However, additional testing with more stem-to-stem-nut combinations will be needed to verify such a hypothesis.

The load-sensitive behavior of a dc-powered motor operator is very similar to that observed during testing with an ac-powered motor operator, discussed earlier in this report. The results of the dc-powered motor operator may appear to be worse because of the increase in the stroke time; however, the final thrusts and associated stem nut coefficients of friction are nearly equal to

similarly loaded ac tests. The output torque of a dc motor, as shown in the motor torque versus speed curve presented in Figure 48, is linear and not significantly influenced as the unit slows down. On the other hand, the speed-torque relationship of an ac motor is relatively constant until it reaches the knee in the motor torque versus speed curve and can thus stall from a relatively high speed. Consequently, marginally sized motor operators equipped with an ac motor may stall more easily than a unit equipped with a dc motor. In addition, we observed that this credible valve operation did not cause the dc motor to overheat and adversely influence motor operator performance any more than with an ac motor.

Direct-current motors do have potential installation problems. The higher current demands of a dc motor before stalling, up to five times their nameplate current, were not always recognized, and the larger cabling necessary to handle these large currents was not always installed. Units operating with undersized cables at these higher currents will experience cable heating, and subsequent voltage drops from cable heatup will quickly influence the performance of a dc motor. The difficulty with measuring the voltage drop in a dc motor operator circuit were discussed earlier in this report.

Figure 45, shown earlier in this report, shows how quickly dc motor heating can reduce the output of the motor. Undersized cables and motor heating from a marginally sized motor can significantly reduce the output of a dc motor-operated valve. These installation problems have been observed in operating plants and support the finding identified here.



M450 rs-1091-02

Figure 75. Typical stem nut coefficient of friction histories from the dc-powered MOVLS test. Note the increase in friction between low-load Test 1 and high-load Test 12. The load was doubled between Tests 12 and 15 without a significant increase in stem nut coefficient of friction.

5. WRITING A PERFORMANCE STANDARD

5.1 Overview

Development of a performance standard is a two-fold process: original qualification and maintenance of qualification (in situ testing). The current original qualification standard for motor-operated valves is ANSI/ASME B16.41, which was developed in 1983 and reaffirmed in 1989. This standard is being outdated by the results of NRC and other valve testing. The valve subcommittee of ASME Qualification of Mechanical Equipment (QME) has rewritten the document under the title "QV, Functional Qualification Requirements for Power-Operated Active Valve Assemblies for Nuclear Power Plants" (same title as B16.41). QV will be a section in the QME family of qualification standards. The rewritten standard is an improvement over B16.41, but incorporates the NRC test results findings only up to the start of the analysis of Phase I gate valve test results (DeWall and Steele, 1989). Subsequent analysis of Phase I testing, the results from the Phase II testing, and the results of separate effects testing on the INEL MOVLS have not been incorporated.

The flow interruption section of QV, Annex G, has been improved to incorporate the NRC butterfly and early gate valve test results, but it still allows family groupings and extrapolation that our test results have shown to be faulty. The qualification philosophy is still go/no-go without guidance for margins determination, which is a definite concern for aging. The standard should also address Generic Letter 89-10 concerns, as there are currently no guidelines that would aid a utility in procuring a replacement valve that would meet the recommendations of the generic letter. The QV document has been approved by subcommittees and the main committee, over the objections of INEL and NRC representatives. On the second vote, the document was approved over NRC objections. Subcommittee and main committee chairmen did agree to start the rewrite of the standard to consider incorporating the recent findings with regard to NRC and other testing. This new task group, formed to rewrite the

standard, was finalized at the QME meeting in New York in 1991.

Maintenance of qualification (in situ testing of valves) is the responsibility of the ASME Operation and Maintenance (OM) Committee, which is split into many subcommittees and working groups with varying responsibilities. Those of major interest here are OM-8 and OM-10; of minor interest are OM-18 and OM-19. OM-8 is the working group on motor operators, OM-10 is the working group on valves, and OM-18 and OM-19 are the working groups on air and hydraulic operators.

These OM groups have two major problems: (a) they must consider the in situ valves qualified and write in situ tests accordingly, when in actuality every possible level of valve qualification exists in the plants, and (b) the valve cannot be considered separate from its operator, as it is by OM. The three operator types, referenced above, the valves, and their functions are different enough that they should be considered as separate integrated units instead of being separated by operator type and valves. The OM-10 standard, currently known as ISTC, has been issued and is referenced in Section XI of the 1989 ASME Code. Utilities are required to update their in-service inspection plans every ten years, so, by 1999, all utilities will be using OM 10 for valve testing requirements. Unfortunately, the requirements of OM-10 are only marginally better than the previous Section XI requirements. OM-10 still treats stroke time as the measure of MOV functionality. At the working group level, OM-10 is trying to add a requirement for motor current signature analysis to the stroke time requirements. However, this is not expected to be adopted. OM-8, driven by Generic Letter 89-10, has redrafted their document for motor operators into an integrated MOV standard. We believe this is an improvement over anything else that has been done for in situ testing of MOVs. Representatives of the INEL and NRC sit on the OM-8 committee and have informed the committee of

NRC-sponsored and other testing. The standard reflecting this input is now in the balloting stage.

5.2 Detailed Observations

The valve problem starts with qualification and continues with the maintenance of qualification. Most of the plants were built or in construction before we had a valve qualification standard. Each valve manufacturer had its own proprietary methods (mostly analytic) for determining qualification and for sizing the operator. Globe valves are more likely to be challenged in daily operation than gate or butterfly valves. Early globe valve problems included plug guidance problems and bent stems. Most of these have been corrected. As discussed earlier in the report, we are not certain whether a gate valve is predictable or nonpredictable without a design-basis test. We also do not know if the extrapolation of butterfly valve response was always performed in the conservative configuration we identified in our tests. The OM standards cannot help with these

problems. The original qualification requirements for a valve and operator must be upgraded for replacement valves. The upgraded qualification requirements can then serve as guidelines for the OM standards to provide for the maintenance of qualification.

NRC, utility, European, and Electric Power Research Institute test programs may provide insights on how to quantify the capability of current in-place valves and quantify the risk that might be involved with those designs. The recommendations contained in Generic Letter 89-10 and the improved diagnostic testing described earlier in this report can help to identify some of the more obvious problems. It is clear that design-basis tests cannot be performed for every valve. We expect that, during the next year, more information on these remaining problems will become available. The INEL considers the development of adequate standards a necessary part of this work that must be performed to improve the reliability of MOVs in the operating plants.

6. REFERENCES

- Allis-Chalmers Corporation, *Test Report on an Allis-Chalmers 6" STREAMSEAL Butterfly Valve in Air Concerning Nuclear Containment Isolation Valves*, VER-0209, December 17, 1979.
- DeWall, K. G., and R. Steele, Jr., *BWR Reactor Water Cleanup System Flexible Wedge Gate Isolation Valve Qualification and High Energy Flow Interruption Test*, NUREG/CR-5406, EGG-2569, 1989.
- MPR Associates, Inc., *Application Guide for Motor-Operated Valves in Nuclear Power Plants*, NP-6660, March, 1990.
- NRC, *NRC Action Plan as a Result of the TMI-2 Accident*, Volumes 1 and 2, Revision, NUREG-0660, August, 1980a.
- NRC, *Clarification of TMI Action Plan Requirements*, NUREG-0737, November, 1980b.
- Steele, R., Jr., and J. G. Arendts, *SHAG Test Series: Seismic Research on an Aged United States Gate Valve and on a Piping System in the Decommissioned Heissdampfreaktor (HDR)*, NUREG/CR-4977, EGG-2505, 1989.
- Steele, R., Jr., K. D. DeWall, and J. C. Watkins, *Generic Issue 87 Flexible Wedge Gate Valve Test Program, Phase II Results and Analysis*, NUREG/CR-5558, EGG-2600, 1990.
- Watkins, J. C., R. Steele, Jr., R. C. Hill, and K. G. DeWall, *A Study of Typical Nuclear Containment Purge Valves in an Accident Environment*, NUREG/CR-4648, EGG-2459, 1986.

BIBLIOGRAPHIC DATA SHEET

(See instructions on the reverse)

1. REPORT NUMBER
*(Assigned by NRC, Add Vol., Supp., Rev.,
and Addendum Numbers, if any.)*

NUREG/CR-5720
EGG-2643

2. TITLE AND SUBTITLE

Motor-Operated Valve Research Update

3. DATE REPORT PUBLISHED

MONTH | YEAR
June | 1992

4. FIN OR GRANT NUMBER

A6857, B5529

5. AUTHOR(S)

Robert Steele, Jr.
John C. Watkins
Kevin G. DeWall
Mark J. Russell

6. TYPE OF REPORT

Technical

7. PERIOD COVERED *(Inclusive Dates)*

8. PERFORMING ORGANIZATION - NAME AND ADDRESS *(If NRC, provide Division, Office or Region, U.S. Nuclear Regulatory Commission, and mailing address; if contractor, provide name and mailing address.)*

Idaho National Engineering Laboratory
EG&G Idaho, Inc.
P.O. Box 1625
Idaho Falls, Idaho 83415

9. SPONSORING ORGANIZATION - NAME AND ADDRESS *(If NRC, type "Same as above"; if contractor, provide NRC Division, Office or Region, U.S. Nuclear Regulatory Commission, and mailing address.)*

Division of Engineering
Office of Nuclear Regulatory Research
U.S. Nuclear Regulatory Commission
Washington, D.C. 20555

10. SUPPLEMENTARY NOTES

11. ABSTRACT *(200 words or less)*

This report provides an update on the valve research sponsored by the U.S. Nuclear Regulatory Commission (NRC) that is being conducted at the Idaho National Engineering Laboratory. The update focuses on the information applicable to the following requests from the NRC staff:

- Examine the use of in situ test results to estimate the response of a valve at design-basis conditions
- Examine the methods used by industry to predict required valve stem forces or torques
- Identify guidelines for satisfactory performance of motor-operated valve diagnostics systems
- Participate in writing a performance standard or guidance document for acceptable design-basis tests.

The authors have reviewed past, current, and ongoing research programs to provide the information available to address these items.

12. KEY WORDS/DESCRIPTORS *(List words or phrases that will assist researchers in locating the report.)*

Motor-operated valve (MOV)
Gate valve—stem force
Butterfly valve—stem torque
MOV diagnostic systems

13. AVAILABILITY STATEMENT

Unlimited

14. SECURITY CLASSIFICATION

(This Page)

Unclassified

(This Report)

Unclassified

15. NUMBER OF PAGES

16. PRICE

THIS DOCUMENT WAS PRINTED USING RECYCLED PAPER

**UNITED STATES
NUCLEAR REGULATORY COMMISSION
WASHINGTON, D.C. 20555-0001**

**OFFICIAL BUSINESS
PENALTY FOR PRIVATE USE, \$300**

**SPECIAL FOURTH-CLASS RATE
POSTAGE AND FEES PAID
USNRC
PERMIT NO. G-67**